OAK RIDGE
NATIONAL LABORATORY
MANAGED BY UT-BATTELLE
FOR THE DEPARTMENT OF ENERGY

ORNL/SUB/00-85B99398V-9

Validation Report for FY 1997

Final Report

Project Manager

A. M. Pavlovichev

Executed by

S. Bychkov
A. Kalashnikov
M. Kalugin
A. Lazarenko
L. Maiorov
A. Pavlovichev
V. Sidorenko

A Russian Contribution to the
Fissile Materials Disposition Program

UT-BATTELLE
ORNL-27 (4-00)

ORNL/SUB/00-85B99398V-9

VALIDATION REPORT FOR FY 1997

Final Report

Project Manager

A. M. Pavlovichev

Executed by

S. Bychkov
A. Kalashnikov
M. Kalugin
A. Lazarenko
L. Maiorov
A. Pavlovichev
V. Sidorenko

Date Published: September 2001

Prepared by
Russian Research Center "Kurchatov Institute"
Institute of Nuclear Reactors
under subcontract 85B-99398V

Funded by
Office of Fissile Materials Disposition
U.S. Department of Energy

Prepared for
Computational Physics and Engineering Division
OAK RIDGE NATIONAL LABORATORY
Oak Ridge, Tennessee 37831
managed by
UT-BATTELLE, LLC
for the
U.S. DEPARTMENT OF ENERGY
under contract DE-AC05-00OR2272

RUSSIAN RESEARCH CENTER "KURCHATOV INSTITUTE"
INSTITUTE OF NUCLEAR REACTORS
VVER DIVISION

Joint U.S./Russian Project to Update, Verify and Validate Reactor Design/Safety Computer Codes Associated with Weapons-Grade Plutonium Disposition in VVER Reactors.

VALIDATION REPORT FOR FY1997

(Final report)

General Order 85B-99398V

Project manager

A.M.Pavlovichev

Executed by

S. Bychkov
A. Kalashnikov
M. Kalugin
A. Lazarenko
L. Maiorov
A. Pavlovichev
V. Sidorenko

Moscow 2000

ABSTRACT

The report issued according to **Work Release 02. P. 99-8** presents a comparison of results on VVER Calculational Benchmarks computed with various codes: design code TVS-M and precision code MCU-REA elaborated in RRC KI, IPPE codes WIMS-ABBN, TRIANG-PWR and CONKEMO and 2-D fuel assembly analysis code HELIOS developed by Studsvik Scandpower.

CONTENT

LIST OF TABLES

LIST OF FIGURES

INTRODUCTION

Up to now all design and operational calculations of VVER type reactors have been carried out with the use of the code package developed in RRC "Kurchatov Institute" and certified by Nuclear Regulatory Body of Russian Federation (GOSATOMNADZOR) [1]. MCU-RFFI/A code [2] developed in RRC "Kurchatov Institute" and certified by GOSATOMNADZOR has been used as a precision one. In recent years the large work has been carried out to update neutronic codes in the context of the necessity of substantiation of improved VVER fuel cycles (zirconium fuel assemblies, uranium-gadolinium burnable absorbers). In particular, the new modern code TVS-M has been developed to prepare few-group constants; the coarse-mesh (BIPR-7) and the fine-mesh (PERMAK) codes for VVER core calculation have been updated. This package allows one to perform design and operational calculations of the VVER type reactors' updated fuel cycles.

It is supposed to use the mentioned code package for neutronic calculation of VVER-1000 partially loaded by MOX fuel fabricated from weapon-grade plutonium. Obviously, the large amount of data on uranium fuel neutronic characteristics (criticality experiments, VVER-1000 operation data, post-reactor studies of uranium fuel, and etc.) should be effectively used in the verification process. At the same time, this database should be complemented by the data on MOX fuel characteristics, such as:

- multiplication properties of MOX fuel as a function of plutonium contents and its isotopic composition;
- power distribution in MOX fuel, in particular at LEU-MOX interfaces;
- the effects of cold-to-operating temperature change and effect of moderator voiding;
- Doppler effect;
- Xe and Sm poisoning effects;
- soluble boron efficiency;
- absorbers rod worth (boron, dysprosium);
- burnable absorber worth (boron rods, gadolinium integrated into fuel);
- kinetics parameters (effective fraction of delayed neutrons, neutron life time);
- change of fuel nuclide content;

All these characteristics should be considered depending on the fuel burnup.

No experiments have been carried out in Russia with MOX fuel and there is no experience on its usage in VVER type reactors. Therefore, international co-operation becomes very important at the current stage of the verification process.

Starting several years ago employees of RRC "Kurchatov Institute" together with colleagues USA, and employees of SRC "Institute of Physic and Power Engineering" (IPPE) have been engaged in the verification of the RRC KI code package with reference to calculation of VVER-1000 reactors with MOX fuel. The verification procedure was suggested to include the following main stages:

- comparison with measured data (critical facilities with LEU and MOX lattices);
- comparison with calculations computed with various codes including precision ones (calculational benchmarks);
- use of data on post-reactor studies of irradiated fuel;
- comparison with operation data;

As can be seen one of the important parts of code verification activity is a joint solving of various calculational benchmarks. So in 1997 within the framework of joint U.S.-Russia project two sets of calculational benchmark problems have been formulated.

The first set [3] covers different aspects of UO_2 and MOX in normal operating condition. The second set was formulated to cover off-normal conditions and provides for a comparison of kinetics parameters. These sets consider of pin cell, single assembly, and multi-assembly geometries with LEU (low enriched uranium) and weapon-grade and reactor MOX fuel.

The calculations call for a wide range of water temperatures, soluble boron concentrations including states with inserted control rods. Several variants require burnup analysis.

The detailed description of this VVER Benchmark is given in [4].

The presented report is devoted to comparison of calculations of VVER Benchmark performed in Russian Federation with the use of codes MCU-REA (RRC KI), TVS-M (RRC KI), WIMS-ABBN (SRC IPPE), TRIANG-PWR (SRC IPPE), CONKEMO (SRC IPPE) and in U.S.(ORNL) using the HELIOS code.

1. CODES USED IN CALCULATIONS

1.1 MCU-RFFI/A AND MCU-REA CODES

The calculations reported were performed with the use of two versions of the MCU Monte Carlo code: MCU-RFFI/A and MCU-REA codes based on nuclear data libraries DLC/MCUDAT-1.0 and DLC/MCUDAT-2.1.

MCU-RFFI/A [2] is a general-purpose Monte Carlo code for solving the neutron transport problems certified by Russian safety authorities (Gosatomnadzor GAN, Passport № 61 17.10.96). The code verification and validation was based on the data library DLC/MCUDAT-1.0.

MCU-RFFI/A is a pointwise continuous energy code permitting one to model systems with any geometry. The subgroup method is used to describe the unresolved resonance cross section. It is possible to use a detailed description of cross sections in the resolved resonance region. For the most important isotopes an "infinite" number of energy points is used to describe the resonance curve. In this case cross sections are calculated during the Monte Carlo run at every energy point on the basis of the resonance parameter library. It permits one to perform the calculations without preliminary tabulation of cross sections and allows the user to estimate temperature effects independently of the cross section library state. For the thermal energy region, the Monte Carlo game is played using the $S(\alpha,\beta)$ scattering law for hydrogen bonded in water or free gas model for others isotopes. One may solve the problems taking into account both the prompt neutron and the delayed neutron fission spectra.

The more detailed description of MCU-RFFI/A code is given in [3].

The MCU-REA [5] code is the advanced version of the MCU-RFFI/A, which can also solve the burnup problems.

The MCU-REA code and DLC/MCUDAT-2.1 library were verified and validated by using the results of more than 400 criticals.

The calculations of variants V1-V12 for zero burnup point were performed with MCU-RFFI/A code based on DLC/MCUDAT-1.0 library. The results of these calculations are included in [3]. Variants V15-V20 were calculated with the same code but with different

data library (DLC/MCUDAT-2.1) and corresponding results are presented in [6]. The code MCU-REA was used to perform the burnup calculations of pin cell variants V1 and V2.

1.2 TVS-M CODE

The code is intended for a generation of few-group neutron constant libraries for codes BIPR and PERMAK which include the multi-parametric dependencies of cross-sections for FAs and their constituent cells (fuel rods, absorber rods, burnable absorber rods and other cells) as well as derivatives of these cross sections as functions of reactor state and fuel burnup.

Nuclear data libraries

The nuclear data library is based on the same files of estimated nuclear data as precision code MCU-RFFI/A (nuclear data library DLC/MCUDAT-1.0), which uses the Monte Carlo method.

In the epithermal energy region (E>0.625 eV) the calculation is based on slightly modified micro-cross section library BNAB (see, e.g., [7]) with 24 energy groups. The nuclide libraries can contain both the group and subgroup constants and for some nuclides with temperature dependence.

For the calculation of neutron spectrum in the energy region of resolved resonances E_n<1 keV (15 and higher BNAB group) the library includes files of resonance parameters of individual nuclides obtained on the base of the LIPAR-3 library. For all fissile nuclei the library contains prompt and delayed neutron spectra, group β values and decay constants for six groups of delayed neutrons.

The thermal energy region is divided into 24 groups. For the nuclides with the "1/v" cross-section behavior the absorption cross sections at 2200 m/s are used, for the rest ones the group values of the absorption, scattering and fission cross sections are specified. In addition, for oxygen and carbon the scattering matrices obtained in terms of gas model at 300, 373, 473, 558, 623K are given. For hydrogen bonded in water molecule the scattering matrix is obtained from the ENDF/B recommended data in terms of the Koppel model [8] at the same temperatures.

The library contains the files of cross sections and yields of 98 fission products including ^{135}Xe and ^{149}Sm. The files of fission product yields are based on the ENDF/B-VI data [9].

There is a modified version of TVS-M library, which differs from the standard one by the only file containing parameters of resolved resonances for ^{238}U. This file was taken from the resonance parameter library LIPAR-5 being a part of the MCU code library DLC/MCUDAT-2.1. The TVS-M results given in [3] were calculated with the standard data library while the ones from [6] were obtained with a modified version of the library. The current report contains both results and by default they correspond to the calculation using the standard data library.

Uniform lattice

In the energy region of epithermal neutrons (10.5MeV>E_n>0.625 eV, BNAB groups 1-24) a detailed calculation of group spatial-energy distribution of neutron flux is performed. Each group is divided into an arbitrary number of intervals equal in lethargy, and then the calculation is performed at each point of group division. The of elastic scattering process is calculated without use of any approximations when the scattering is isotropic in the inertia center system (i.e.s), otherwise the scattering anisotropy is taken into account by the term not higher than linear in cosine of scattering angle. The slowing down due to inelastic scattering

is taken into account via the matrix of inelastic transitions under the assumption of uniform energy distribution of neutrons scattering into the given group.

For nuclides with the subgroup description of cross sections the heterogeneous subgroup calculation of their micro cross sections is performed.

In the energy region of resolved resonances (groups 13-24 BNAB) for resonance nuclides the calculation of all types of cross sections is performed with the use of nuclide resonance parameters. In so doing it is possible to take into account temperature dependence of resonance cross sections.

In the thermal energy region the standard calculation technique is used. It suggests solving the multi-group equation of thermalization with the neutron sources from the epithermal energy region formed when calculation for this energy range was performed. The model of the thermalization matrix construction is described above.

Calculation of neutron spatial distribution is carried out by dividing the cells into an arbitrary number of annular material zones and by the use of the passing through probability (PTP) method [10]. In the calculation the actual form of the cell boundary is taken into account.

The calculation of the point kinetics parameters $\beta_{eff.}$, ℓ is made by the standard formulas using the value function ψ with respect to K_{eff} and with six groups of delayed neutrons.

The calculation of the fuel nuclide composition during fuel burnup is performed for heavy nuclides from ^{232}Th to ^{244}Cm and for 98 fission products from ^{82}Kr to ^{163}Dy. The burnup equations can be solved both by the Runge-Kutt method and by a faster analytical method described in [11].

Calculation of supercells and fuel assemblies

For the determination of FA neutronic characteristics the code uses the diffusion fine-mesh calculation with an arbitrary number of groups from 4 to 48 and with the mesh width equal to the pitch between fuel rods in the FA. For the boundary mesh cells the compression coefficient is used. Along with the standard six-point scheme the refined scheme whose principles of construction are described in [12] can be used. The use of this scheme permits keeping of the *accurate* (i.e. obtained from solving of transport equation for the cell) connection between cell averaged neutron flux and values of flux and current at the cell boundary. In this way it becomes possible to avoid errors peculiar to the standard calculation scheme associated with the finite size and heterogeneous structure of mesh points.

Each mesh point pertains to a definite type: fuel rod, cell with absorber rod, cell corresponding to the gap between FAs, etc. The constants for the background type are always calculated in the asymptotic mode, i.e. as for the uniform fuel cell. The constants for non-fuel cells are calculated in the mode of supercell. For the non-background fuel cells including those with the tvegs the calculation can be performed both in the asymptotic and supercell modes. The homogenized background cell is always considered as the external zone of supercell.

1.3 CONKEMO CODE COMPLEX

Code complex CONKEMO was specially developed for burnup calculation. It consists of the following main program units:

- CONSYST prepares the group (299 groups) cross-sections of medium based on ABBN-93 neutron data library [13];

- KENO-VI is used for neutron flux calculations in arbitrary geometry (including hexagonal one) by the Monte-Carlo method;
- ORIGEN-S performs isotope evaluation calculations;
- MAYAK provides the joint work of the codes in the complex, information flows, process the results.

Short description of the above mentioned codes are given below.

The CONSYST code is the main part of CONSYST2 cross-section provision system, which provides the use of ABBN-93 cross sections for various practical applications. CONSYST calculates microscopic group cross-sections of nuclides in the medium, neutron and photon cross-section of the medium etc. CONSYST provides cross-sections for such transport codes as ANISN, DOT, TWODANT, also it gives an opportunity to make use of ABBN-93 data in KENO-VI Monte Carlo calculations etc. CONSYST2 system also includes sets of service procedures.

KENO-VI [14] is a part of American SCALE 4.3 system and performs precision calculations in arbitrary 3-D geometry by the Monte Carlo method.

ORIGEN-S [15] is also a part of SCALE 4.3 system. Cross-sections from original ORIGEN libraries are updated during calculations. Multi-group (299 groups) library of fission products contains only capture cross-sections (as original ORIGEN library). These cross-sections produced on the base of the FOND 2.2 library of evaluated neutron files for 169 nuclides.

MAYAK makes possible the joint use of CONSYST processing code together with neutron and photon transport codes (TWODANT, KENO and MCNP) with burnup codes (ORIGEN or CARE [16]). Set of batch files provides sequential code start up.

1.4 WIMS-ABBN CODE

The WIMS-ABBN code is an updated, English WIMS-D4 code. The modernization mainly was done to introduce minor actinide chains and to update the library.

Updating and Supplementing the WIMS-D4 Library

Data for almost all structural materials, all neutron moderators, and all actinides were updated in the WIMS-D4 library. Data for Sn, Mo, Hf, Ta, and W were added. Data for minor actinides ^{237}Np, ^{238}Pu, ^{241}Am, ^{242}Am, ^{242m}Am, ^{243}Am, ^{242}Cm, ^{243}Cm, ^{244}Cm, and ^{245}Cm were also added.

The FP list was preserved as in the original version, but all the neutron data for FPs were updated and replenished. Now, full neutron constant sets are included in the library, not simply the capture cross sections as in earlier versions of the library. The FP yields are updated for ^{235}U and ^{239}Pu, and the yields for all other fissile materials are added.

Group constants for the new WIMS-D4 library were calculated on the basis of the FOND-2 evaluated neutron data library. In many cases, the evaluated nuclear data libraries of ENDF/B-6 and JEF-2 are also used.

Resonance self-shielding data were calculated using the GRUCON code but only in the cases when the narrow resonance approximation may be considered as adequate. The NJOY code was used for calculation of resonance self-shielding, taking into account the fluctuations of collision density in the vicinities of resonance. The NJOY calculations were performed for all fuel nuclides.

Thermalization matrices for moderators were calculated on the basis of ENDF/B-6 data by the NJOY code. Anisotropy of scattering is described in P1 approximation. Average

group cross-section and matrices of inter-group transitions were calculated using the NJOY code.

The additional neutron reaction cross-section library ACTWIMS is compiled. This library includes the data for many more nuclides and reaction types than does the main WIMS-D4 library. But energy grids in these libraries are the same, and thus the ACTWIMS data can be collapsed using the neutron spectra calculated by WIMS.

In WIMS calculations, a set of 48 nuclides, consisting of 16 actinides, 31 FPs, and oxygen, were used to represent fuel composition.

WIMS-D4 Improvements

Improvements were introduced in WIMS-D4. Resonance self-shielding of neutron cross-sections is extended to the thermal region. This improvement is especially important for the accurate treatment of neutron capture in ^{242}Pu, which has a resonance at very low energy. The second improvement consists of the addition of a special module (AVERAGE) for collapsing the ACTWIMS cross sections using WIMS's cell-averaged neutron spectra. Collapsed one-group cross sections are then used in kinetics calculations.

The number of nuclear reactions considered in the WIMS library during actinide generation was considerably extended. However, the structure of the WIMS-D4 library does not allow the inclusion of some nuclear reactions.

The production of ^{242}Am and ^{242m}Am by the ^{241}Am neutron capture cannot be taken into account today because the current version of the WIMS-D4 code cannot treat branching in the capture process. Thus, channels for the production of ^{242}Cm and ^{243}Cm are closed. For this reason, for any nuclide, the reaction (n, 2n) cannot be considered if the reaction (n, γ) has been included.

The CREDE code was produced to correct these flaws. This code works together with WIMS and AVERAGE. The CREDE code is used for calculations of heavy metal (HM) concentrations during burnup and over a long period after unloading.

1.5 TRIANG-PWR CODE

The program complex TRIANG-PWR is a new version of TRIANG [17] code for 3-D calculations of VVER reactors. It is used for simulation of reactor burnup while maintaining criticality by adjusting the concentration of dissolved boron in the coolant and refueling.

3-D neutron fluxes are calculated by the diffusion approximation.

Number of points in a plane is 6000 (base variant). Symmetry angles from 30° to 180° on a triangular (in a plane) grid are accepted.

TRIANG-PWR is used mainly for 3-D rough-mesh calculation of VVER type reactors. A grid with 7 nodes per assembly is usually used. If needed, more detailed geometric descriptions with tighter grids are possible. In this case the specific cells containing, for example, absorber regions (absorber/burnable absorber rods surrounded by fuel pins) are formed within the assembly. A grid pitch will be something like the trebled fuel pin one. Fine mesh (pin-by-pin) calculations are possible too.

To save computation time a few-group approach is used. The homogenized macroscopic cross-sections of zones of 3-D model are determined from cell (fuel assembly) calculations. Generally speaking the macro constants depend on instantaneous conditions of fuel assembly operation: water density, temperature of water and fuel, concentration of dissolved boron, etc.

To obtain accurate macroscopic cross-sections an iterative process is required. In a complex TRIANG mode the correction of constants can be produced through a given number of external iteration.

The WIMS-ABBN code is used to make cell burnup calculations and, as a result, to obtain few-group macroscopic cross-sections. Then the code PARSEC determines approximation coefficients as a function of state variables for zone required. These coefficients are used by the TRIANG-PWR code to calculate and correct macroscopic cross-sections during reactor calculations.

In the present report the TRIANG-PWR code was used for calculation of pin-by-pin power distributions for assembly and multi-assembly variants (variants V11-14, V19-20).

1.6 HELIOS CODE

HELIOS [18] is a 2-D code that is used for the analysis of fuel assemblies and the generation of collapsed cross sections for full-core analysis codes. The code uses the collision probability method with current coupling for the transport equation solution. The subgroup method is used for resonance treatment. A detailed set of nuclides is used for the fuel depletion.

HELIOS's cross-section libraries are based on ENDF/B-VI revision 2 with ^{235}U from revision 3. The ^{238}U resonance integral in the production libraries has been reduced by 3.4% to produce better agreement with critical experiments. The cross-sections used are in 190-group structure.

The more detailed description of the HELIOS code and its modelling options are given in [4].

2. COMPARISON OF THE RESULTS

All materials on comparison of VVER Benchmarks calculation results can be subdivided into the following principal parts:

- comparison of pin cell results:
  - pre-defined fuel composition, separate states;
  - reactivity effects;
  - micro cross sections;
  - burnup calculations (K_{eff} and nuclide composition);
  - kinetic parameters;
- comparison of fuel assembly results;
  - burnup calculations (K_{eff} and nuclide composition);
  - separate states calculations;
  - reactivity effects;
  - pin by pin power distribution;
- comparison of multi-assembly results
  - K_{eff} burnup calculations;
  - pin by pin power distribution;

  Each of the parts (figures and tables) is enclosed in corresponding Appendix.

The statistical error in MCU calculations of separate states at burnups 0, 10, 30, 40, 50, and 60 MWd/kgHM is less than 0.1% for K_{eff} and less than 2% for local values of fission rate. All burnup calculations were performed with statistical errors less than 0.15% in K_{eff} value.

The statistical deviation in K_{inf} calculations obtained by KENO-VI code included in CONKEMO complex is equal to about 0.02% in states with power distribution calculations and is about 0.04 % in the other states.

All statistical errors given above correspond to 1σ-confident interval.

2.1 COMPARISON OF PIN CELL RESULTS

The pin cell is the simplest geometry type considered in the system of benchmark variants specified in [4]. These variants differ both in fuel composition and in states to be calculated. They are of two main groups: *V1-V10* variants requiring calculation of standard operating conditions states (S1-S6) and *V15-V18* variants, which call for calculations of off-normal and accident condition states (S7-S12). Below one can see brief characteristics of the states:

S1 – T_f=1027K /T_m=579K /C_B=600 ppm /ρ(Xe,Sm)≠0 /B_z^2=0.003 cm^{-2};
S3 – T_f=1027K /T_m=579K /C_B=0 /ρ(Xe,Sm)≠0 / B_z^2=0.003 cm^{-2};
S4 – T_f=1027K /T_m=579K /C_B=600 ppm /ρ(Xe,Sm)=0 /B_z^2=0.003 cm^{-2};
S5 – T_f=579K /T_m=579K /C_B=600 ppm /ρ(Xe,Sm)=0 /B_z^2=0.003 cm^{-2};
S6 – T_f=300K /T_m=300K /C_B=600 ppm /ρ(Xe,Sm)=0 /B_z^2 =0.003 cm^{-2};
S7 – T_f=1027K /T_m=579K /C_B=0 /ρ(Xe,Sm)=0 /B_z^2 =0.0;
S8 – T_f=2000K /T_m=579K /C_B=0 /ρ(Xe,Sm)=0 /B_z^2 =0.0;
S9 – T_f=1027K /T_m=579K /C_B=0 /ρ(Xe,Sm)=0 /B_z^2 =0.0 /γ_m=0.2 g/cm^3
S10 – T_f=1027K /T_m=579K /C_B=1200 ppm/ρ(Xe,Sm)=0 /B_z^2 =0.0;
S11 – T_f=1027K /T_m=579K /C_B=0 /ρ(Xe,Sm)=0 /B_z^2 =critical;
S12 – T_f=300K /T_m=579K /C_B=0 /ρ(Xe,Sm)=0 /B_z^2 =critical;

This section contains materials of comparison of K_{eff}, reactivity effects, kinetic parameters and micro cross sections for the fresh fuel as well as K_{eff} and fuel nuclide content burnup dependence calculated by various codes. The corresponding Tables and Figures are given in Appendix A.

2.1.1 Separate states calculation for the variants with pre-defined isotopic composition

The results of K_{eff} and K_o calculation obtained by codes TVS-M, HELIOS, WIMS-ABBN and MCU-RFFI/A for pin cells with pre-defined nuclide composition are listed in Table A- 1 and Table A- 3. Comparison results are presented in the form of deviations from TVS-M values (in %). They are given in Table A- 2 and Table A- 4 as well as in Fig. A- 1 and Fig. A- 2. Data of these Tables and Figures show that:

- in case of LEU pin cells all codes demonstrate a good agreement: scattering of K_{eff} values does not exceed 0.5-0.6%, WIMS-ABBN systematically giving lower value of K_{eff} for the fresh fuel in comparison with the others;
- for MOX pin cells the result scattering increases, but in most of the cases it is less than ~1%;
- HELIOS differs significantly from the others in case of MOX fuel with ^{239}Pu only;

- significant deviations (3-4%) between MCU,TVS-M and HELIOS, WIMS are observed in case of MOX fuel with ^{241}Pu only. In view of coincidence of MCU and TVS-M nuclear data the probable reason of discrepancies lies in differences of their nuclear data for ^{241}Pu;
- comparing of two spent fuel cells (with and without fission products) gives a reason to say that TVS-M code obviously overestimates somewhat fission products efficiency. It can lead to underestimating of multiplication factor at high burnups;
- maximum deviations are observed in case of pin cell with reactor grade Pu;
- two options of MCU code (*pointwise* and *multigroup*) give significantly different results in case of MOX fuel cells (TVS-M results are very close to results of MCU/*multigroup*).

On the whole in case of pin cells with specified nuclide composition the agreement between various codes based on various nuclear data can be considered as rather good. Codes with the same nuclear data (TVS-M and MCU-RFFI/A) agree better.

2.1.2 Reactivity effects

The multiplication factors for pin cell variants were used to compute reactivity effects of the fuel temperature (Doppler), boron concentration, poisoning (^{135}Xe and ^{149}Sm), total temperature (isothermal) and voiding. A comparison of the reactivity effects with respect to the TVS-M results for the zero burnup point are given in Table A- 5 and Table A- 6 as well as in Fig. A- 3 and Fig. A- 4. The results show generally good agreement with a few exceptions:

- TVS-M gives noticeably (by ~10%) higher values of the poisoning effect relative to the other codes;
- as it was noted above TVS-M overestimates somewhat (up to 6%) a fission products efficiency;
- in comparison with the other codes WIMS-ABBN significantly overestimates Doppler effect for fresh LEU and MOX cells and total temperature effect in case of MOX pin cells.

2.1.3 Micro cross-sections comparison

To clarify possible reasons of discrepancy of the results obtained by different codes the benchmark specification calls for computation of one group microscopic cross-sections of the main nuclides. These cross-sections are averaged over fuel volume and correspond to the working state S1.

In Table A- 7 the cross-sections computed with TVS-M, HELIOS, WIMS-ABBN and MCU-RFFI/A codes for the zero burnup point are presented. Table A- 8 contains the comparison results in terms of deviations from TVS-M. Generally good agreement is observed but nevertheless it should be noted that:

- there is a systematic difference of about 3-3.5% between TVS-M, MCU-RFFI/A and others in ($\nu\sigma_f/\sigma_a$) for ^{241}Pu, which probably explains a large deviation in K_{eff} value mentioned above for Variant 9 (MOX fuel with ^{241}Pu only);
- these codes (TVS-M, MCU) slightly underestimate multiplicative properties (α) of ^{239}Pu in comparison with the others;

- TVS-M code systematically overestimates σ_a for ^{135}Xe and ^{149}Sm by 5-10%, which corresponds to the overestimation of poisoning effect mentioned above. It should be noted that the discrepancy is more in case of MOX cells;
- TVS-M underestimates ^{240}Pu absorption by ~7-10%. It can noticeably affect the K_{eff} burnup dependence if a large amount of ^{240}Pu in fuel (reactor grade Pu, Variant 10)
- HELIOS undervalues σ_a for ^{238}U by 1.5-1.8% relative to TVS-M and MCU-RFFI/A and by 3.4-3.7% in comparison with WIMS-ABBN (for fresh fuel cells);
- WIMS-ABBN differs from TVS-M in σ_a for ^{236}U by ~15% and in the most of cases overestimates σ_a for ^{238}U by 1.5-2%. It possibly can result in discrepancies in K_{eff} burnup dependence predicted by these codes;
- deviation in σ_a for ^{238}U given by WIMS-ABBN is different for fresh fuel cells (except for V9) and spent fuel cells. It corresponds to the discrepancy character observed for Doppler effect. It is difficult to find a reasonable cause of the fact.

2.1.4 Kinetics parameters

For variants 15-18 kinetic parameters were also calculated. For computing of effective fraction of delayed neutrons and prompt neutrons lifetime different codes use different approaches. In MCU-RFFI/A β_{eff} is defined as follows:

$\beta_{eff} = (K_{eff} - K_{prompt})/K_{eff}$, where K_{prompt} is a multiplication factor with only prompt neutrons taking into account.

In TVS-M and WIMS-ABBN codes β_{eff} and ℓ were calculated with the use of neutron value function. TRIANG used the so-called "direct" method [19].

The effective delayed neutron fractions are presented in Table A- 11, β_{eff}/β values – in Table A- 12, and the prompt neutron lifetimes are given in Table A- 13.

As it is seen from Table A- 11 values of β_{eff} obtained with different codes are close and maximum deviation does not exceed 5%. The β_{eff}/β values given in Table A- 12 have better agreement than β_{eff}, because β_{eff}/β characterizes the computer code algorithms quality, while β_{eff} also depends on the cross section libraries used in a code. Prompt neutron lifetime values also agree very well, discrepancies being less than 5%.

2.1.5 Burnup calculations

Burnup calculations were performed for pin cell variants 1,2 and 10. A comparison of *K_{eff} and K_o burnup dependence* is presented in Fig. A- 5, 6 and 7 respectively in the form of deviation from TVS-M values. It is seen from these Figures that:

- in case of LEU pin cell (V1) all codes demonstrate a good agreement and all K_{eff} discrepancies find out to be within ±0.6% for the whole depletion interval. However, TVS-M code shows a slight tendency to underestimate K_{eff} at high burnups in comparison with other codes, especially with WIMS-ABBN, which gives a minimum rate of K_{eff} decreasing. This fact can be explained by several reasons mentioned above such as: a greater value of fission product efficiency (see Table A- 6), a large overestimation of σ_a (^{236}U) relative to WIMS-ABBN and so on. It should be noted that using of updated data on ^{238}U resonance parameters (from LIPAR-5 as in MCU-REA code) results in a better agreement with the others in K_{eff} depletion trend.
- for MOX pin cell with weapon grade Pu (V2) discrepancies in K_{eff} values are somewhat increased and exceed 1% at high burnups. It is seen that the tendency of TVS-M code

to overstate an inclination of K_{eff} (W) curve relative to HELIOS and WIMS-ABBN became more pronounced. Agreement with MCU-REA results is better (especially when TVS-M use ^{238}U data from LIPAR-5). Possible reasons of observed disagreements can be an underestimation of both ^{240}Pu absorption and $\nu\sigma_f/\sigma_a$ value of ^{241}Pu mentioned above for TVS-M code.

- for MOX pin cell with reactor grade Pu (V10), which is remarkable for higher ^{240}Pu and ^{241}Pu content, discrepancies in K_{eff} become even greater and exceed 2% by 60 MWd/kgHM. HELIOS and WIMS-ABBN codes show similar trends in K_{eff} but noticeably differ in K_{eff} itself. In case of TVS-M the reasons of observed disagreements are probably the same as for V2 variant.

Comparisons of burnup dependence of main *nuclide concentrations* are presented in Fig. A- 8 - Fig. A- 19. As before they are given in the form of deviation (%) from TVS-M code. On the base of this comparison generally showing a satisfactory agreement one can say that:

- codes based on the same nuclear data (TVS-M and MCU-REA) show rather close results for the most of main nuclides. In case of codes using nuclear data libraries of different origin the discrepancies in concentrations are somewhat larger;
- data on ^{235}U for LEU fuel cell agree very well, the maximum deviation is about 1% at 60 MWd/kgHM and is observed for WIMS-ABBN and TVS-M (with LIPAR-5 data for ^{238}U). The noted deviation is most likely a result of these codes overestimate ^{238}U capture in comparison with the others, which leads to increasing of ^{239}Pu generation and so to increasing of contribution of ^{239}Pu fission into burnup. In case of MOX cells a discrepancy in ^{235}U concentration increases but it is not practically important because of its small value.
- codes TVS-M and MCU-REA demonstrate a good agreement in ^{236}U concentration whereas the other codes give somewhat higher value of this isotope content. Data on microscopic cross-section comparison indicate that in case of WIMS-ABBN possible reason of observed discrepancy is underestimation of σ_a (^{236}U) and for HELIOS the likely cause is understating of $\nu\sigma_f/\sigma_a$ value.
- all the codes show a good agreement in ^{238}U concentration, only HELIOS slightly overestimates its concentration.
- TVS-M systematically shows a significant overestimation of ^{238}Pu concentration. It should be noted that is practically negligible in reactivity balance.
- all the codes but the HELIOS give very close results in ^{239}Pu concentration, the discrepancies do not exceed 3%. As for HELIOS, the observed underestimation of ^{238}U capture obviously results in a remarkable (up to 4-6%) undervaluing of ^{239}Pu concentration.
- in comparison with the other codes TVS-M gives noticeably higher (up to ~10%) values of ^{240}Pu concentration, which is explained by the noted earlier underestimation of absorption cross-section of this isotope. An additional difference between HELIOS and TVS-M in precursor (^{239}Pu) concentration leads to the fact that the discrepancy between these two codes is the largest.
- previously noted difference in ^{240}Pu concentration between TVS-M and other codes can be one of the reasons responsible for discrepancies in ^{241}Pu concentration, which are about 2-6% at the end of burnup.

- TVS-M code gives 5-6% lower value of ^{242}Pu in comparison with MCU-REA and 10-15% higher value relative to WIMS-ABBN and HELIOS.
- TVS-M significantly overestimates concentrations of ^{135}Xe and ^{149}Sm in comparison with WIMS-ABBN and HELIOS (by 5-7% for ^{135}Xe and 15-18% for ^{149}Sm). Relative to MCU-REA results the difference is lower by 1.5-2 times.

In addition to the computation of various *reactivity effects* carried out for fresh fuel cells the calculation of these effects in several burnup points was performed for V1 and V2 variants. Unfortunately, burnup calculations with MCU-REA code were performed for a working state S1 only. So reactivity effects calculated by this code are unavailable. Results of these calculations are given in Table A- 9 and Table A- 10. It is seen that:

- the maximum deviation from TVS-M result (about 13.5%) in *Doppler effect* is observed for MOX fuel cell at zero burnup. With a burnup increase the difference between TVS-M and HELIOS increases steadily from 1.3% up to ~6% in case of UO_2 cell and from ~4% up to 8% for the MOX cell. WIMS-ABBN–TVS-M difference has an opposite burnup trend: it decreases from 10.5% to –2.9% for UO_2 cell and from 13.7% to –2% for MOX cell. In a view of a small value of this effect the agreement can be considered as good.
- all codes demonstrate rather good agreement in *boron effect* calculation for all burnup points. Differences do not exceed 2.5-3.5% in case of LEU cell and 5-6% in case of MOX cell, TVS-M giving as a rule lower value of the effect.
- the determination of *poisoning effect* for the fresh fuel cells differs from the one for non-zero burnup points: at zero burnup point concentration of ^{135}Xe and ^{149}Sm are fixed and the same for all codes, whereas in case of spent fuel cells each code calculates equilibrium concentrations of these fission products. And we observe different deviation from TVS-M values: when ^{135}Xe, ^{149}Sm concentrations are fixed the code overestimates poisoning effect relative to the others (up to 10%) and vice versa systematically underestimates this effect when the equilibrium concentrations are computed[1].
- codes TVS-M and WIMS-ABBN give very close results when calculating a *total temperature effect* for LEU fuel cell (V1). Results lie within 2.5% interval for all burnup points. Agreement of HELIOS results with the others is somewhat worse, the deviation increases with burnup increase and runs up to ~11% (HELIOS gives a lower value). In case of MOX fuel cell (V2) all results are within ±10% interval: at zero burnup point WIMS-ABBN and HELIOS overestimate a total temperature effect value relative to TVS-M, this overestimation decreases with burnup increase and in case of HELIOS turns into an underestimation.

2.2 COMPARISON OF SINGLE ASSEMBLY RESULTS

The single assembly is a geometry type of the most interest from the practical point of view because just assembly characteristics are used in core calculations. When you know the

[1] It should be noted that TVS-M considers separately ^{149}Sm appearing just after fission (via ^{149}Pm) and ^{149}Sm emerging fission product chain with mass number A=147. In other words some amount of ^{149}Sm (up to 12-15% at high burnups) is in the fuel even for non-poisoned states. This can partially explain the fact that TVS-M systematically underestimates a poisoning effect at the end of burnup.

single assembly calculation uncertainty you can separate the cross-section component from the error of the whole core calculation.

The considered set of benchmarks contains two variants V11 and V12 corresponding to non-graded VVER-1000 fuel assemblies with UOX and WG-MOX fuel accordingly. Unfortunately, Monte Carlo code results (MCU-RFFI/A with DLC/MCUDAT-1.0 library) are available for zero burnup only.

The corresponding materials are given in Appendix B.

2.2.1 K_{eff} burnup dependence. Separate states

The benchmark specification called for depletion calculation of two VVER-1000 fuel assemblies (UOX and MOX) being in the working state S1. Additionally, for some burnup points calculation of several assembly states, including the state with absorber rods inserted, is required.

Figure B- 1 shows the result of comparison of K_{eff} burnup dependence obtained for the state S1 by various codes and given in the form of deviation from TVS-M. The results are close to the ones for the pin cell cases and show that:

- TVS-M and HELIOS agree very well in case of uranium assembly (variant V11), difference does not exceed 0.5% and the trends in K_{eff} are almost the same. WIMS-ABBN noticeably underestimates K_{eff} at the beginning of burnup (~1% relatively to HELIOS) and gives somewhat different inclination of K_{eff} curve in comparison with the others.
- in case of MOX fuel assembly (variant V12) all the codes demonstrate large scattering of the results both in K_{eff} values (from –1% at 0 MWd/kgHM to +1.5% at 60 MWd/kgHM) and K_{eff} trends (TVS-M gives maximum inclination of the curve, WIMS-ABBN – the minimum one)
- discrepancies between TVS-M and WIMS-ABBN are somewhat increased relative to the pin cell cases.

Results of separate state calculation obtained for several burnup points as well as corresponding comparison results are given in Table B- 1÷Table B- 3. It is seen that maximum differences are observed at high burnups and for some states they run up to ~1.5% in case of uranium assembly and up to ~2.5% in case of MOX one.

2.2.2 Reactivity effects

The multiplication factors for fuel assembly variants were used to compute various reactivity effects including a control rod worth. Corresponding results obtained with TVS-M, HELIOS and WIMS-ABBN are presented in Table B- 5 and Table B- 6 and show that:

- all the codes demonstrate a very good agreement when computing *a control rod worth;*
- differences between TVS-M and HELIOS in *Doppler effect* value are almost the same as observed in case of pin cell variants. As for WIMS-ABBN, the deviations observed for the pin cells have been increased by 1.5-2 times and come to ~20%;
- discrepancies in *boron effect* value are very similar to the ones observed in case of pin cell variants. Only deviations of WIMS-ABBN results from the others are somewhat increased and come to –6-7% at high burnups.
- as in case of pin cell variants TVS-M code noticeably differs from the others in the value of *poisoning effect*: the code overestimates (by 5-9%) this effect at zero burnup point, when ^{135}Xe and ^{149}Sm concentrations are pre-defined, and underestimates its

value when corresponding concentrations are equilibrium, underestimation increasing with burnup and reaching 10-12%.

- greater (in comparison with pin cell) amount of water containing boric acid results in a smaller value of *total temperature effect* having a tendency to decrease with burnup. At high burnups it tends to zero and can even reverse sign, so the relative differences can reach significant values and we should probably pay main attention to the absolute values. Table B- 5 and Table B- 6 show generally good agreement between codes in a total temperature effect with the only exception of WIMS-ABBN, which systematically gives greater absolute values of the effect.

2.2.3 Pin power distribution

The results of detailed comparison of pin-by-pin power distributions computed by various codes are shown in Figure B- 1÷Figure B- 17. Codes used in calculations are: TVS-M, MCU-RFFI/A (only for zero burnup point), HELIOS and TRIANG code. Comparison results are presented in the form of deviations relative to TVS-M[1] and correspond to four burnup points (0, 10, 30 and 60 MWd/kgHM) and to the states S1 and S2. Calculations carried out with TRIANG code are available only for S1 state. The figures make it possible to conclude that:

- in the absence of control rods all the codes demonstrate a very good agreement, differences lie within ±2% interval for all burnup points. The only exception is TRIANG results, whose difference from the others increases with burnup and run up to 7-9%. The reason is the insufficiently correct technique of deriving of fuel rod macroscopic cross-section versus burnup. The agreement between the program TRIANG and others was essentially improved after the refinement of this technique (see results of pin power distribution calculation V13 and V14, Fig. C- 2, Fig. C- 3, Fig. C- 5, Fig. C- 6, Fig. C- 9). It should be noted that scattering of the results is slightly greater for MOX assembly than for LEU one.
- when control rods are inserted discrepancies in a local pin power somewhat increase, but, nevertheless, agreement remains good especially between MCU-RFFI/A and transport code HELIOS. Maximum differences are less than 5% for all burnup points and are located mainly near absorber rods and in the corner cells.

In general it is possible to conclude that all the codes, including the ones using diffusion approach, show a good agreement in pin power distribution in the absence of strong absorber. When the assembly contains absorber rods, deviation of diffusion results from the others somewhat increases.

2.3 COMPARISON OF THE RESULTS ON MULTI-ASSEMBLY SYSTEMS

Multi-assembly geometries (variants labelled V13, V14, V19 and V20) are of interest because they give information about accuracy of neutron flux distribution calculation near the boundary between MOX and LEU. In this analysis, a uniform MOX bundle and a graded MOX bundle surrounded by both fresh and spent UO_2 assemblies are studied. Codes used in these studies are the following: MCU-RFFI/A, CONKEMO, TVS-M, HELIOS and WIMS-ABBN/TRIANG.

[1] To be more precise, it is a deviation of TVS-M from the other code, calculated by the formula: δ=100*(value(TVS-M)-value(code))

2.3.1 K_{eff} burnup dependence

The benchmark specification calls for burnup computations in case of variants V13 and V14 only. Calculation results given in the form of deviations from TVS-M are presented in Fig. C- 1. It is seen from the Figure that:

- all the codes demonstrate approximately the same agreement as in case of single assembly geometry: maximum deviation does not exceed 1.5%.
- results obtained with precision code CONKEMO and WIMS-ABBN/TRIANG complex practically coincide for variant V13. In case of V14 variants the codes differ somewhat larger and the difference runs up to ~1% by the end of burnup.
- contrary to the single assembly case TVS-M code gives a lower average inclination of the K_{eff}(W) curve relative to HELIOS. It is rather difficult to explain this fact reasonably. Preliminary HELIOS results given in [20] agree better with TVS-M.
- for the whole burnup range with the only exception of initial interval from 0 to 10 MWd/kgHM the deviation of TVS-M results from the ones of WIMS-ABBN/TRIANG is of the same shape as in case of more simple geometries (see Fig. A- 5,Fig. A- 6 and Figure B- 1).

2.3.2 Separate state calculations. Reactivity effects

Unlike variants V13 and V14 requiring calculations for the working state S1 only, computing of several states is needed in case of variants V19 and V20. This allows to calculate some reactivity effects such as: Doppler, boron effect and effect of voiding. It should be noted that the range of variation of corresponding parameters is increased in comparison with V1-V10 and V11-V12 variants[1]. Calculation results as well as results of comparison are given in Table C- 1 and Table C- 2. They make it possible to conclude that:

- a good agreement is observed between TVS-M and MCU-RFFI/A codes, TVS-M being especially close to the multigroup version of MCU.
- HELIOS systematically overestimates K_{eff} values in comparison with TVS-M and MCU-RFFI/A. Maximum deviation (about 1.2-1.3%) is observed between MCU-RFFI/A and HELIOS in case of V20 variant.
- WIMS-ABBN/TRIANG code system noticeably underestimates K_{eff} value for the most of states. Maximum deviation (about 1.5%) is observed between WIMS-ABBN and HELIOS.
- for the state with extremely low water density WIMS-ABBN/TRIANG significantly (more than 3.5%) overestimates K_{eff} value in comparison with the others.
- the last fact is the reason of ~15% discrepancy in voiding effect value which is observed between WIMS-ABBN/TRIANG and the others. As for the rest all codes demonstrate a satisfactory agreement in calculation of reactivity effects.

2.3.3 Kinetics parameters

For variants V19-20 kinetic parameters were also calculated. The effective delayed neutron fractions are presented in Table C- 3 and β_{eff}/β values are given in Table C- 4. The values agree rather well across all of considered states.

[1] In case of V15-V18 pin cell variants the range of parameter variations was the same.

2.3.4 Pin power distribution

When comparing pin-by-pin distributions it should be remembered that some of codes compute a fission rate distribution instead of pin power one. It is of no importance when the system contains fuel pins of single type (only UO_2 or only MOX). But in the case that a system consists of regions characterized by different values of released fission energy, pin power and fission rate distributions can noticeably differ from each other especially near the boundary between regions with different properties. So, in the presented report pin power and fission rate distributions are compared separately.

The results of detailed comparison of pin power distribution calculated with the use of TVS-M, CONKEMO and TRIANG codes are shown in Fig. C- 2÷Fig. C- 9. Comparison results are presented in the form of deviations relative to TVS-M[1]. In general the codes agree satisfactory, however, it should be noted that:

- TVS-M code systematically overestimates pin powers (up to 3-4%) in the central part where MOX fuel pins are located. For the most of UO_2 pins a discrepancy does not exceed 2%, TVS-M giving lower values.
- as a rule discrepancies have a tendency to decrease with burnup. The only exception is variant V14: the maximum deviations are observed at 30 MWd/kgHM in the corner UO_2 pins at the boundary between MOX and UO_2 regions.
- for the most of cases fuel pins situated near the water gap are not the pins of maximum discrepancies.

The results of fission rate distribution comparison obtained with TVS-M, MCU-RFFI/A (initial burnup point only) and HELIOS codes are given in Fig. C- 10÷Fig. C- 17. Generally the codes are in satisfactory agreement - for the most of pins deviations do not exceed 2%. However, it should be mentioned that:

- TVS-M systematically underestimates a fission rate in boundary pins (both MOX and UO_2) relative to MCU-RFFI/A code, maximum discrepancy reaching ~7%.
- HELIOS systematically overvalues fission rate in the MOX pins located in the central region, especially in comparison with MCU-RFFI/A results. In addition to that HELIOS, like TVS-M code, underestimates the increasing of fission rate in the pins located near the water gap.

3. CONCLUSION

Variants of pin cell, assembly and multi-assembly VVER-1000 structures have been computed with several different codes used in the U.S. and Russia. The codes use both different methods and different nuclear data. A comparison of the results shows rather good agreement among the various codes. Significant discrepancies were noted in an extreme pin cell case, which contains only ^{241}Pu and are attributed to different nuclear data. The trends in K_{eff} versus burnup were slightly different for the MOX cases resulting in differences of over 1% at the end of burnup. Especially it concerns the TVS-M code, which has a tendency to underestimate somewhat a fuel cycle length. The single assembly and multi-assembly calculations generally show a good agreement both in K_{eff} and in pin power distribution.

---

[1] As in the case of a single assembly the deviations are calculated by the formula:
δ=100*(value(TVS-M)-value(code))

As it was mentioned above the verification of spectral codes is only a part of overall verification of the whole code package for VVERs calculations. And another parts of this package (codes for core coarse-mesh and fine-mesh calculation) need to be verified too. So the work along these lines should be continued and benchmarking efforts should be extended to the whole-core methods involving fuel cycle and kinetics calculations.

It is necessary to emphasize that a verification on the base of calculational benchmarks does not eliminate the necessity of comparing with the results obtained at MOX fuelled experimental facilities.

REFERENCES

1. A.N. Novikov et. al. Problems of VVER In-core Fuel Management, IAEA-TECDOC-567, In-core Fuel Management Practices, IAEA, Vienna,1990
2. Gomin E.A., Majorov L.V. The MCU-RFFI Monte Carlo Code for Reactor Design Applications. Proc. of Int. Conf. on Math. and Comp., Reac. Phys. and Envir. Analyses, April 30 -4 May 1995, Portlend, Oregon, USA
3. Neutronics Benchmarks for the Utilization of Mixed-Oxide Fuel: Joint US/Russian Progress Report for Fiscal Year 1997, Volume 3 – Calculations Performed in the Russian Federation, ORNL/TM-13603/V3, June 1998.
4. J.C. Gehin et al. Analysis of Weapons-Grade MOX VVER-1000 Benchmarks with HELIOS and KENO. ORNL/TM-1999/78, July 1999
5. Abagyan L., Alexeyev N., Bryzgalov V. et all. MCU-REA code with nuclear data library DLC/MCUDAT-2.1. Report of the Russian Research Center "Kurchatov Institute", N: 36/5-98, Moscow 1998. (in Russian)
6. Creation of computational benchmarks for LEU and MOX fuel assemblies under accident conditions. Calculate kinetic parameters, Doppler coefficient, and the effect of decreasing the water density: Joint US/Russian Report for Fiscal Year 1998
7. L.P.Abagyan et al. Group constants for calculation of the reactors and shields. M., Energoizdat, 1981.
8. Koppel J.U., Houston S.H. Reference for ENDF Thermal Neutron Scattering Data, GA-8774, 1978
9. ENDF-102. Data Formats and Procedures for the Evaluated Nuclear Data Files ENDF-6, July 1990, National Nuclear Data Center, Brookhaven National Laboratory, Upton, NewYork, 11973
10. I.E.Rubin. Method of probabilities of transmission in the one-dimensional cylindrical geometry. Izvestiya AN BSSR, ser. fiz-energ. nauk, № 2, p. 25-31, 1983.
11. V.M.Kolobashkin et al. Radiation characteristics of irradiated nuclear fuel M., Energoatomizdat, 1983.
12. V.D.Sidorenko. Homogenization of effective cross sections in the periodic lattice. Preprint IAE-2793, 1977.
13. Manturov G.N., Nikolaev M.N., Tsibulya A.M., "System of group constants ABBN-93. Verification report 1. Recommended reference data", Moscow 1995.
14. D.F. Hollenbach, L.M. Petrie, N.F. Landers. KENO-VI: A General Quadratic Version of the KENO Program. SCALE 4.3, Vol. 2.2, Section F17, 1995
15. O.W. Hermann, R.M. Westfall. ORIGEN-S: SCALE System Module to Calculate Fuel Depletion, Actinide Transmutation, Fission Product Bildup and Decay, and Assosiation Source Terms. SCALE 4.3, Vol.2, Section F7, 1995
16. Kochetkov A.L. The code CARE – calculation of isotopic kinetics, radiation and ecological behavior of nuclear fuel on irradiation and storage. IPPE, 1995 (in Russian).

17. Voronkov A.V. Codes for multi-dimensional calculations of nuclear reactors. In collected articles "Codes and methods of fast reactors neutronics calculation", Dimitrovgrad, 1974 (in Russian)

18. J. J. Casal, et al., HELIOS: Geometric Capabilities of a New Fuel-Assembly Program, Proceedings International Topical Meeting Advances in Mathematics, Computation, and Reactor Physics, American Nuclear Society, April 28-May 2, 1991, p. 10.21-1.

19. G. Toshinski, P.E. Bulavin. "About calculation of relative value of delayed neutrons", Atomnaya Energiya, 1967, V. 23, N 2, p. 146-147 (in Russian)

20. Z.N. Chizhikova, A.G. Kalashnikov, et al. Verification Calculation Results to Validate the Procedures and Codes for Pin-by-Pin Power Computation in VVER Type Reactors with MOX Fuel Loading. ORNL/SUB/98-85B99398V-3, 1998

APPENDIX A. PIN CELL RESULTS

Table A- 1 K_{eff} and K_o values for pin cells with pre-defined isotopic content(variants V1-V9).

State	TVS-M		HELIOS		WIMS-ABBN		MCU-RFFI/A	
	keff	k0	keff	k0	keff	k0	keff	k0
	V1 (fresh LEU fuel)							
s1	1.0617	1.2658	1.0648	1.2703	1.0572	1.2614	1.0639	1.2690
s3	1.1073	1.3212	1.1110	1.3259	1.1024	1.3167	-	-
s4	1.1028	1.3152	1.1039	1.3172	1.0962	1.3091	1.1033	1.3150
s5	1.1159	1.3316	1.1173	1.3339	1.1109	1.3271	1.1161	1.3320
s6	1.2200	1.3717	1.2207	1.3727	1.2160	1.3671	1.2187	1.3700
	V2 (fresh MOX fuel)							
s1	1.0233	1.2146	1.0227	1.2166	1.0149	1.2004	1.0200	1.2100
s3	1.0477	1.2443	1.0469	1.2455	1.0385	1.2290	-	-
s4	1.0412	1.2360	1.0389	1.2358	1.0310	1.2197	1.0368	1.2290
s5	1.0569	1.2552	1.0551	1.2558	1.0483	1.2410	1.0498	1.2480
s6	1.1818	1.3258	1.1832	1.3292	1.1779	1.3171	1.1786	1.3210
	V3 (spent LEU fuel without F.P.)							
s1	0.9127	1.0904	0.9128	1.0915	0.9136	1.0901	-	-
s3	0.9502	1.1360	0.9500	1.1364	0.9506	1.1354	-	-
s4	0.9477	1.1325	0.9453	1.1305	0.9465	1.1303	-	-
s5	0.9621	1.1504	0.9604	1.1492	0.9615	1.1489	-	-
s6	1.0610	1.1950	1.0603	1.1946	1.0619	1.1951	1.0574	-
	V4 (spent LEU fuel with F.P.)							
s1	0.8569	1.0226	0.8602	1.0269	0.8598	1.0236	-	-
s3	0.8905	1.0634	0.8936	1.0672	0.8931	1.0643	0.8915	-
s4	0.8879	1.0598	0.8890	1.0615	0.8890	1.0593	0.8883	-
s5	0.9010	1.0760	0.9029	1.0787	0.9025	1.0760	0.9002	-
s6	0.9982	1.1235	1.0005	1.1262	1.0007	1.1245	0.9984	-
	V7 (fresh MOX fuel with ^{239}Pu only)							
s1	1.0965	1.3030	1.1046	1.3156	1.0967	1.2992	-	-
s3	1.1240	1.3364	1.1321	1.3487	1.1237	1.3318	-	-
s4	1.1166	1.3270	1.1229	1.3376	1.1151	1.3213	-	-
s5	1.1303	1.3440	1.1369	1.3550	1.1303	1.3401	-	-
s6	1.2509	1.4042	1.2595	1.4160	1.2542	1.4036	1.2501	1.4030
	V8 (fresh MOX fuel with ^{240}Pu only)							
s1	0.9281	1.1049	0.9240	1.1005	0.9160	1.0915	-	-
s3	0.9731	1.1594	0.9690	1.1547	0.9599	1.1453	-	-
s4	0.9711	1.1564	0.9646	1.1492	0.9563	1.1408	-	-
s5	0.9856	1.1745	0.9800	1.1682	0.9728	1.1612	-	-
s6	1.0881	1.2225	1.0831	1.2167	1.0780	1.2112	1.0828	1.2160
	V9 (fresh MOX fuel with ^{241}Pu only)							
s1	1.2797	1.5193	1.3228	1.5676	1.3247	1.5697	-	-
s3	1.3096	1.5557	1.3543	1.6052	1.3552	1.6098	-	-
s4	1.3001	1.5437	1.3425	1.5911	1.3443	1.5934	-	-
s5	1.3167	1.5642	1.3593	1.6117	1.3611	1.6140	-	-
s6	1.4337	1.6086	1.4713	1.6484	1.4747	1.6501	1.4372	-

Table A- 2 Deviations from TVS-M in K_{eff} and K_o values for pin cells with pre-defined isotopic content (variants V1-V9).

State	HELIOS		WIMS-ABBN		MCU-RFFI/A	
	Keff	k0	keff	k0	keff	k0
	V1 (fresh LEU fuel)					
s1	0.29	0.36	-0.42	-0.35	0.21	0.25
s3	0.33	0.35	-0.44	-0.34	-	-
s4	0.10	0.16	-0.60	-0.46	0.05	-0.01
s5	0.12	0.17	-0.46	-0.33	0.02	0.03
s6	0.06	0.07	-0.33	-0.33	-0.11	-0.12
	V2 (fresh MOX fuel)					
s1	-0.06	0.16	-0.83	-1.17	-0.33	-0.38
s3	-0.08	0.10	-0.88	-1.23	-	-
s4	-0.22	-0.01	-0.98	-1.32	-0.43	-0.56
s5	-0.17	0.05	-0.81	-1.13	-0.67	-0.57
s6	0.12	0.25	-0.34	-0.66	-0.27	-0.36
	V3 (spent LEU fuel without F.P.)					
s1	0.01	0.10	0.10	-0.03	-	-
s3	-0.02	0.03	0.05	-0.06	-	-
s4	-0.25	-0.17	-0.13	-0.19	-	-
s5	-0.17	-0.10	-0.06	-0.12	-	-
s6	-0.07	-0.03	0.09	0.01	-0.34	-
	V4 (spent LEU fuel with F.P.)					
s1	0.38	0.42	0.34	0.10	-	-
s3	0.35	0.36	0.30	0.09	0.12	-
s4	0.13	0.17	0.13	-0.05	0.05	-
s5	0.22	0.25	0.17	0.00	-0.09	-
s6	0.23	0.24	0.25	0.09	0.02	-
	V7 (fresh MOX fuel with ^{239}Pu only)					
s1	0.74	0.97	0.02	-0.29	-	-
s3	0.72	0.92	-0.03	-0.34	-	-
s4	0.56	0.80	-0.14	-0.43	-	-
s5	0.58	0.82	-0.01	-0.29	-	-
s6	0.69	0.84	0.27	-0.04	-0.06	-0.08
	V8 (fresh MOX fuel with ^{240}Pu only)					
s1	-0.44	-0.39	-1.30	-1.21	-	-
s3	-0.42	-0.40	-1.35	-1.22	-	-
s4	-0.67	-0.63	-1.52	-1.35	-	-
s5	-0.57	-0.53	-1.29	-1.13	-	-
s6	-0.46	-0.47	-0.93	-0.92	-0.49	-0.53
	V9 (fresh MOX fuel with ^{241}Pu only)					
s1	3.37	3.18	3.52	3.32	-	-
s3	3.41	3.18	3.48	3.47	-	-
s4	3.26	3.07	3.40	3.22	-	-
s5	3.24	3.04	3.37	3.18	-	-
s6	2.62	2.47	2.85	2.58	0.24	-

Fig. A- 1 Deviations from TVS-M in K_{eff} for pin cell variants V1-V4

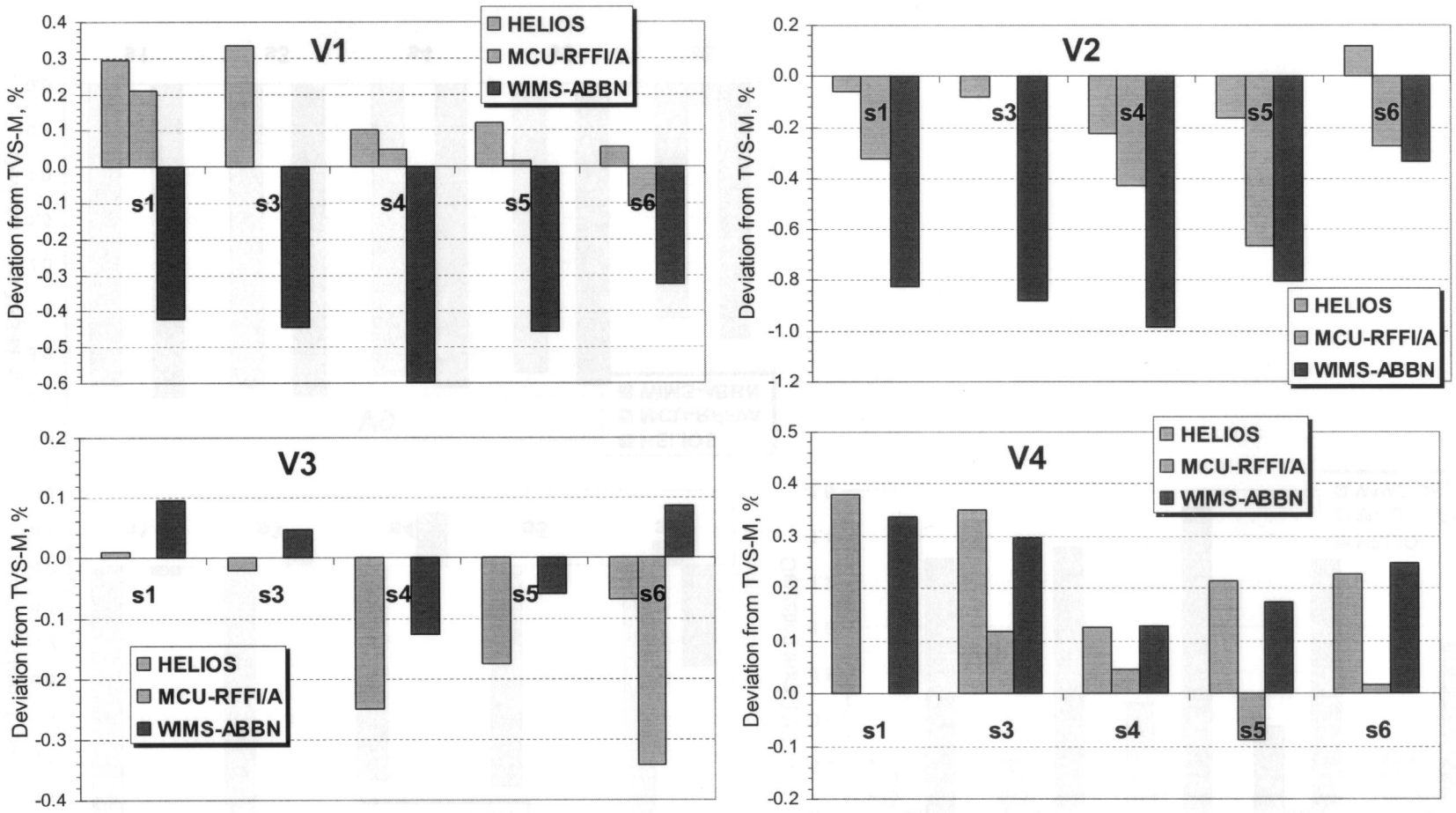

Fig. A- 2 Deviations from TVS-M in K_{eff} for pin cell variants V7-V9

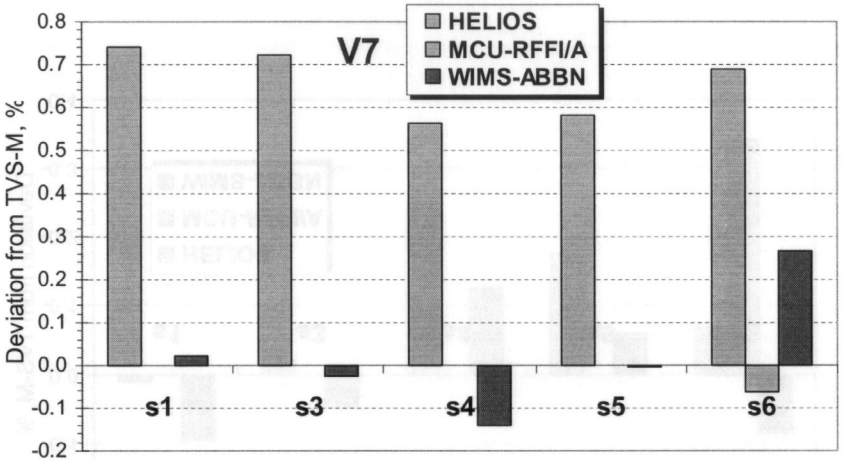

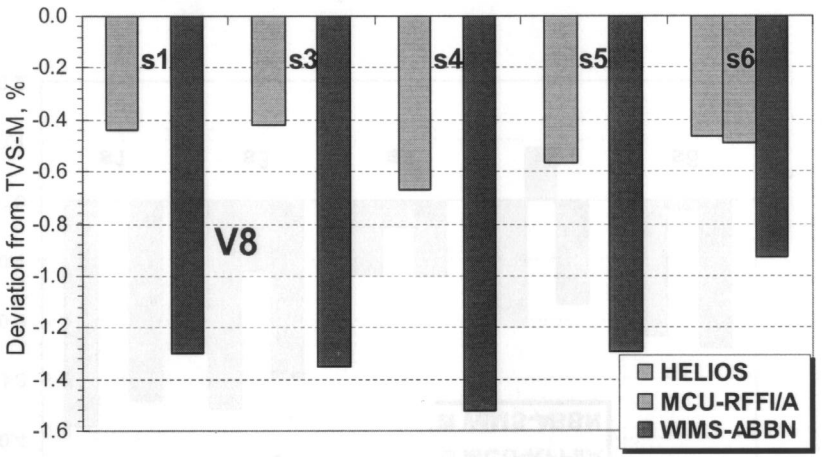

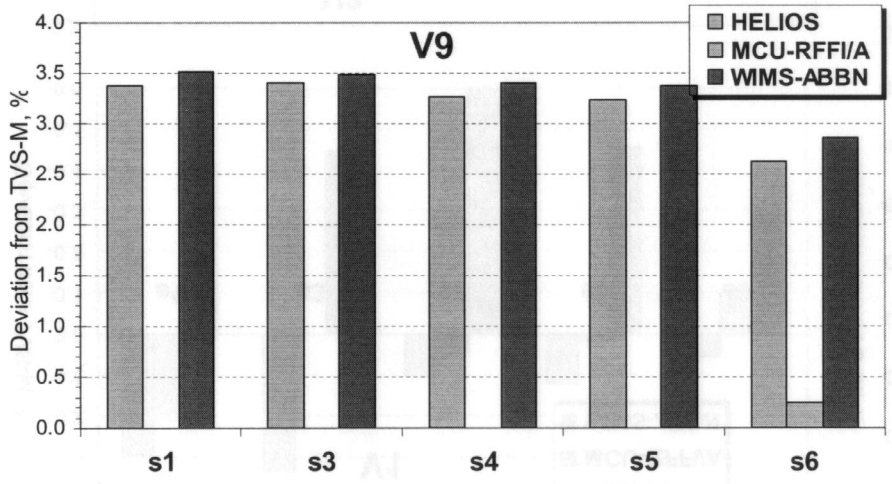

Table A- 3 K_{eff} and K_o values for pin cells with pre-defined isotopic content (variants V15-V18).

State	MCU-RFFI/A		TVS-M	TVS-M	WIMS-ABBN	HELIOS
	Pointwise	Multigroup	U8 - LIPAR-5	U8 - LIPAR-3		
	V15, fresh LEU					
S7	1.3809	1.3805	1.3789	1.3820	1.3745	1.3846
S8	1.3543	1.3547	1.3517	1.3545	1.3448	1.3561
S9	1.0742	1.0729	1.0699	1.0743	1.0634	1.0748
S10	1.2644	1.2633	1.2613	1.2642	1.2581	1.2669
S11	-	-	1.3682	1.3712	1.3631	1.3727
S12	-	-	1.4547	1.4575	1.4518	1.4578
	V16, spent LEU					
S7	1.1032	1.1093	1.1058	1.1083	1.1068	1.1107
S8	-	-	1.0792	1.0816	1.0788	1.0818
S9	-	-	0.7990	0.8024	0.7956	0.8081
S10	1.0173	1.0218	1.0187	1.0213	1.0209	1.0250
S11	-	-	1.1038	1.1063	1.1044	1.1084
S12	-	-	1.1968	1.1992	1.1994	1.2026
	V17, fresh MOX					
S7	1.2610	1.2706	1.2665	1.2695	1.2544	1.2682
S8	1.2311	1.2384	1.2354	1.2382	1.2194	1.2341
S9	0.9700	0.9725	0.9687	0.9733	0.9563	0.9732
S10	1.2024	1.2108	1.2050	1.2084	1.1957	1.2085
S11	-	-	1.2632	1.2662	1.2507	1.2644
S12	-	-	1.3766	1.3795	1.3708	1.3818
	V18, spent MOX					
S7	1.0704	1.0808	1.0782	1.0808	1.0765	1.0809
S8	-	-	1.0497	1.0521	1.0468	1.0498
S9	-	-	0.7844	0.7880	0.7843	0.7911
S10	1.0071	1.0143	1.0119	1.0147	1.0124	1.0164
S11	-	-	1.0773	1.0799	1.0755	1.0798
S12	-	-	1.1718	1.1743	1.1738	1.1771

Table A- 4 Deviations from TVS-M in K_{eff} and K_o values for pin cells with pre-defined isotopic content (variants V15-V18).

State	MCU-RFFI/A		TVS-M	WIMS-ABBN/ TRIANG	HELIOS
	Pointwise	Multigroup	U8 - LIPAR-5		
	V15, fresh LEU				
S7	-0.08	-0.11	-0.22	-0.54	0.19
S8	-0.02	0.01	-0.21	-0.72	0.12
S9	-0.01	-0.13	-0.41	-1.02	0.04
S10	0.02	-0.07	-0.23	-0.48	0.21
S11	-	-	-0.22	-0.59	0.11
S12	-	-	-0.19	-0.39	0.02
	V16, spent LEU				
S7	-0.46	0.09	-0.23	-0.14	0.21
S8	-	-	-0.22	-0.26	0.02
S9	-	-	-0.42	-0.84	0.71
S10	-0.40	0.05	-0.26	-0.04	0.36
S11	-	-	-0.22	-0.17	0.19
S12	-	-	-0.20	0.02	0.29
	V17, fresh MOX				
S7	-0.67	0.09	-0.24	-1.19	-0.10
S8	-0.57	0.02	-0.23	-1.52	-0.33
S9	-0.34	-0.08	-0.47	-1.75	-0.01
S10	-0.49	0.20	-0.28	-1.05	0.01
S11	-	-	-0.24	-1.23	-0.14
S12	-	-	-0.21	-0.63	0.17
	V18, spent MOX				
S7	-0.96	0.00	-0.24	-0.40	0.01
S8	-	-	-0.23	-0.50	-0.22
S9	-	-	-0.46	-0.47	0.39
S10	-0.75	-0.04	-0.28	-0.23	0.16
S11	-	-	-0.24	-0.41	-0.01
S12	-	-	-0.21	-0.04	0.24

Table A- 5 Reactivity effects at zero burnup point.

Effect	Initial state	Final state	Effect value, $(K_i-K_j)/(K_i*K_j)$, %				Deviation from TVS-M		
			TVS-M	HELIOS	WIMS-ABBN	MCU-RFFI/A	HELIOS	WIMS-ABBN	MCU-RFFI/A
			Variant V1						
ppler effect, T_f : 579K→ 1027K	S5	S4	-0.94	-0.95	-1.04	-0.97	1.31	10.94	3.45
ron effect, C_B : 0.0 → 0.6 g/kg	S3	S1	-3.32	-3.30	-3.33	-	-0.44	0.47	-
isoning effect	S4	S1	-2.97	-2.80	-2.89	-2.76	-5.49	-2.65	-7.05
tal temperature effect, T_m : 300K → 579K	S6	S5	-2.20	-2.12	-2.20	-2.08	-3.53	0.29	-5.20
			Variant V2						
ppler effect, T_f : 579K→ 1027K	S5	S4	-1.24	-1.29	-1.41	-1.24	3.91	13.67	-0.12
ron effect, C_B : 0.0 → 0.6 g/kg	S3	S1	-1.96	-1.91	-1.94	-	-2.72	-1.03	-
isoning effect	S4	S1	-1.42	-1.28	-1.32	-1.28	-10.16	-7.30	-10.12
tal temperature effect, T_m : 300K → 579K	S6	S5	-4.24	-4.40	-4.65	-4.43	3.61	9.64	4.33
			Variant V3						
ppler effect, T_f : 579K→ 1027K	S5	S4	-1.37	-1.44	-1.44	-	4.76	4.52	-
ron effect, C_B : 0.0 → 0.6 g/kg	S3	S1	-3.68	-3.62	-3.66	-	-1.71	-0.60	-
isoning effect	S4	S1	-3.41	-3.16	-3.27	-	-7.21	-4.13	-
tal temperature effect, T_m : 300K → 579K	S6	S5	-3.24	-3.31	-3.36	-	1.95	3.67	-
			Variant V4						
ppler effect, T_f : 579K→ 1027K	S5	S4	-1.42	-1.50	-1.47	-	5.54	3.14	-
ron effect, C_B : 0.0 → 0.6 g/kg	S3	S1	-3.75	-3.68	-3.73	-	-1.92	-0.48	-
isoning effect	S4	S1	-3.43	-3.17	-3.29	-	-7.46	-4.19	-
tal temperature effect, T_m : 300K → 579K	S6	S5	-3.93	-3.91	-4.01	-	-0.47	2.07	-
			Variant V10						
ppler effect, T_f : 579K→ 1027K	S5	S4	-1.34	-1.46	-1.44	-	9.36	7.29	-
ron effect, C_B : 0.0 → 0.6 g/kg	S3	S1	-1.07	-1.06	-1.10	-	-1.52	2.36	-
isoning effect	S4	S1	-0.52	-0.46	-0.46	-	-10.53	-10.81	-
tal temperature effect, T_m : 300K → 579K	S6	S5	-4.87	-5.03	-5.26	-	3.46	8.17	-
			Variant V15						
ppler effect, T_f : 1027K→ 2000K	S7	S8	-1.47	-1.52	-1.61	-1.42	3.43	9.49	-3.07
ron effect, C_B : 0.0 → 1.2 g/kg	S7	S10	-6.74	-6.71	-6.73	-6.67	-0.48	-0.16	-1.03
iding effect, γ_m : 0.716 → 0.2 g/cm^3	S7	S9	-20.72	-20.82	-21.28	-20.68	0.46	2.71	-0.22
			Variant V16						
ppler effect, T_f : 1027K→ 2000K	S7	S8	-2.23	-2.41	-2.35	-	7.70	5.01	-
ron effect, C_B : 0.0 → 1.2 g/kg	S7	S10	-7.68	-7.53	-7.60	-7.65	-2.04	-1.07	-0.40
iding effect, γ_m : 0.716 → 0.2 g/cm^3	S7	S9	-34.40	-33.71	-35.34	-	-2.01	2.72	-
			Variant V17						
ppler effect, T_f : 1027K→ 2000K	S7	S8	-1.99	-2.18	-2.29	-1.93	9.39	14.88	-3.30
ron effect, C_B : 0.0 → 1.2 g/kg	S7	S10	-3.99	-3.90	-3.91	-3.86	-2.26	-1.80	-3.03
iding effect, γ_m : 0.716 → 0.2 g/cm^3	S7	S9	-23.97	-23.90	-24.85	-23.79	-0.29	3.66	-0.76
			Variant V18						
ppler effect, T_f : 1027K→ 2000K	S7	S8	-2.52	-2.74	-2.64	-	8.63	4.46	-
ron effect, C_B : 0.0 → 1.2 g/kg	S7	S10	-6.02	-5.87	-5.88	-5.87	-2.53	-2.35	-2.51
iding effect, γ_m : 0.716 → 0.2 g/cm^3	S7	S9	-34.37	-33.89	-34.61	-	-1.40	0.69	-

Fig. A- 3 Results of reactivity effects calculations for zero burnup point (variants V1-V12).

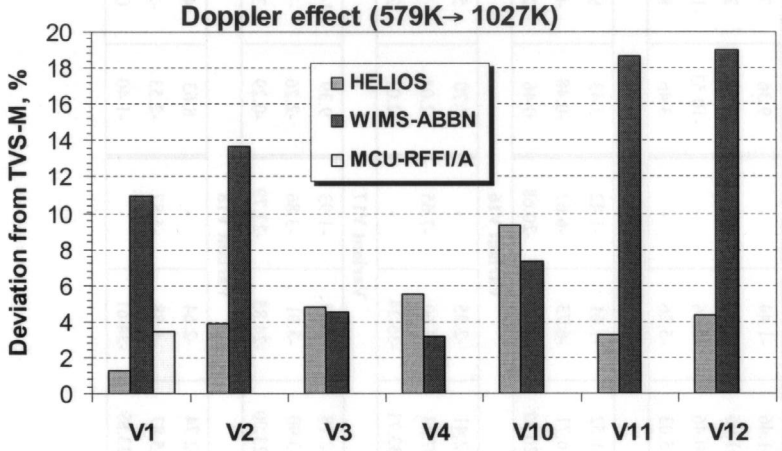

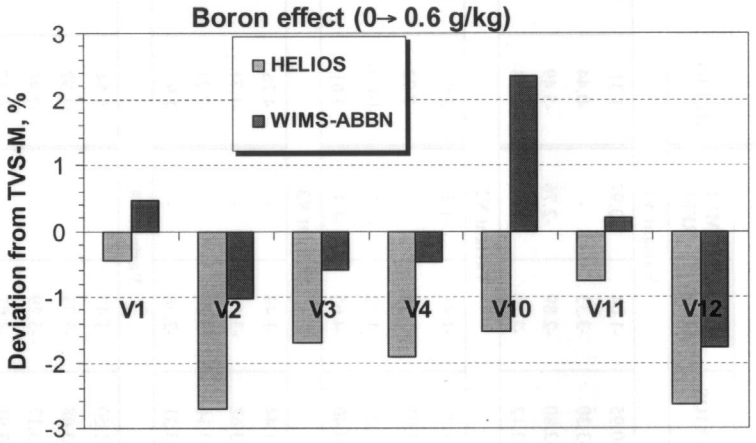

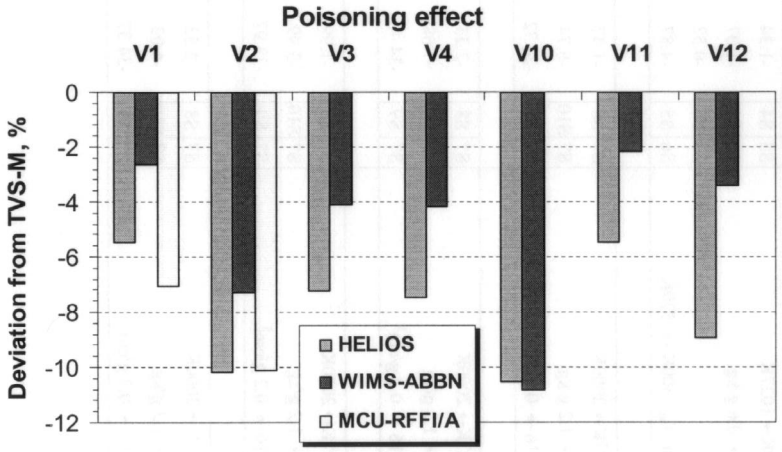

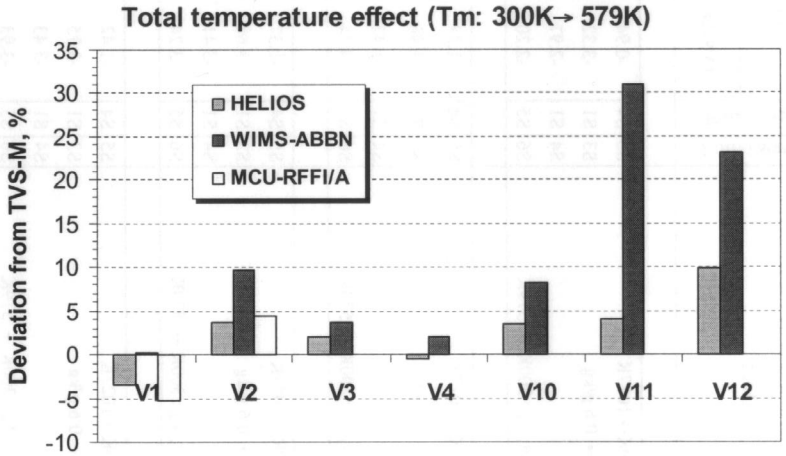

Fig. A- 4 Results of reactivity effects calculations for zero burnup point (variants V15-V18).

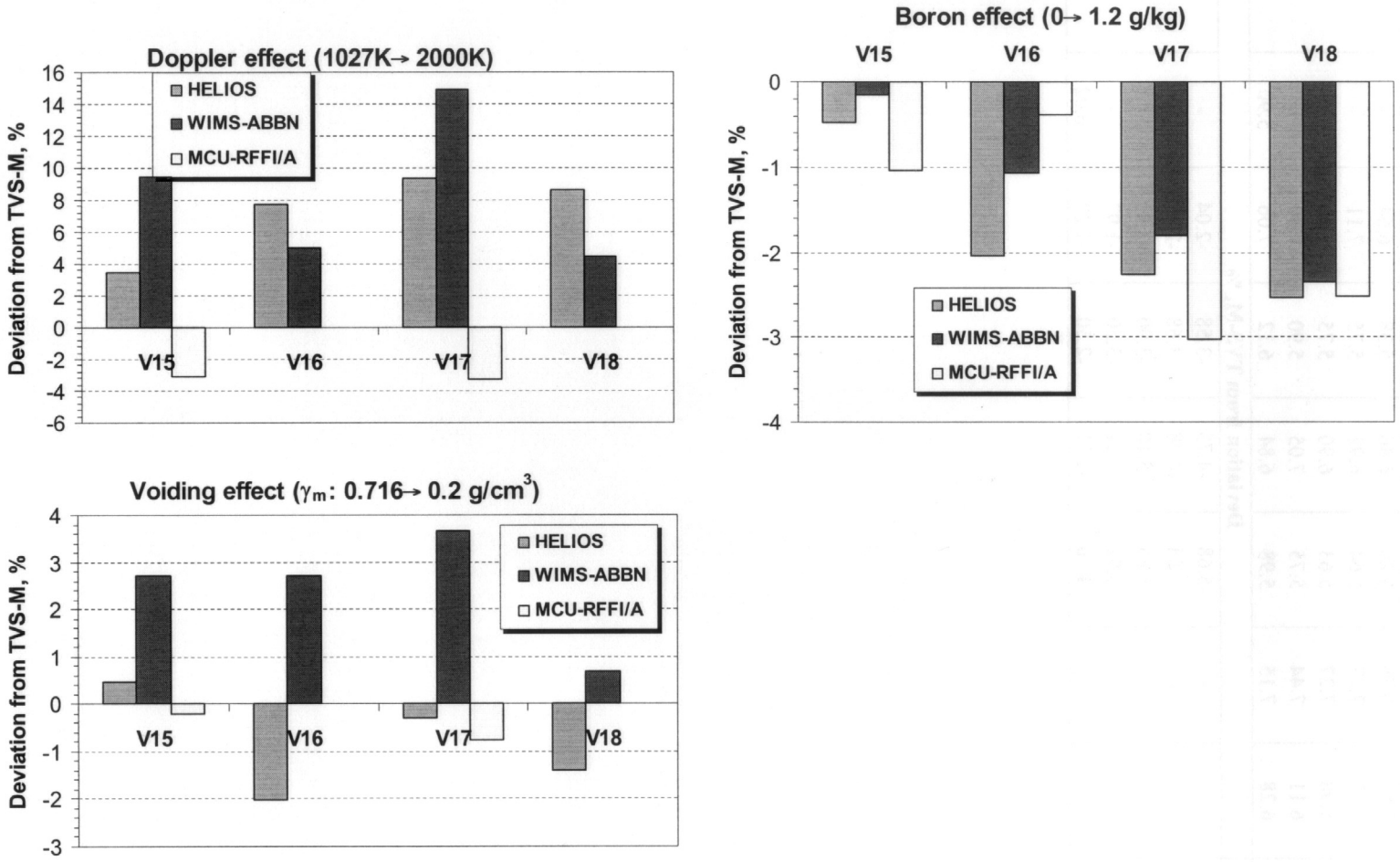

Table A- 6 Results of comparison of fission products efficiency

State	TVS-M		HELIOS		WIMS-ABBN		MCU-RFFI/A	
	Δkeff	Δk0	Δkeff	Δk0	Δkeff	Δk0	Δkeff	Δk0
	V3 -> V4							
s1	5.58	6.78	5.26	6.46	5.38	6.64	-	-
s3	5.97	7.27	5.64	6.92	5.75	7.11	-	-
s4	5.98	7.27	5.63	6.90	5.75	7.10	-	-
s5	6.11	7.44	5.75	7.05	5.90	7.30	-	-
s6	6.28	7.15	5.98	6.84	6.12	7.06	5.90	-
	Deviation from TVS-M, %							
s1	-	-	-5.68	-4.75	-3.58	-2.04	-	-
s3	-	-	-5.54	-4.78	-3.68	-2.18	-	-
s4	-	-	-5.85	-5.10	-3.90	-2.31	-	-
s5	-	-	-5.92	-5.22	-3.50	-1.92	-	-
s6	-	-	-4.76	-4.31	-2.50	-1.22	-6.02	-

Table A- 7 Results of micro cross-sections calculations for zero burnup point (barn).

State	TVS-M (U8-LIPAR-3)		HELIOS		WIMS-ABBN		MCU-RFFI/A	
	σ_a	$\nu\sigma_f$	σ_a	$\nu\sigma_f$	σ_a	$\nu\sigma_f$	σ_a	$\nu\sigma_f$
	V1 (fresh LEU fuel)							
^{235}U	42.420	83.910	42.920	84.54	42.622	84.46	42.596	84.223
^{238}U	0.9870	0.2875	0.9693	0.2813	1.0025	0.2811	0.9835	0.2874
^{135}Xe	150800	-	142880	-	145699	-	145572	-
^{149}Sm	4738.0	-	4526.0	-	4592.1	-	4476	-
	V2 (fresh MOX fuel)							
^{235}U	25.520	48.570	25.305	47.478	25.280	47.806	25.208	47.855
^{238}U	0.9656	0.3143	0.9465	0.3134	0.9822	0.3000	0.9642	0.3160
^{239}Pu	59.010	109.100	59.055	109.430	59.588	110.279	58.933	108.710
^{240}Pu	90.100	1.9890	99.968	1.9733	101.865	1.9083	96.896	2.0007
^{241}Pu	62.820	135.300	60.572	134.870	61.468	137.282	61.687	132.79
^{135}Xe	69810	-	62623	-	64246	-	64917	-
^{149}Sm	2204.0	-	2002.8	-	2046.8	-	2018.3	-
	V3 (spent LEU fuel without F.P.)							
^{235}U	39.760	78.230	39.524	77.228	39.711	78.120	-	-
^{236}U	7.1780	0.7559	6.9925	0.7713	6.0858	0.5611	-	-
^{238}U	1.0020	0.2968	0.9843	0.2929	1.0001	0.2861	-	-
^{238}Pu	25.440	6.6160	25.493	6.4580	25.366	7.0175	-	-
^{239}Pu	115.60	211.90	118.53	217.61	118.95	218.52	-	-
^{240}Pu	100.80	1.8970	111.17	1.8721	113.37	1.8271	-	-
^{241}Pu	111.30	238.50	109.10	240.92	110.78	245.05	-	-
^{242}Pu	27.630	1.2850	32.617	1.4253	29.845	1.3322	-	-
^{135}Xe	141300	-	130740	-	135198	-	-	-
^{149}Sm	4378.0	-	4088.2	-	4203.1	-	-	-
	V4 (spent LEU fuel with F.P.)							
^{235}U	37.620	73.880	37.571	73.201	37.663	73.943	-	-
^{236}U	6.9330	0.7554	6.7092	0.7699	5.8962	0.5670	-	-
^{238}U	0.9902	0.3002	0.9765	0.2961	0.9852	0.2890	-	-
^{238}Pu	24.000	6.5270	24.131	6.3822	24.018	6.9390	-	-
^{239}Pu	109.30	200.20	112.36	206.12	112.74	206.94	-	-
^{240}Pu	96.32	1.9150	106.07	1.8887	108.09	1.8427	-	-
^{241}Pu	105.00	224.90	103.23	228.03	104.64	231.50	-	-
^{242}Pu	26.840	1.2990	31.773	1.4407	29.110	1.3462	-	-
^{135}Xe	131400	-	121750	-	125959	-	-	-
^{149}Sm	4079.0	-	3815.1	-	3924.8	-	-	-

Table A- 7 (continuation)

State	TVS-M (U8-LIPAR-3)		HELIOS		WIMS-ABBN		MCU-RFFI/A	
	σ_a	$\nu\sigma_f$	σ_a	$\nu\sigma_f$	σ_a	$\nu\sigma_f$	σ_a	$\nu\sigma_f$
V7 (fresh MOX fuel with ^{239}Pu only)								
^{235}U	27.270	52.230	27.173	51.371	27.187	51.780	-	-
^{238}U	0.9676	0.3112	0.9485	0.3099	0.9842	0.2965	-	-
^{239}Pu	63.720	117.90	64.224	119.140	64.857	120.160	-	-
^{135}Xe	76950	-	69636	-	71490	-	-	-
^{149}Sm	2428.0	-	2227.6	-	2277.2	-	-	-
V8 (fresh MOX fuel with ^{240}Pu only)								
^{235}U	45.420	90.030	45.700	90.211	45.304	89.896	-	-
^{238}U	1.0010	0.2843	0.9836	0.2775	1.0156	0.2644	-	-
^{240}Pu	96.890	1.8350	106.12	1.8017	107.07	1.7808	-	-
^{135}Xe	167500	-	158210	-	160629	-	-	-
^{149}Sm	5215.0	-	4964.9	-	5013.5	-	-	-
V9 (fresh MOX fuel with ^{241}Pu only)								
^{235}U	26.170	50.040	27.017	51.143	26.533	50.648	-	-
^{238}U	0.9480	0.3142	0.9373	0.2985	0.9392	0.2986	-	-
^{241}Pu	64.690	139.10	65.811	145.97	66.544	147.32	-	-
^{135}Xe	68910	-	65418	-	65987	-	-	-
^{149}Sm	2210.0	-	2119.6	-	2131.1	-	-	-

Table A- 8 Micro cross-sections comparison (deviation from TVS-M, %).

State	HELIOS		WIMS-ABBN		MCU-RFFI/A	
	σ_a	$\nu\sigma_f$	σ_a	$\nu\sigma_f$	σ_a	$\nu\sigma_f$
	V1 (fresh LEU fuel)					
^{235}U	1.18	0.75	0.48	0.66	0.41	0.37
^{238}U	-1.79	-2.14	1.57	-2.21	-0.35	-0.05
^{135}Xe	-5.25	-	-3.38	-	-3.47	-
^{149}Sm	-4.47	-	-3.08	-	-5.53	-
	V2 (fresh MOX fuel)					
^{235}U	-0.84	-2.25	-0.94	-1.57	-1.22	-1.47
^{238}U	-1.98	-0.29	1.72	-4.55	-0.15	0.53
^{239}Pu	0.08	0.30	0.98	1.08	-0.13	-0.36
^{240}Pu	10.95	-0.79	13.06	-4.06	7.54	0.59
^{241}Pu	-3.58	-0.32	-2.15	1.46	-1.80	-1.86
^{135}Xe	-10.30	-	-7.97	-	-7.01	-
^{149}Sm	-9.13	-	-7.13	-	-8.43	-
	V3 (spent LEU fuel without F.P.)					
^{235}U	-0.59	-1.28	-0.12	-0.14	-	-
^{236}U	-2.58	2.03	-15.22	-25.77	-	-
^{238}U	-1.77	-1.30	-0.19	-3.62	-	-
^{238}Pu	0.21	-2.39	-0.29	6.07	-	-
^{239}Pu	2.53	2.69	2.90	3.12	-	-
^{240}Pu	10.29	-1.31	12.47	-3.68	-	-
^{241}Pu	-1.98	1.01	-0.46	2.75	-	-
^{242}Pu	18.05	10.92	8.01	3.67	-	-
^{135}Xe	-7.47	-	-4.32	-	-	-
^{149}Sm	-6.62	-	-3.99	-	-	-

Table A- 8 (continuation)

State	HELIOS		WIMS-ABBN		MCU-RFFI/A	
	σ_a	$\nu\sigma_f$	σ_a	$\nu\sigma_f$	σ_a	$\nu\sigma_f$
	V4 (spent LEU fuel with F.P.)					
^{235}U	-0.13	-0.92	0.11	0.08	-	-
^{236}U	-3.23	1.92	-14.95	-24.94	-	-
^{238}U	-1.38	-1.37	-0.50	-3.72	-	-
^{238}Pu	0.55	-2.22	0.07	6.31	-	-
^{239}Pu	2.80	2.96	3.15	3.37	-	-
^{240}Pu	10.12	-1.37	12.22	-3.77	-	-
^{241}Pu	-1.69	1.39	-0.35	2.93	-	-
^{242}Pu	18.38	10.91	8.46	3.63	-	-
^{135}Xe	-7.34	-	-4.14	-	-	-
^{149}Sm	-6.47	-	-3.78	-	-	-
	V7 (fresh MOX fuel with ^{239}Pu only)					
^{235}U	-0.36	-1.64	-0.31	-0.86	-	-
^{238}U	-1.97	-0.40	1.72	-4.72	-	-
^{239}Pu	0.79	1.05	1.78	1.92	-	-
^{135}Xe	-9.50	-	-7.10	-	-	-
^{149}Sm	-8.25	-	-6.21	-	-	-
	V8 (fresh MOX fuel with ^{240}Pu only)					
^{235}U	0.62	0.20	-0.26	-0.15	-	-
^{238}U	-1.74	-2.41	1.46	-7.00	-	-
^{240}Pu	9.53	-1.81	10.50	-2.95	-	-
^{135}Xe	-5.55	-	-4.10	-	-	-
^{149}Sm	-4.80	-	-3.86	-	-	-
	V9 (fresh MOX fuel with ^{241}Pu only)					
^{235}U	3.24	2.20	1.39	1.22	-	-
^{238}U	-1.13	-5.01	-0.93	-4.95	-	-
^{241}Pu	1.73	4.94	2.87	5.91	-	-
^{135}Xe	-5.07	-	-4.24	-	-	-
^{149}Sm	-4.09	-	-3.57	-	-	-

Fig. A- 5 K_{eff} and K_o comparison results for variant V1 (deviation from TVS-M, %)

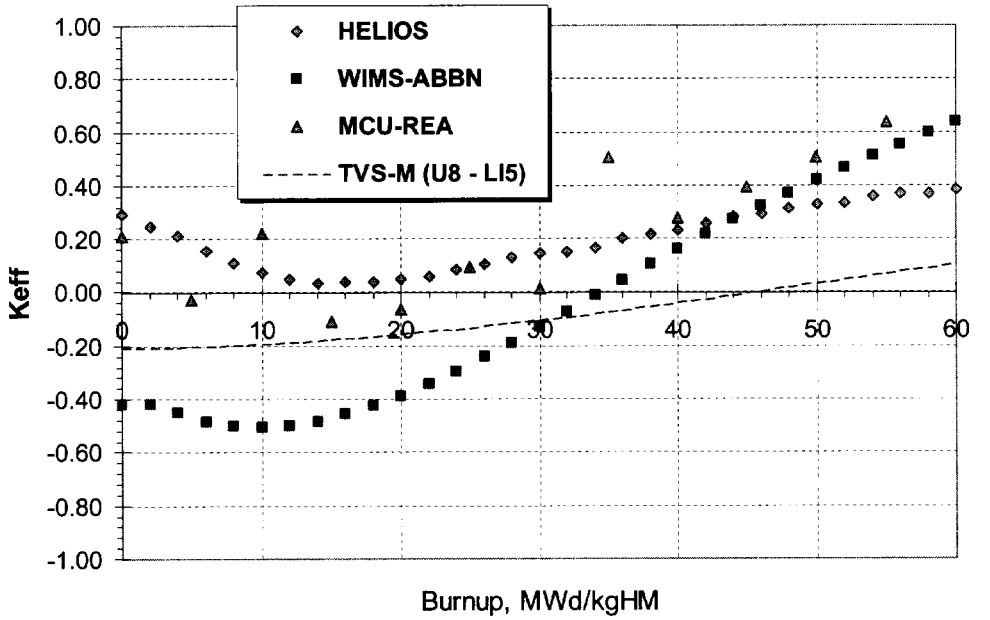

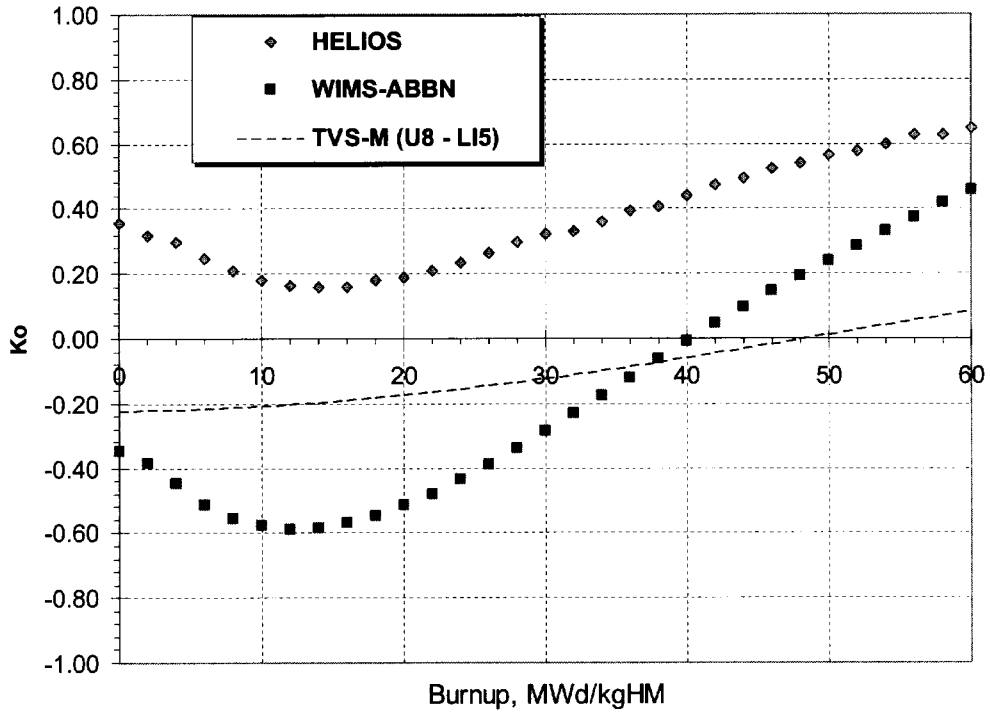

Fig. A- 6 K_{eff} and K_o comparison results for variant V2 (deviation from TVS-M,%)

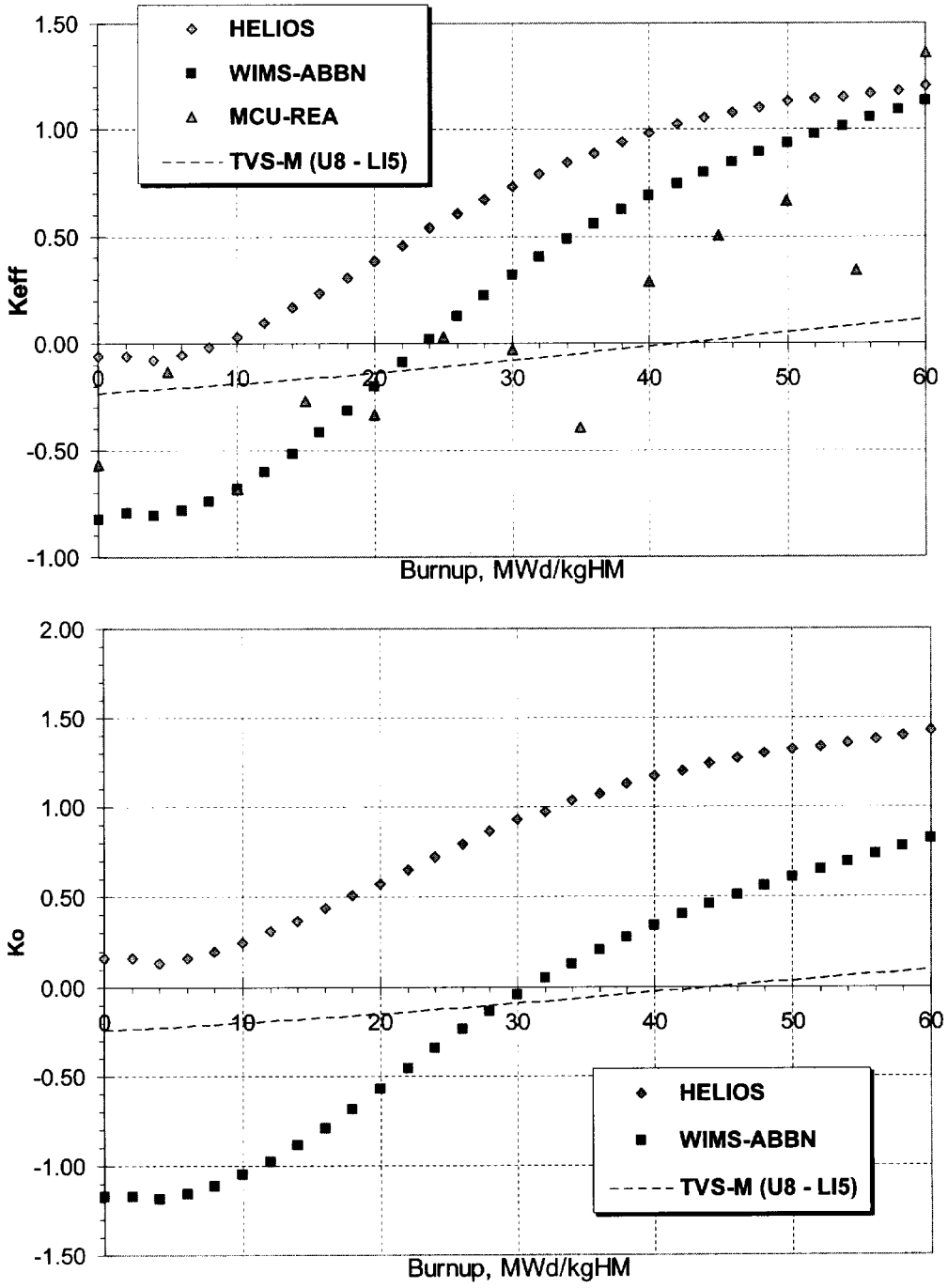

Fig. A- 7 K_{eff} and K_o comparison results for variant V10 (deviation from TVS-M, %)

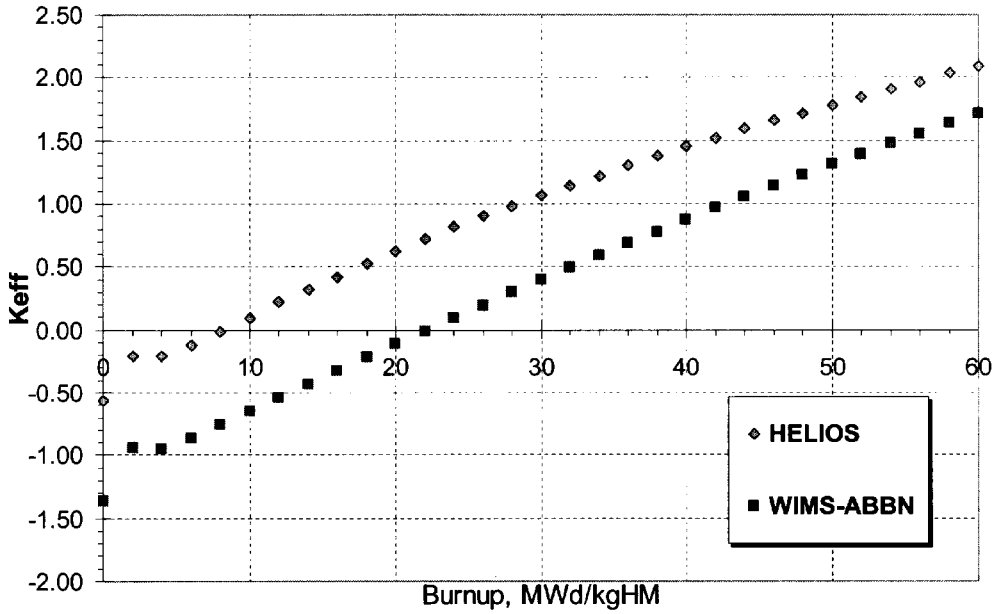

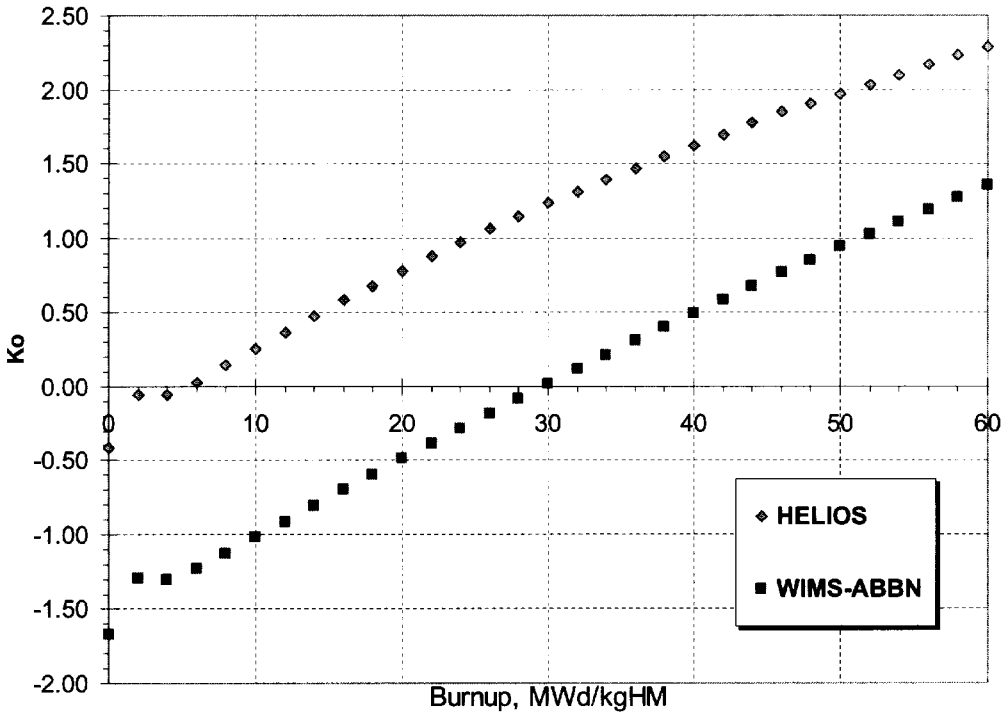

Fig. A- 8 ^{235}U and ^{236}U concentrations comparison results for variant V1 (deviation from TVS-M, %)

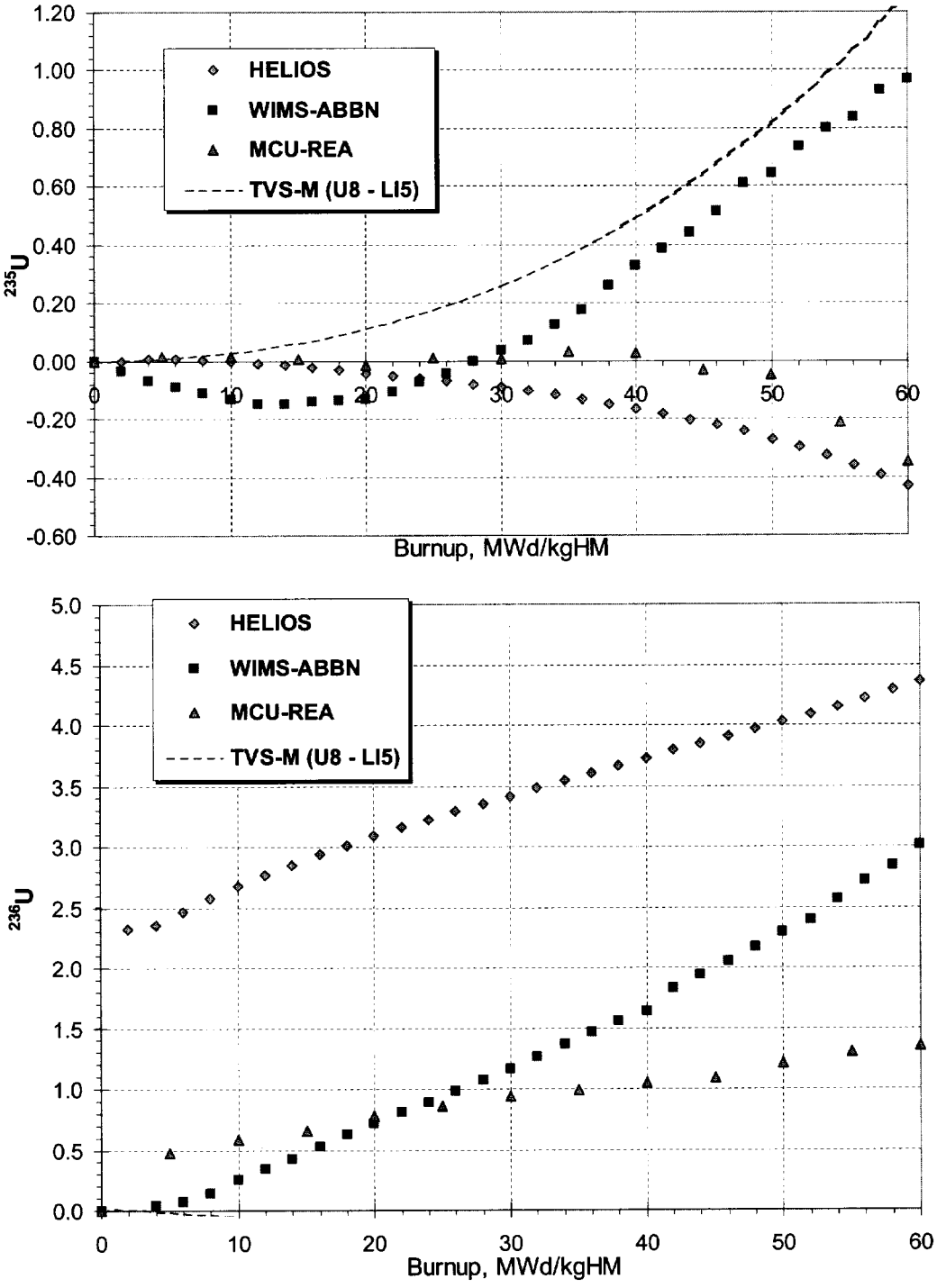

Fig. A- 9 ^{235}U and ^{236}U concentrations comparison results for variant V2 (deviation from TVS-M, %)

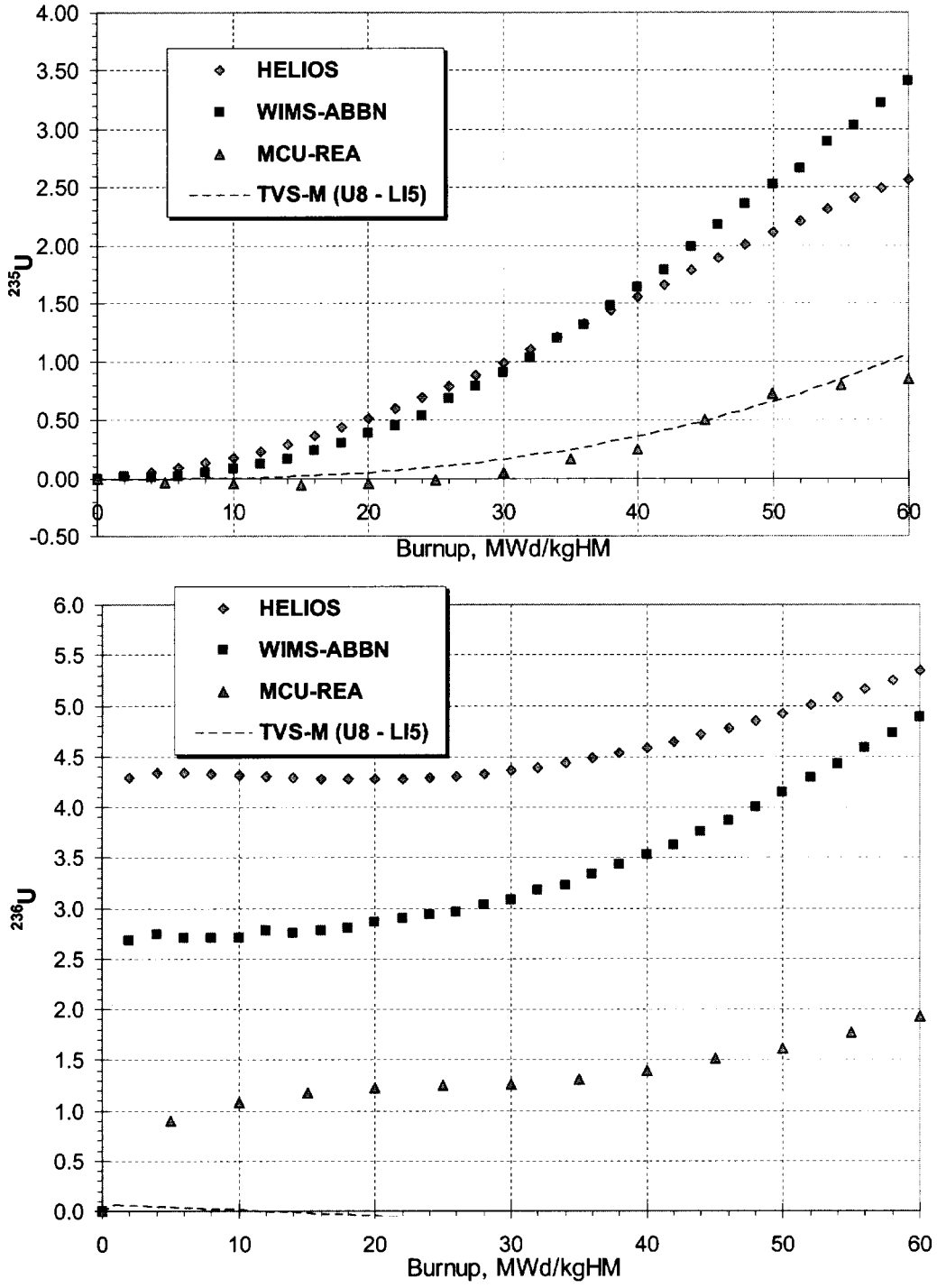

Fig. A- 10 ^{238}U and ^{238}Pu concentrations comparison results for variant V1 (deviation from TVS-M, %)

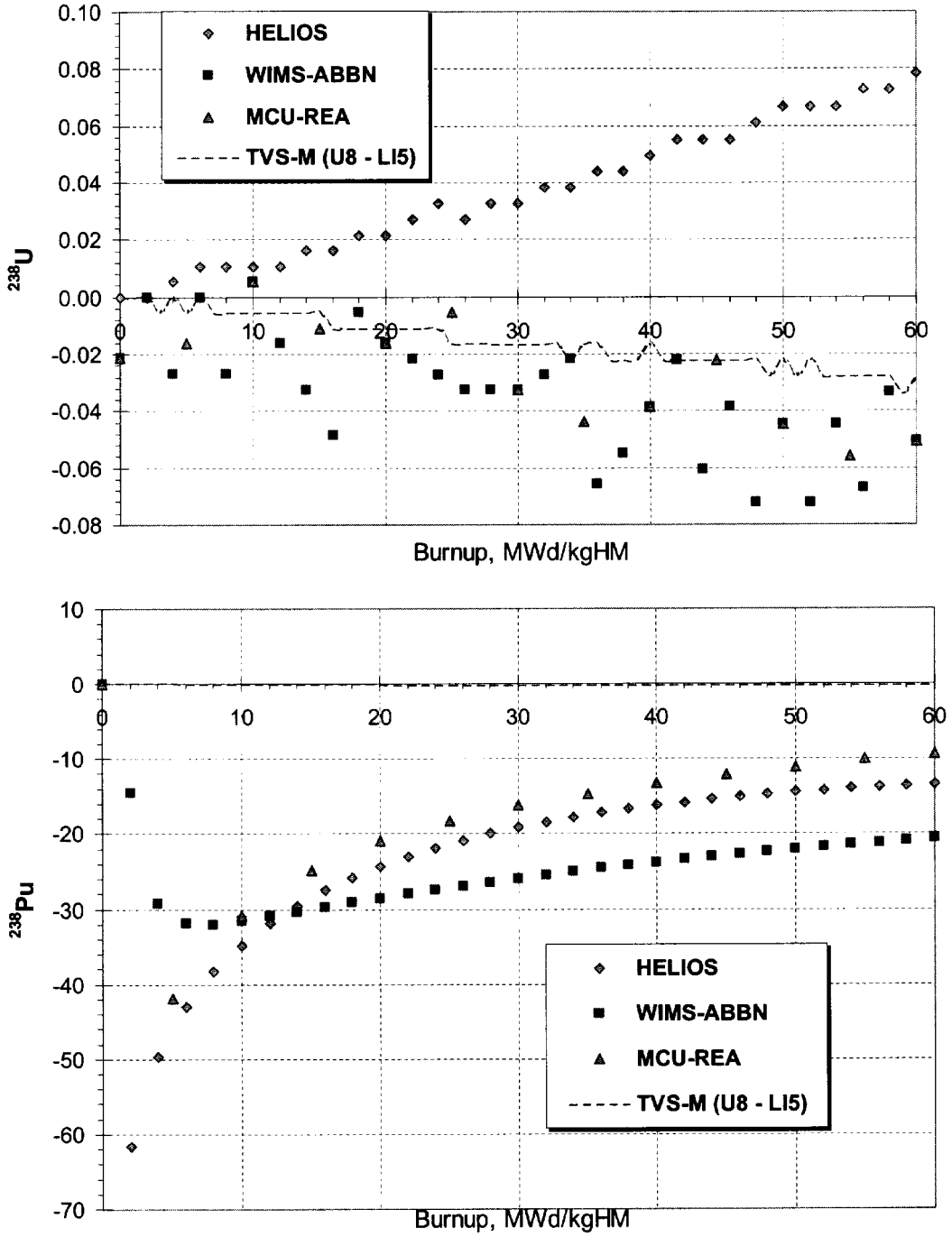

Fig. A- 11 ^{238}U and ^{238}Pu concentrations comparison results for variant V2 (deviation from TVS-M, %)

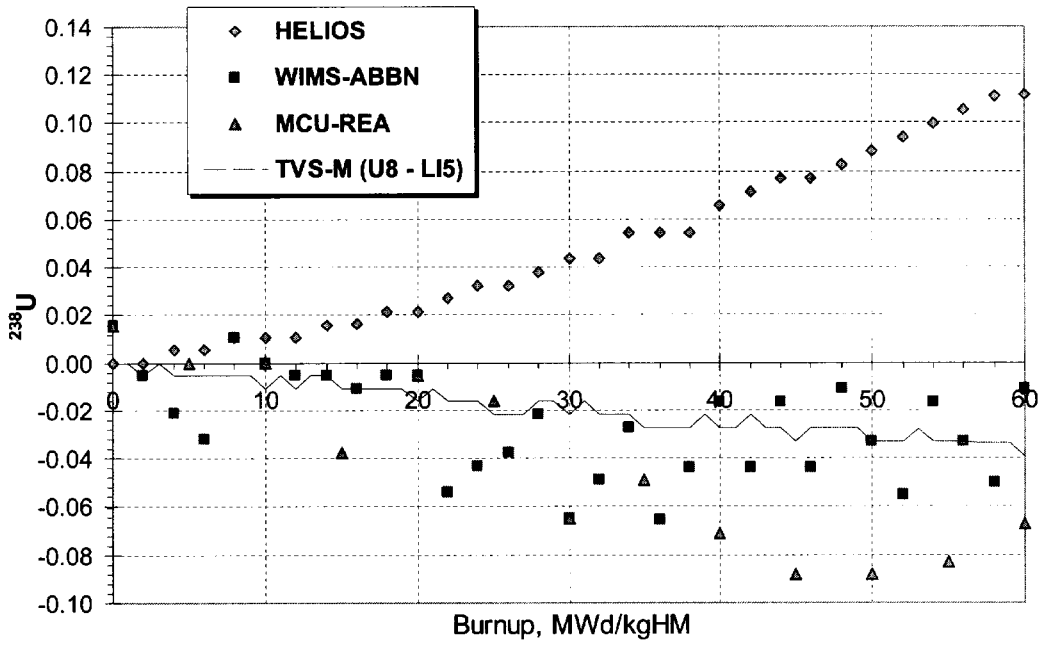

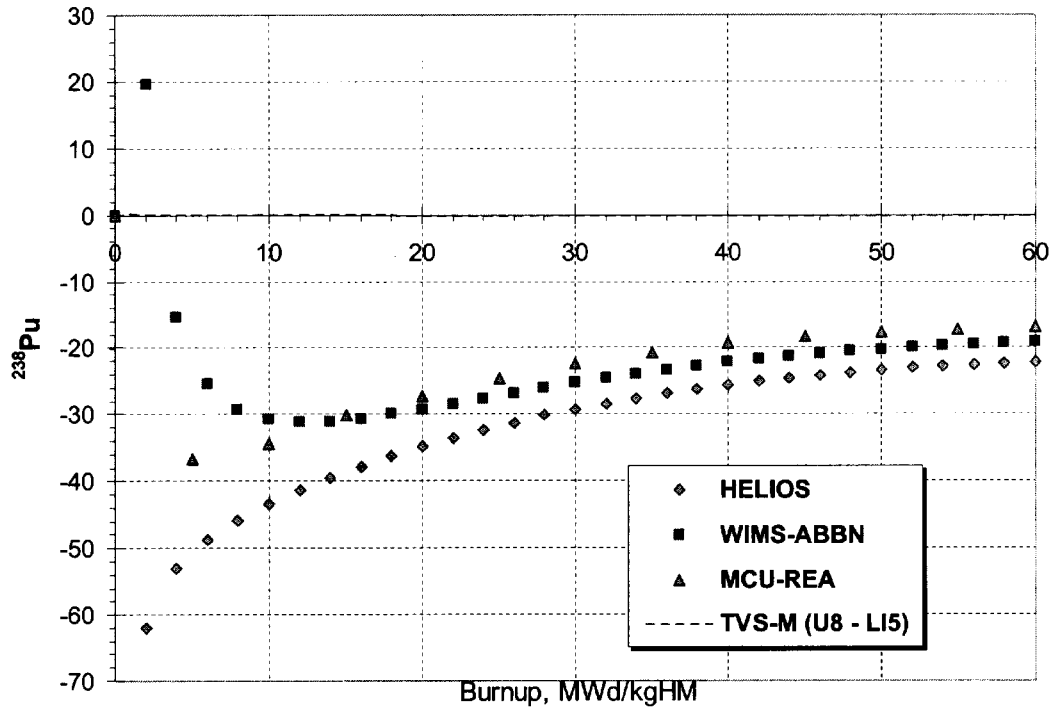

Fig. A- 12 ^{239}Pu and ^{240}Pu concentrations comparison results for variant V1 (deviation from TVS-M, %)

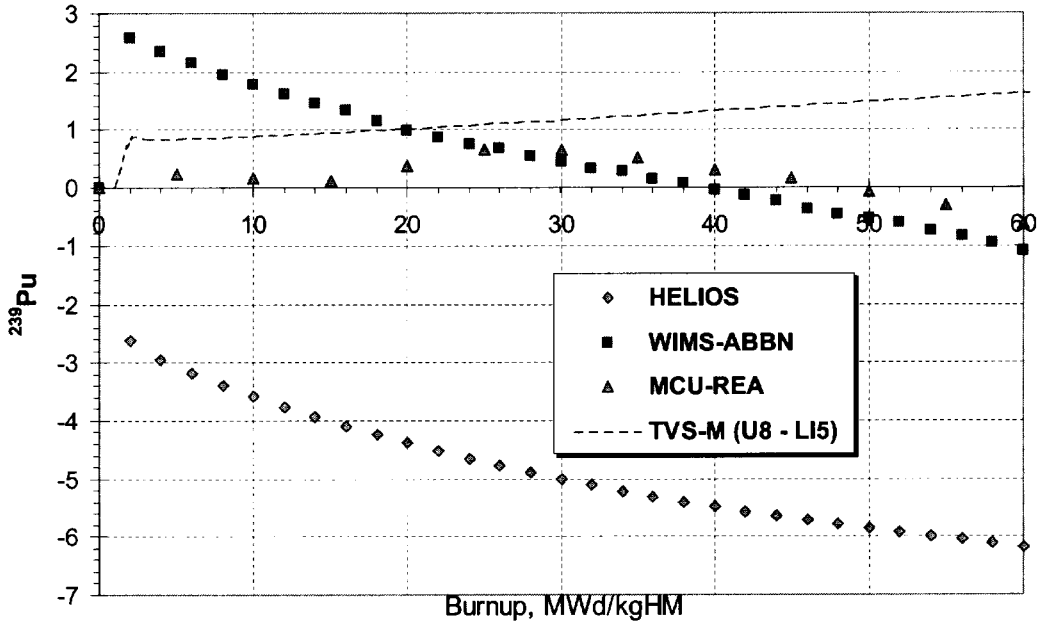

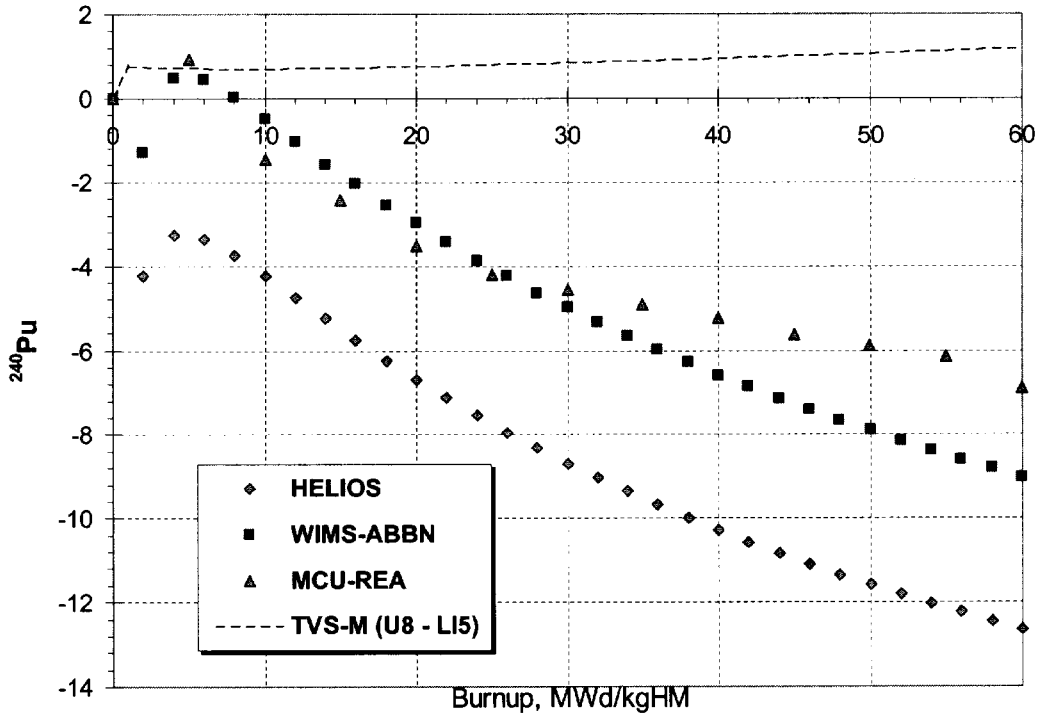

Fig. A- 13 ^{239}Pu and ^{240}Pu concentrations comparison results for variant V2 (deviation from TVS-M, %)

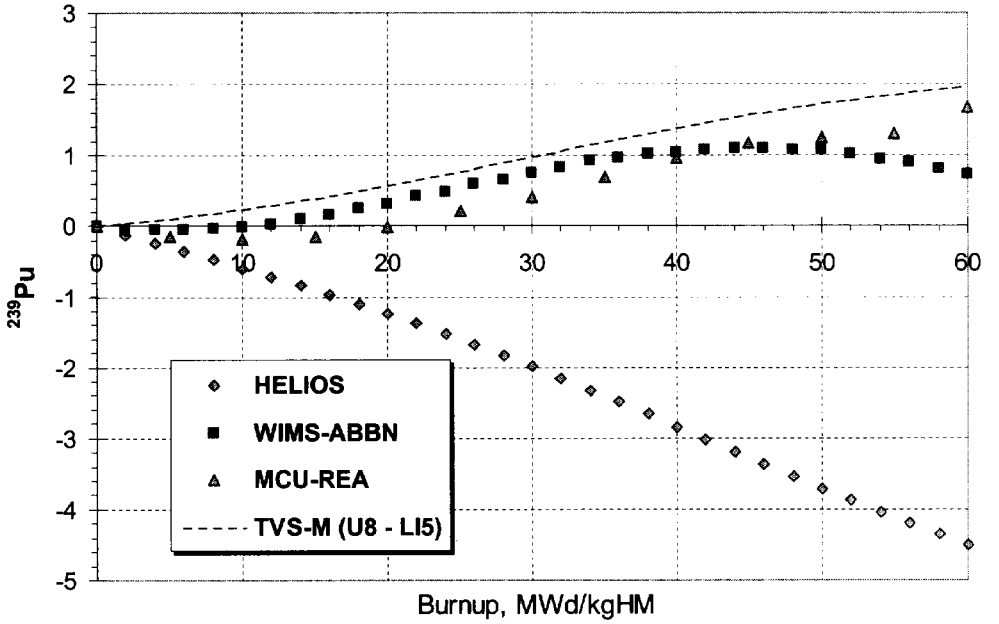

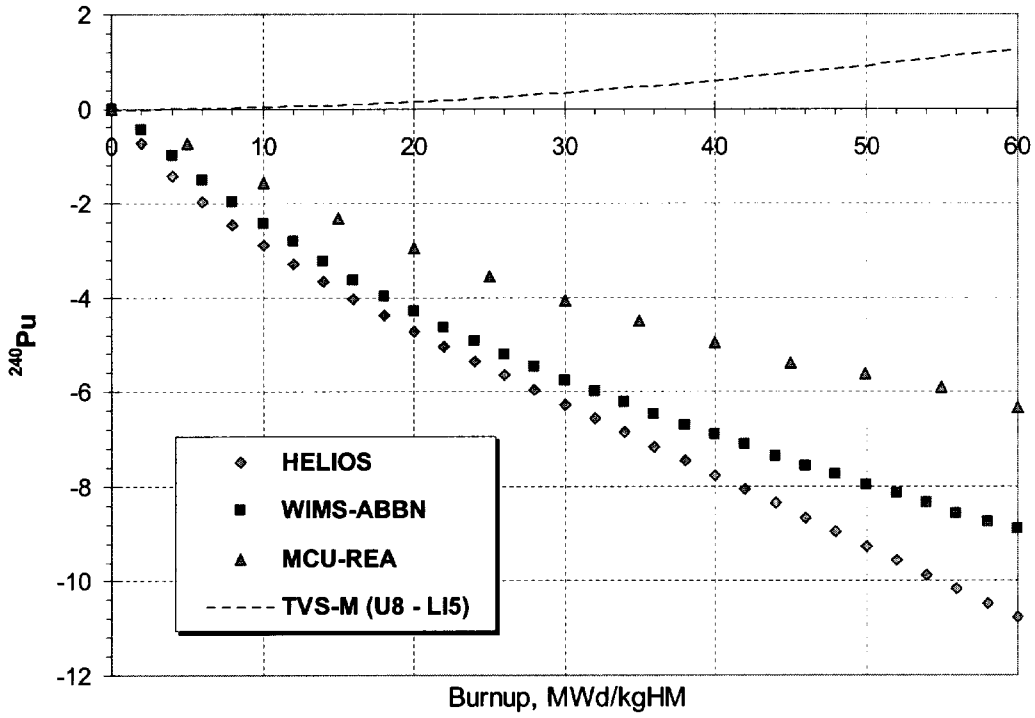

Fig. A- 14 ^{239}Pu and ^{240}Pu concentrations comparison results for variant V10 (deviation from TVS-M, %)

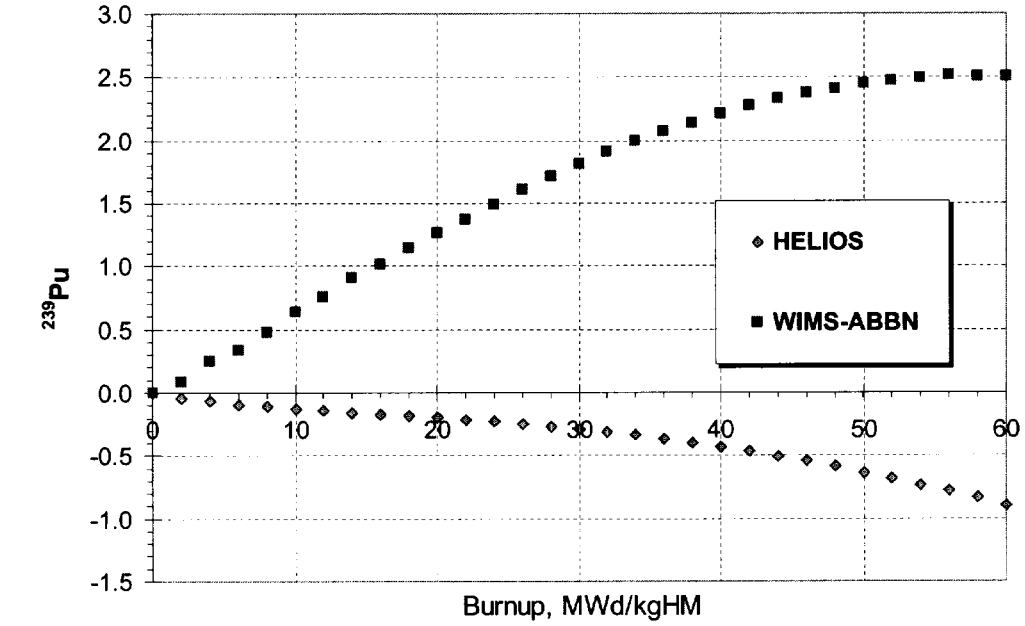

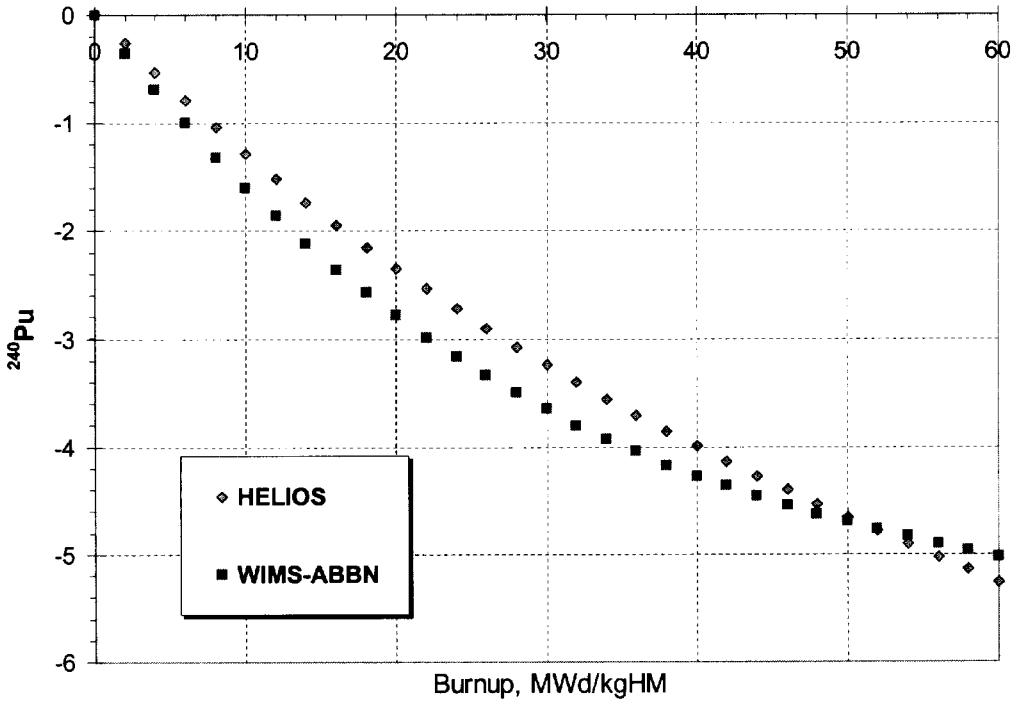

Fig. A- 15 ^{241}Pu and ^{242}Pu concentrations comparison results for variant V1 (deviation from TVS-M, %)

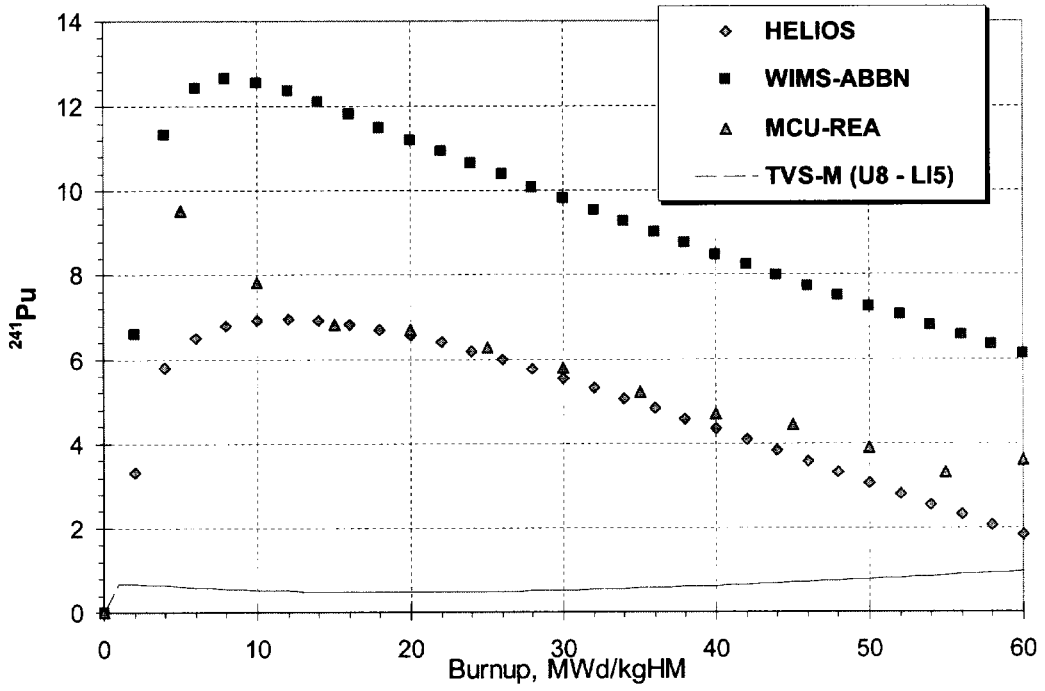

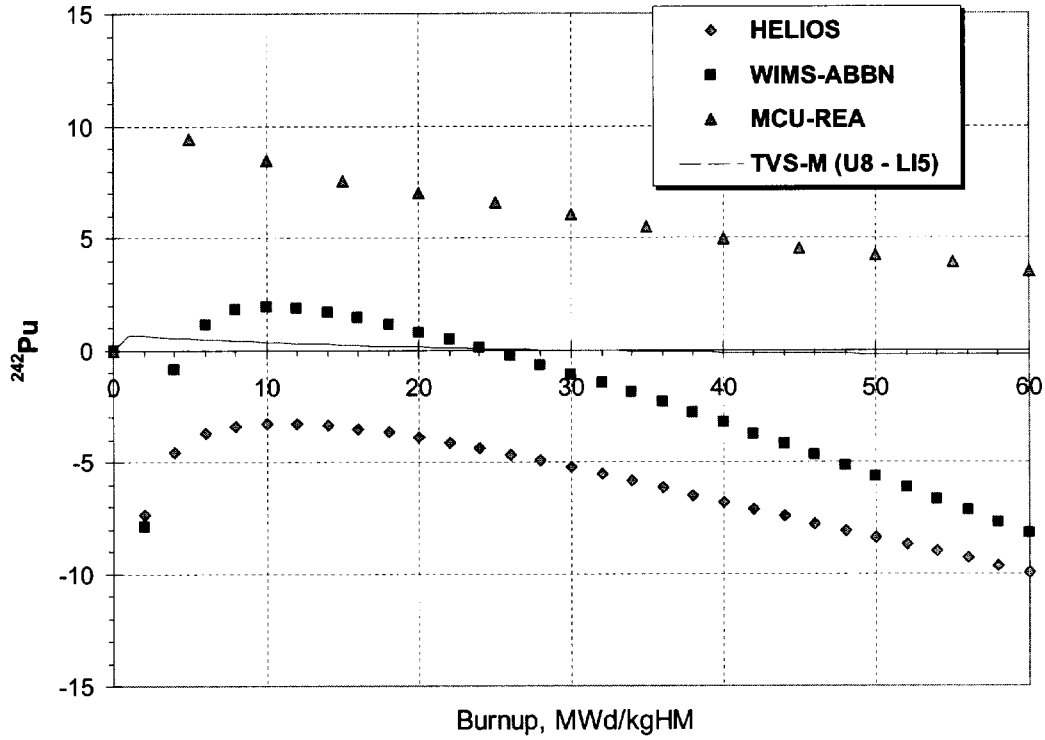

Fig. A- 16 ^{241}Pu and ^{242}Pu concentrations comparison results for variant V2 (deviation from TVS-M, %)

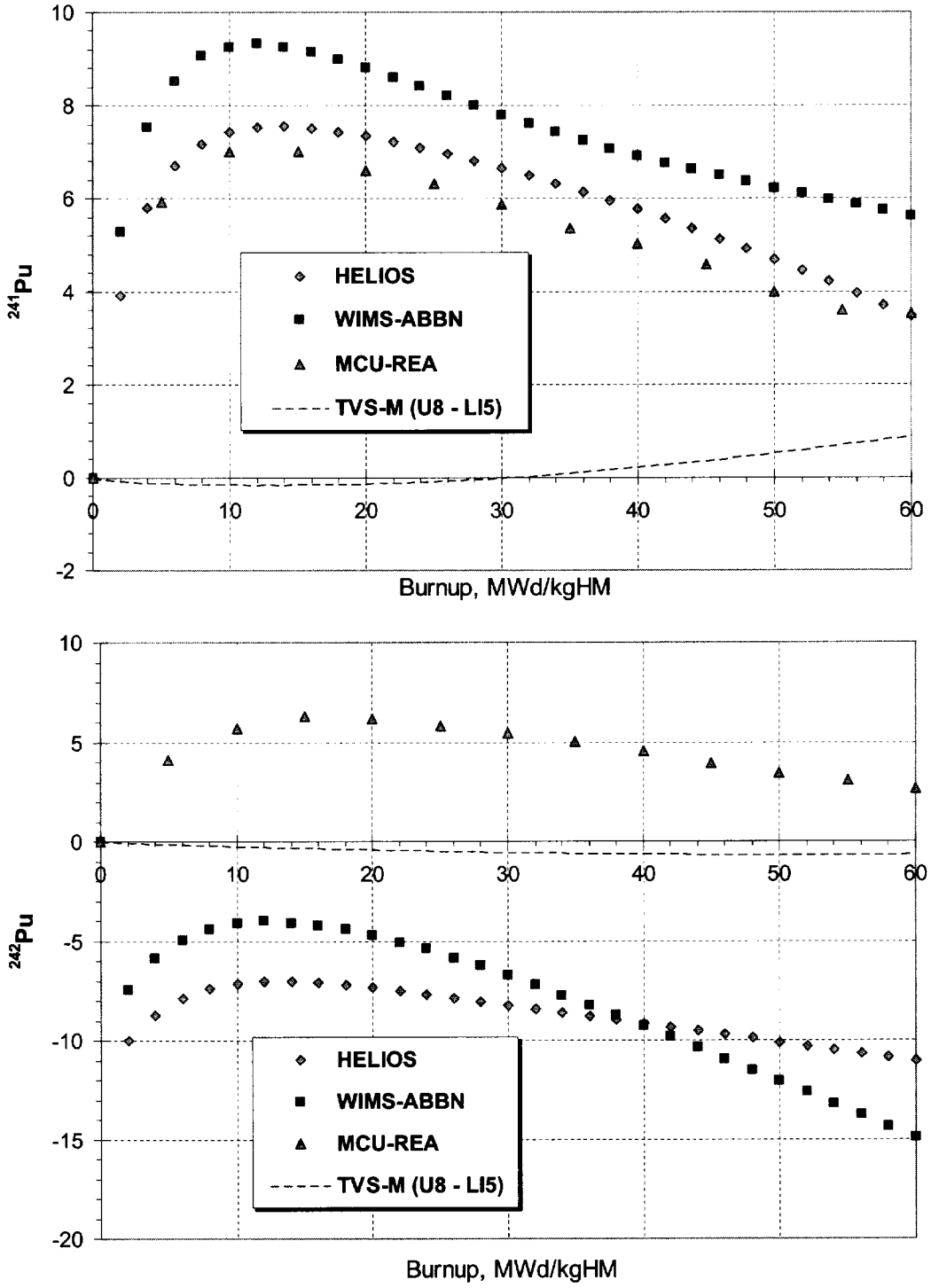

Fig. A- 17 ^{241}Pu and ^{242}Pu concentrations comparison results for variant V10 (deviation from TVS-M, %)

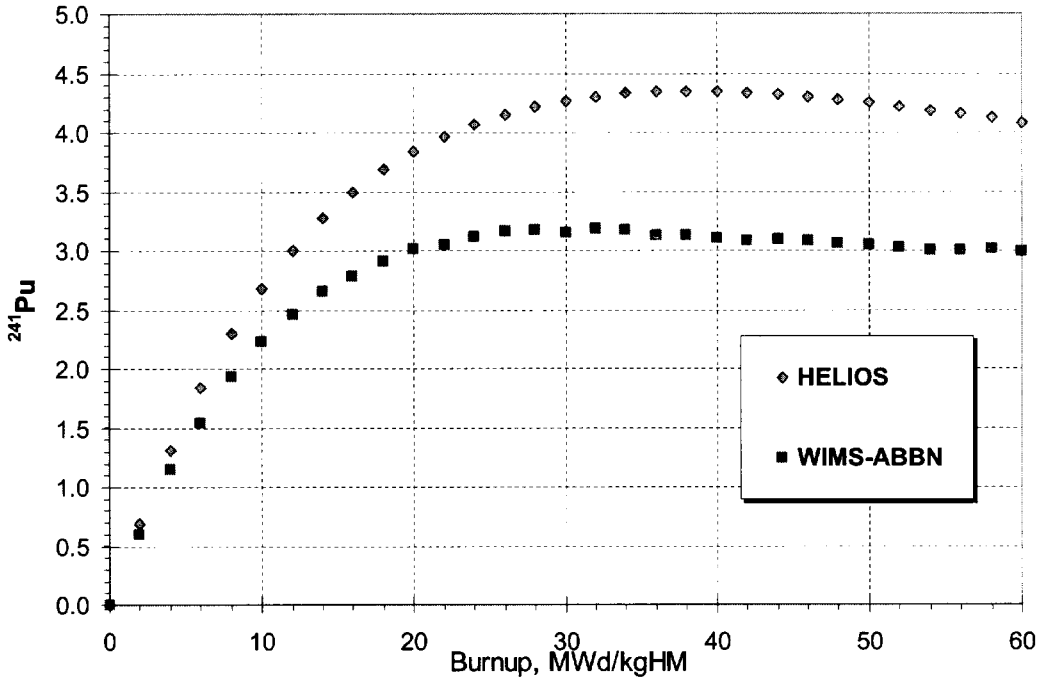

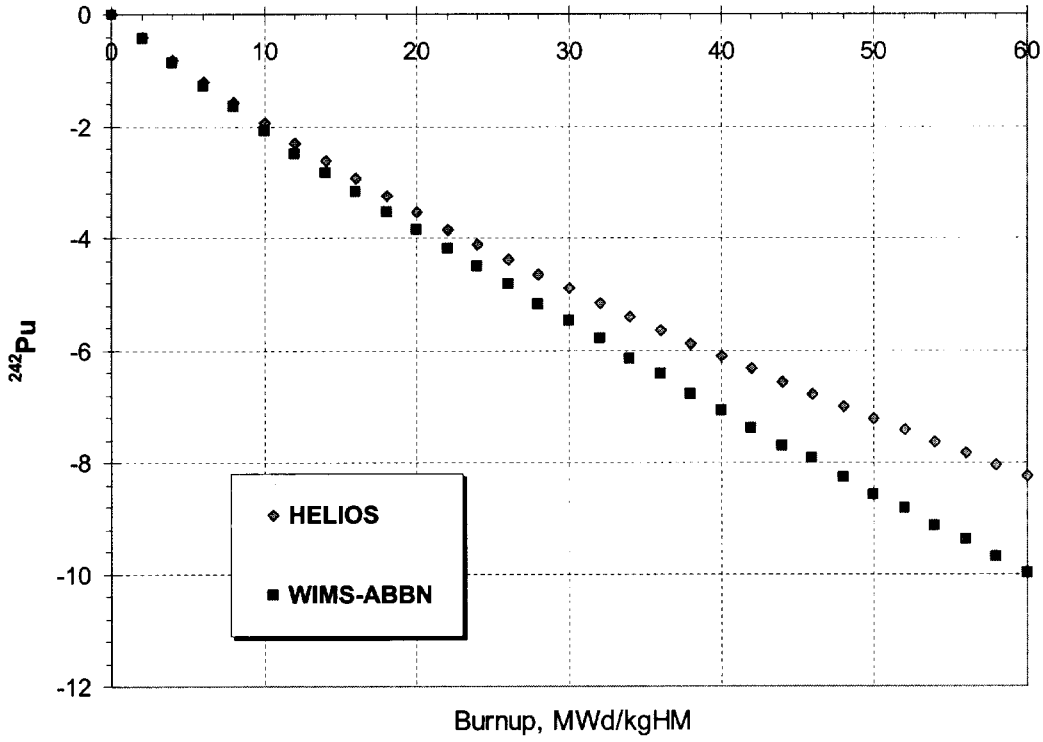

Fig. A- 18 ^{135}Xe and ^{149}Sm concentrations comparison results for variant V1 (deviation from TVS-M, %)

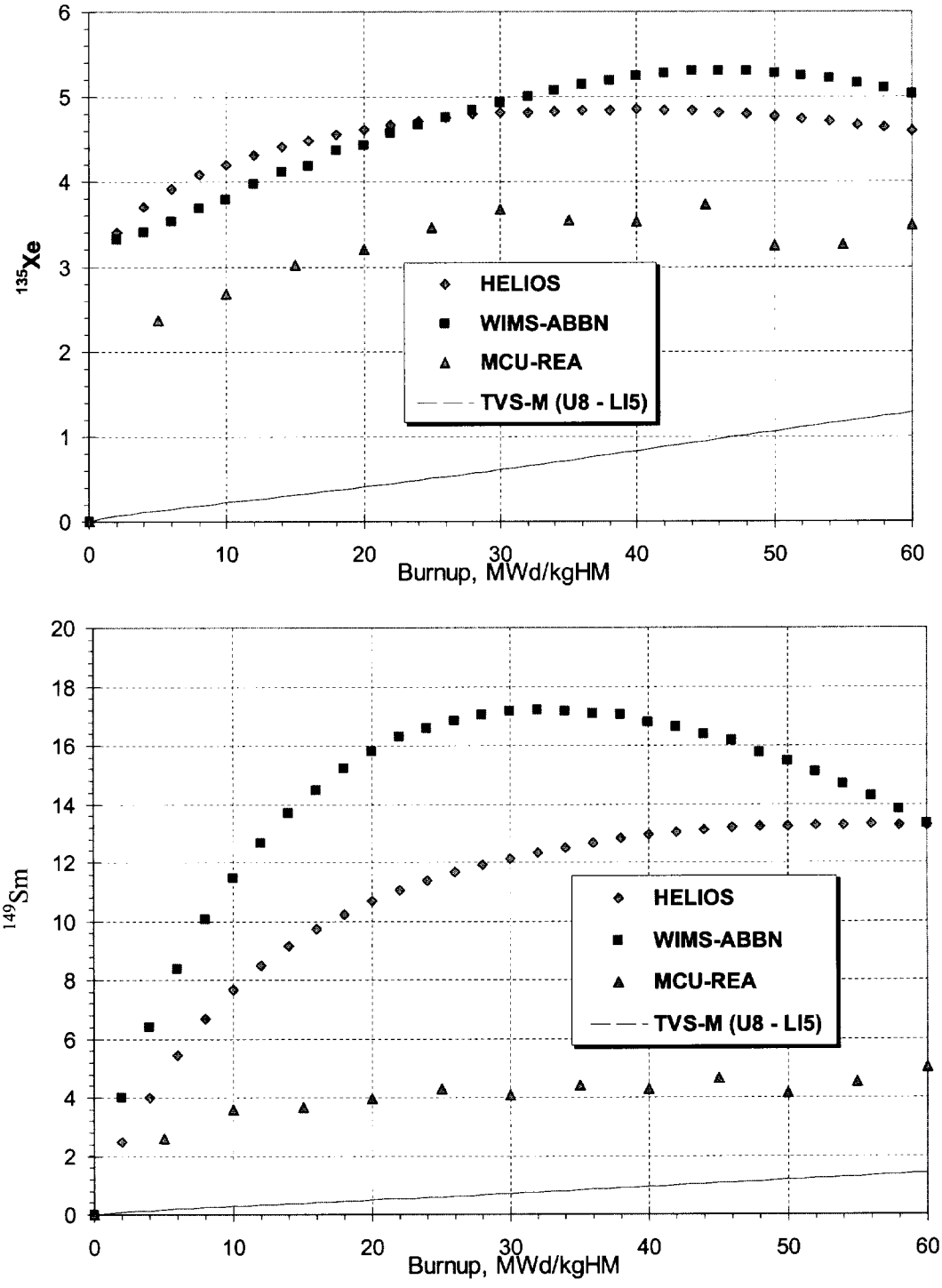

Fig. A- 19 ^{135}Xe and ^{149}Sm concentrations comparison results for variant V2 (deviation from TVS-M, %)

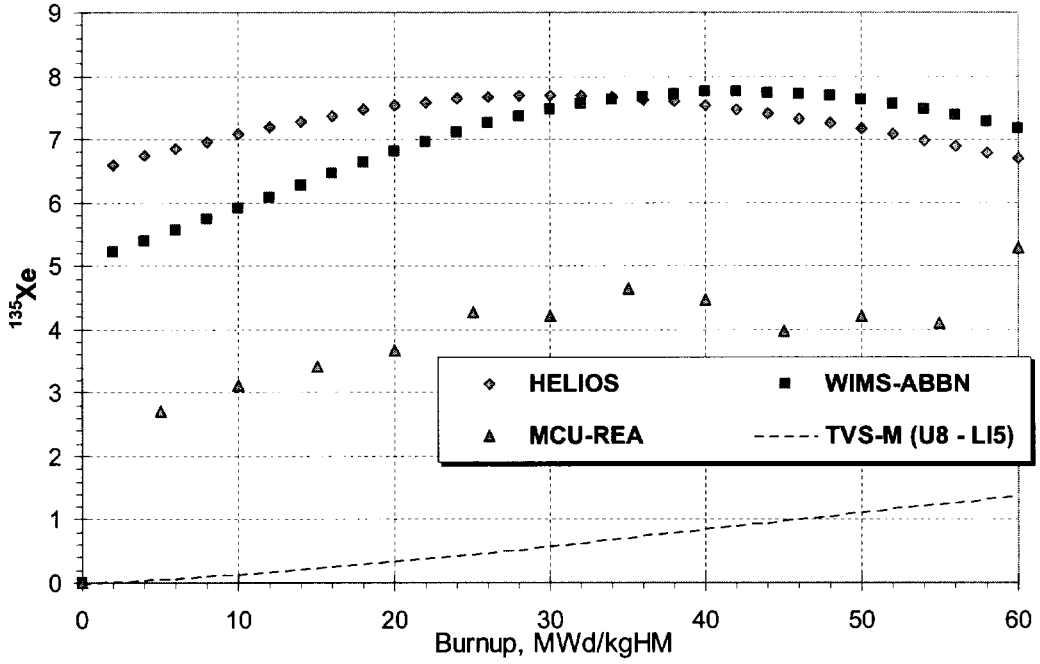

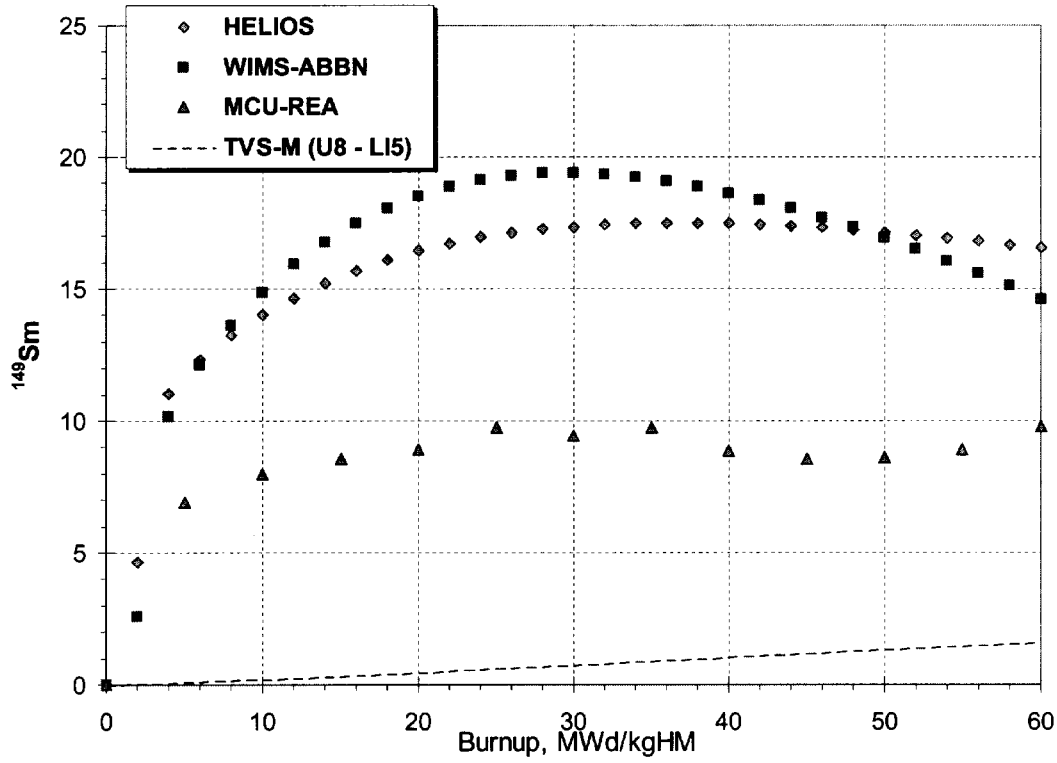

Table A- 9 Comparison of various reactivity effects values for several burnup points (LEU pin cell, variant V1)

Effect	Initial state	Final state	Effect value, $(K_i-K_j)/(K_i*K_j)$, %			Deviation from TVS-M	
			TVS-M	HELIOS	WIMS-ABBN	HELIOS	WIMS-ABBN
	Burnup 0.0 MWd/kgHM						
Doppler effect, T_f : 579K→ 1027K	S5	S4	-0.94	-0.95	-1.04	1.31	10.94
Boron effect, C_B : 0.0 → 0.6 g/kg	S3	S1	-3.32	-3.30	-3.33	-0.44	0.47
Poisoning effect	S4	S1	-2.97	-2.80	-2.89	-5.49	-2.65
Total temperature effect, Tm : 300K → 579K	S6	S5	-2.20	-2.12	-2.20	-3.53	0.29
	Burnup 10.0 MWd/kgHM						
Doppler effect, T_f : 579K→ 1027K	S5	S4	-1.08	-1.10	-1.19	2.49	10.25
Boron effect, C_B : 0.0 → 0.6 g/kg	S3	S1	-3.37	-3.29	-3.30	-2.42	-1.99
Poisoning effect	S4	S1	-3.12	-3.19	-3.27	2.15	4.77
Total temperature effect, Tm : 300K → 579K	S6	S5	-3.11	-3.06	-3.19	-1.64	2.43
	Burnup 20.0 MWd/kgHM						
Doppler effect, T_f : 579K→ 1027K	S5	S4	-1.28	-1.33	-1.38	3.84	7.82
Boron effect, C_B : 0.0 → 0.6 g/kg	S3	S1	-3.56	-3.47	-3.47	-2.77	-2.51
Poisoning effect	S4	S1	-3.25	-3.43	-3.52	5.71	8.51
Total temperature effect, Tm : 300K → 579K	S6	S5	-3.72	-3.64	-3.81	-2.04	2.39
	Burnup 30.0 MWd/kgHM						
Doppler effect, T_f : 579K→ 1027K	S5	S4	-1.44	-1.50	-1.52	4.22	5.23
Boron effect, C_B : 0.0 → 0.6 g/kg	S3	S1	-3.82	-3.71	-3.71	-2.90	-2.92
Poisoning effect	S4	S1	-3.37	-3.65	-3.72	8.28	10.65
Total temperature effect, Tm : 300K → 579K	S6	S5	-4.03	-3.89	-4.09	-3.47	1.58
	Burnup 40.0 MWd/kgHM						
Doppler effect, T_f : 579K→ 1027K	S5	S4	-1.58	-1.67	-1.62	5.79	2.59
Boron effect, C_B : 0.0 → 0.6 g/kg	S3	S1	-4.11	-3.99	-3.98	-2.90	-3.21
Poisoning effect	S4	S1	-3.47	-3.81	-3.88	9.85	11.84
Total temperature effect, Tm : 300K → 579K	S6	S5	-4.13	-3.90	-4.14	-5.44	0.45
	Burnup 50.0 MWd/kgHM						
Doppler effect, T_f : 579K→ 1027K	S5	S4	-1.70	-1.79	-1.70	5.52	-0.20
Boron effect, C_B : 0.0 → 0.6 g/kg	S3	S1	-4.40	-4.28	-4.26	-2.68	-3.22
Poisoning effect	S4	S1	-3.56	-3.96	-4.01	11.29	12.52
Total temperature effect, Tm : 300K → 579K	S6	S5	-4.05	-3.71	-4.02	-8.20	-0.70
	Burnup 60.0 MWd/kgHM						
Doppler effect, T_f : 579K→ 1027K	S5	S4	-1.81	-1.91	-1.75	5.93	-2.89
Boron effect, C_B : 0.0 → 0.6 g/kg	S3	S1	-4.68	-4.58	-4.53	-2.06	-3.06
Poisoning effect	S4	S1	-3.63	-4.10	-4.10	12.81	12.77
Total temperature effect, Tm : 300K → 579K	S6	S5	-3.84	-3.41	-3.77	-11.40	-1.91

Table A- 10 Comparison of various reactivity effects values for several burnup points (MOX pin cell, variant V2)

Effect	Initial state	Final state	Effect value, $(K_i-K_j)/(K_i*K_j)$, %			Deviation from TVS-M	
			TVS-M	HELIOS	WIMS-ABBN	HELIOS	WIMS-ABBN
	Burnup 0.0 MWd/kgHM						
Doppler effect, T_f : 579K→ 1027K	S5	S4	-1.24	-1.29	-1.41	3.91	13.67
Boron effect, C_B : 0.0 → 0.6 g/kg	S3	S1	-1.96	-1.91	-1.94	-2.72	-1.03
Poisoning effect	S4	S1	-1.42	-1.28	-1.32	-10.16	-7.30
Total temperature effect, Tm : 300K → 579K	S6	S5	-4.24	-4.40	-4.65	3.61	9.64
	Burnup 10.0 MWd/kgHM						
Doppler effect, T_f : 579K→ 1027K	S5	S4	-1.39	-1.46	-1.57	5.27	12.79
Boron effect, C_B : 0.0 → 0.6 g/kg	S3	S1	-2.30	-2.17	-2.23	-5.86	-3.00
Poisoning effect	S4	S1	-2.80	-2.80	-2.90	-0.12	3.36
Total temperature effect, Tm : 300K → 579K	S6	S5	-4.69	-4.79	-5.08	2.08	8.19
	Burnup 20.0 MWd/kgHM						
Doppler effect, T_f : 579K→ 1027K	S5	S4	-1.48	-1.58	-1.63	6.71	10.56
Boron effect, C_B : 0.0 → 0.6 g/kg	S3	S1	-2.64	-2.50	-2.55	-5.50	-3.72
Poisoning effect	S4	S1	-3.01	-3.13	-3.23	3.87	7.03
Total temperature effect, Tm : 300K → 579K	S6	S5	-4.86	-4.89	-5.19	0.48	6.66
	Burnup 30.0 MWd/kgHM						
Doppler effect, T_f : 579K→ 1027K	S5	S4	-1.57	-1.68	-1.69	6.76	7.54
Boron effect, C_B : 0.0 → 0.6 g/kg	S3	S1	-3.00	-2.84	-2.87	-5.43	-4.27
Poisoning effect	S4	S1	-3.19	-3.40	-3.48	6.57	9.18
Total temperature effect, Tm : 300K → 579K	S6	S5	-4.90	-4.82	-5.12	-1.47	4.63
	Burnup 40.0 MWd/kgHM						
Doppler effect, T_f : 579K→ 1027K	S5	S4	-1.67	-1.79	-1.74	7.28	4.17
Boron effect, C_B : 0.0 → 0.6 g/kg	S3	S1	-3.35	-3.19	-3.20	-4.85	-4.43
Poisoning effect	S4	S1	-3.34	-3.64	-3.69	8.91	10.53
Total temperature effect, Tm : 300K → 579K	S6	S5	-4.84	-4.68	-5.00	-3.45	3.26
	Burnup 50.0 MWd/kgHM						
Doppler effect, T_f : 579K→ 1027K	S5	S4	-1.76	-1.90	-1.78	8.33	0.96
Boron effect, C_B : 0.0 → 0.6 g/kg	S3	S1	-3.69	-3.53	-3.53	-4.38	-4.42
Poisoning effect	S4	S1	-3.46	-3.81	-3.85	10.20	11.28
Total temperature effect, Tm : 300K → 579K	S6	S5	-4.74	-4.49	-4.85	-5.42	2.27
	Burnup 60.0 MWd/kgHM						
Doppler effect, T_f : 579K→ 1027K	S5	S4	-1.85	-1.99	-1.81	7.97	-2.10
Boron effect, C_B : 0.0 → 0.6 g/kg	S3	S1	-4.00	-3.83	-3.84	-4.21	-4.18
Poisoning effect	S4	S1	-3.55	-3.95	-3.97	11.26	11.65
Total temperature effect, Tm : 300K → 579K	S6	S5	-4.61	-4.27	-4.71	-7.55	2.04

Table A- 11 β_{eff} comparison in case of pin cell variants (V15-V18).

State	β_{eff} value				Deviation from TVS-M		
	MCU-RFFI/A	TVS-M	WIMS-ABBN	HELIOS	MCU-RFFI/A	WIMS-ABBN	HELIOS
	V15, fresh LEU						
S7	7.130E-03	7.202E-03	7.161E-03	7.192E-03	-1.00	-0.57	-0.14
S8	7.120E-03	7.203E-03	7.161E-03	7.194E-03	-1.15	-0.58	-0.12
S9	7.330E-03	7.392E-03	7.369E-03	7.500E-03	-0.84	-0.31	1.46
S10	7.120E-03	7.203E-03	7.164E-03	7.202E-03	-1.15	-0.54	-0.01
S11	-	8.218E-03	8.143E-03	8.225E-03	-	-0.91	0.09
S12	-	8.404E-03	8.312E-03	8.354E-03	-	-1.09	-0.59
	V16, spent LEU						
S7	5.150E-03	5.309E-03	5.211E-03	5.289E-03	-2.99	-1.85	-0.38
S8	-	5.318E-03	5.200E-03	5.276E-03	-	-2.22	-0.79
S9	-	5.949E-03	5.879E-03	6.061E-03	-	-1.18	1.89
S10	5.170E-03	5.328E-03	5.232E-03	5.317E-03	-2.97	-1.80	-0.20
S11	-	5.559E-03	5.454E-03	5.558E-03	-	-1.89	-0.02
S12	-	5.853E-03	5.755E-03	5.846E-03	-	-1.67	-0.12
	V17, fresh MOX						
S7	3.140E-03	3.170E-03	3.169E-03	3.231E-03	-0.95	-0.03	1.93
S8	3.170E-03	3.184E-03	3.184E-03	3.248E-03	-0.44	0.00	2.01
S9	3.890E-03	3.962E-03	3.977E-03	4.160E-03	-1.82	0.38	5.01
S10	3.170E-03	3.200E-03	3.200E-03	3.266E-03	-0.94	0.00	2.05
S11	-	3.576E-03	3.550E-03	3.657E-03	-	-0.73	2.28
S12	-	3.542E-03	3.511E-03	3.583E-03	-	-0.88	1.17
	V18, spent MOX						
S7	3.730E-03	3.874E-03	3.752E-03	3.896E-03	-3.72	-3.15	0.57
S8	-	3.890E-03	3.761E-03	3.908E-03	-	-3.32	0.47
S9	-	4.764E-03	4.642E-03	4.880E-03	-	-2.56	2.43
S10	3.750E-03	3.912E-03	3.789E-03	3.938E-03	-4.14	-3.14	0.65
S11	-	4.023E-03	3.891E-03	4.055E-03	-	-3.28	0.79
S12	-	4.035E-03	3.901E-03	4.046E-03	-	-3.32	0.28

Table A- 12 β_{eff}/β comparison in case of pin cell variants (V15-V18).

State	MCU-RFFI/A	TVS-M	WIMS-ABBN	HELIOS
	V15, fresh LEU			
S7	9.750E-01	9.760E-01	9.750E-01	9.754E-01
S8	9.710E-01	9.740E-01	9.740E-01	9.740E-01
S9	9.270E-01	9.220E-01	9.210E-01	9.199E-01
S10	9.670E-01	9.690E-01	9.690E-01	9.693E-01
S11	-	1.103E+00	1.099E+00	1.103E+00
S12	-	1.147E+00	1.142E+00	1.144E+00
	V16, spent LEU			
S7	9.570E-01	9.590E-01	9.600E-01	9.589E-01
S8	-	9.570E-01	9.580E-01	9.567E-01
S9	-	8.700E-01	8.720E-01	8.670E-01
S10	9.500E-01	9.520E-01	9.540E-01	9.520E-01
S11	-	9.990E-01	9.990E-01	1.001E+00
S12	-	1.050E+00	1.050E+00	1.053E+00
	V17, fresh MOX			
S7	9.630E-01	9.650E-01	9.640E-01	9.638E-01
S8	9.640E-01	9.630E-01	9.610E-01	9.616E-01
S9	8.880E-01	8.930E-01	8.890E-01	8.870E-01
S10	9.610E-01	9.610E-01	9.600E-01	9.598E-01
S11	-	1.062E+00	1.057E+00	1.063E+00
S12	-	1.122E+00	1.116E+00	1.121E+00
	V18, spent MOX			
S7	9.540E-01	9.540E-01	9.520E-01	9.537E-01
S8	-	9.520E-01	9.490E-01	9.511E-01
S9	-	8.590E-01	8.540E-01	8.545E-01
S10	9.450E-01	9.480E-01	9.470E-01	9.482E-01
S11	-	9.840E-01	9.810E-01	9.858E-01
S12	-	1.038E+00	1.037E+00	1.041E+00

Table A- 13 Prompt neutrons lifetime comparison in case of pin cell variants (V15-V18).

State	TVS-M	WIMS-ABBN	HELIOS
	V15, fresh LEU		
S7	2.109E-05	2.110E-05	2.111E-05
S8	2.101E-05	2.110E-05	2.106E-05
S9	1.604E-05	1.600E-05	1.591E-05
S10	1.877E-05	1.880E-05	1.881E-05
S11	2.047E-05	2.040E-05	2.035E-05
S12	2.106E-05	2.120E-05	2.089E-05
	V16, spent LEU		
S7	1.945E-05	1.920E-05	1.909E-05
S8	1.936E-05	1.900E-05	1.876E-05
S9	1.290E-05	1.260E-05	1.253E-05
S10	1.719E-05	1.700E-05	1.692E-05
S11	1.926E-05	1.900E-05	1.888E-05
S12	2.177E-05	2.190E-05	2.159E-05
	V17, fresh MOX		
S7	1.118E-05	1.080E-05	1.088E-05
S8	1.109E-05	1.070E-05	1.057E-05
S9	8.639E-06	8.300E-06	8.483E-06
S10	1.034E-05	1.010E-05	1.011E-05
S11	1.098E-05	1.060E-05	1.065E-05
S12	1.321E-05	1.310E-05	1.303E-05
	V18, spent MOX		
S7	1.470E-05	1.430E-05	1.427E-05
S8	1.460E-05	1.410E-05	1.388E-05
S9	9.847E-06	9.400E-06	9.493E-06
S10	1.325E-05	1.290E-05	1.292E-05
S11	1.460E-05	1.420E-05	1.417E-05
S12	1.757E-05	1.750E-05	1.739E-05

APPENDIX B. FUEL ASSEMBLIES CALCULATION RESULTS

Figure B- 1 Comparison of K_{eff} burnup dependence for fuel assembly variants (V11-V12).

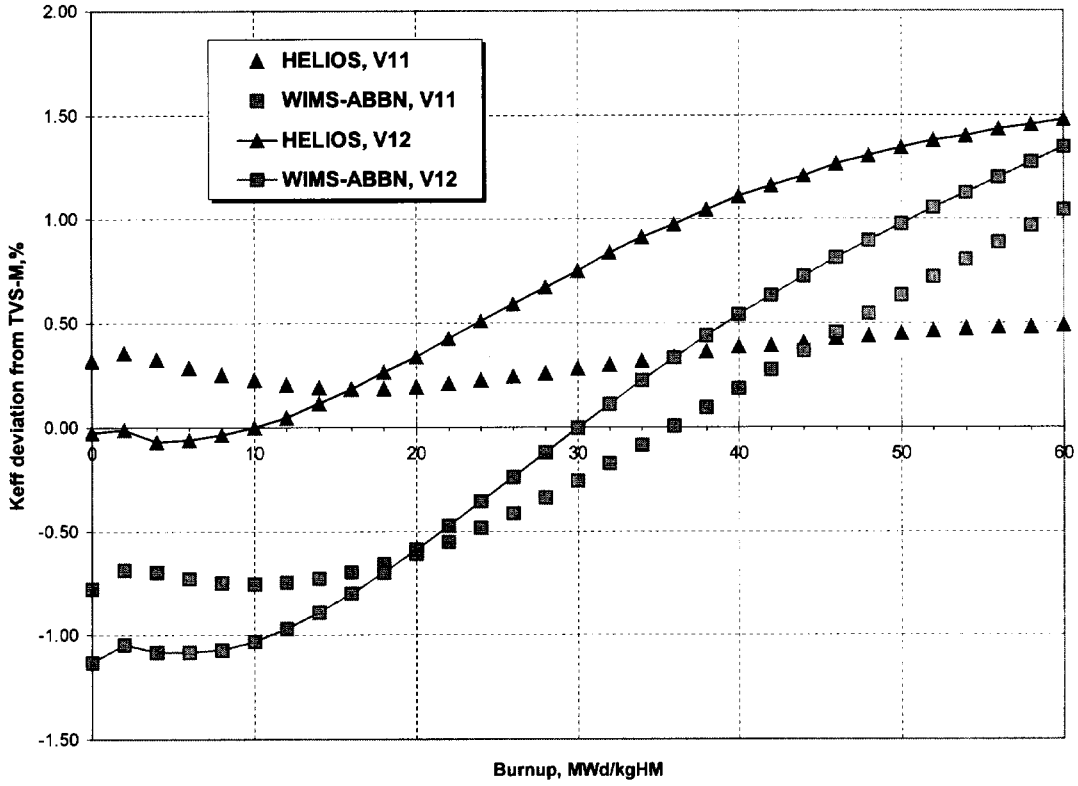

Table B- 1 K_{eff} and K_o values for various states as a function of burnup for LEU fuel assembly (V11).

State	TVS-M		HELIOS		WIMS-ABBN		MCU-RFFI/A	
	keff	k0	keff	k0	keff	k0	keff	k0
	Burnup 0. MWd/kg/HM							
s1	1.0757	1.2803	1.0791	1.2854	1.0673	1.2687	-	-
s2	0.8416	0.9990	0.8412	0.9991	0.8361	0.9933	-	-
s2*	0.8701	1.0331	0.8681	1.0312	-	-	0.8662	1.0280
s3	1.1313	1.3477	1.1351	1.3528	1.1221	1.3349	-	-
s4	1.1189	1.3321	1.1203	1.3347	1.1085	1.3184	1.1172	1.3290
s5	1.1307	1.3469	1.1326	1.3500	1.1226	1.3356	-	-
s6	1.2197	1.3673	1.2226	1.3713	1.2156	1.3619	1.2182	1.3650
	Burnup 10. MWd/kg/HM							
s1	0.9929	1.1814	0.9952	1.1855	0.9854	1.1701	-	-
s2	0.7800	0.9259	0.7817	0.9288	0.7777	0.9230	-	-
s3	1.0423	1.2412	1.0439	1.2441	1.0327	1.2271	-	-
s4	1.0311	1.2272	1.0336	1.2316	1.0237	1.2162	-	-
s5	1.0427	1.2415	1.0457	1.2466	1.0372	1.2327	-	-
s6	1.1323	1.2693	1.1368	1.2756	1.1313	1.2672	-	-
	Burnup 20. MWd/kg/HM							
s1	0.9195	1.0942	0.9213	1.0979	0.9139	1.0852	-	-
s2	0.7229	0.8583	0.7246	0.8613	0.7210	0.8557	-	-
s3	0.9655	1.1498	0.9665	1.1522	0.9575	1.1378	-	-
s4	0.9537	1.1351	0.9569	1.1406	0.9494	1.1280	-	-
s5	0.9655	1.1498	0.9694	1.1561	0.9629	1.1445	-	-
s6	1.0508	1.1782	1.0560	1.1854	1.0530	1.1797	-	-
	Burnup 30. MWd/kg/HM							
s1	0.8552	1.0180	0.8576	1.0225	0.8530	1.0132	-	-
s2	0.6716	0.7975	0.6736	0.8012	0.6711	0.7966	-	-
s3	0.8990	1.0711	0.9007	1.0745	0.8945	1.0633	-	-
s4	0.8858	1.0547	0.8904	1.0619	0.8857	1.0527	-	-
s5	0.8975	1.0691	0.9028	1.0773	0.8987	1.0686	-	-
s6	0.9748	1.0933	0.9809	1.1016	0.9809	1.0994	-	-
	Burnup 40. MWd/kg/HM							
s1	0.7967	0.9487	0.7998	0.9541	0.7982	0.9487	-	-
s2	0.6244	0.7418	0.6267	0.7459	0.6256	0.7428	-	-
s3	0.8390	0.9999	0.8414	1.0043	0.8381	0.9969	-	-
s4	0.8241	0.9816	0.8297	0.9901	0.8281	0.9849	-	-
s5	0.8353	0.9954	0.8417	1.0049	0.8402	0.9997	-	-
s6	0.9026	1.0126	0.9090	1.0212	0.9125	1.0233	-	-
	Burnup 50. MWd/kg/HM							
s1	0.7443	0.8865	0.7476	0.8924	0.7490	0.8908	-	-
s2	0.5822	0.6919	0.5846	0.6961	0.5838	0.6934	-	-
s3	0.7851	0.9360	0.7881	0.9413	0.7876	0.9376	-	-
s4	0.7687	0.9159	0.7749	0.9252	0.7762	0.9237	-	-
s5	0.7793	0.9290	0.7863	0.9393	0.7873	0.9374	-	-
s6	0.8358	0.9380	0.8419	0.9463	0.8491	0.9526	-	-
	Burnup 60. MWd/kg/HM							
s1	0.6993	0.8332	0.7027	0.8393	0.7066	0.8409	-	-
s2	0.5463	0.6493	0.5485	0.6534	0.5472	0.6502	-	-
s3	0.7387	0.8810	0.7421	0.8868	0.7441	0.8864	-	-
s4	0.7212	0.8596	0.7277	0.8693	0.7313	0.8709	-	-
s5	0.7313	0.8720	0.7383	0.8825	0.7415	0.8835	-	-
s6	0.7777	0.8729	0.7831	0.8805	0.7934	0.8906	-	-

Table B- 2 Comparison of K_{eff} and K_o for various states as a function of burnup for LEU fuel assembly (V11).

State	HELIOS		WIMS-ABBN		MCU-RFFI/A	
	keff	k0	keff	k0	keff	k0
	Burnup 0. MWd/kg/HM					
s1	0.32	0.40	-0.78	-0.91	-	-
s2	-0.04	0.01	-0.64	-0.57	-	-
s2*	-0.23	-0.18	-	-	-0.45	-0.49
s3	0.34	0.38	-0.81	-0.95	-	-
s4	0.12	0.19	-0.93	-1.03	-0.15	-0.24
s5	0.16	0.23	-0.72	-0.84	-	-
s6	0.24	0.30	-0.34	-0.39	-0.12	-0.16
	Burnup 10. MWd/kg/HM					
s1	0.23	0.34	-0.76	-0.96	-	-
s2	0.22	0.32	-0.29	-0.30	-	-
s3	0.15	0.23	-0.92	-1.14	-	-
s4	0.24	0.36	-0.72	-0.90	-	-
s5	0.29	0.41	-0.52	-0.71	-	-
s6	0.40	0.50	-0.08	-0.17	-	-
	Burnup 20. MWd/kg/HM					
s1	0.19	0.34	-0.61	-0.82	-	-
s2	0.23	0.35	-0.26	-0.30	-	-
s3	0.11	0.21	-0.82	-1.05	-	-
s4	0.34	0.48	-0.44	-0.63	-	-
s5	0.41	0.55	-0.26	-0.46	-	-
s6	0.49	0.61	0.21	0.13	-	-
	Burnup 30. MWd/kg/HM					
s1	0.28	0.45	-0.26	-0.47	-	-
s2	0.31	0.46	-0.06	-0.11	-	-
s3	0.19	0.32	-0.51	-0.73	-	-
s4	0.52	0.69	-0.01	-0.18	-	-
s5	0.59	0.77	0.14	-0.05	-	-
s6	0.63	0.76	0.63	0.56	-	-
	Burnup 40. MWd/kg/HM					
s1	0.39	0.57	0.18	0.00	-	-
s2	0.36	0.55	0.19	0.14	-	-
s3	0.29	0.44	-0.10	-0.30	-	-
s4	0.68	0.87	0.49	0.34	-	-
s5	0.77	0.96	0.59	0.43	-	-
s6	0.71	0.85	1.10	1.05	-	-
	Burnup 50. MWd/kg/HM					
s1	0.45	0.66	0.63	0.48	-	-
s2	0.41	0.61	0.27	0.23	-	-
s3	0.39	0.57	0.33	0.17	-	-
s4	0.81	1.02	0.97	0.85	-	-
s5	0.89	1.10	1.02	0.90	-	-
s6	0.73	0.88	1.58	1.56	-	-
	Burnup 60. MWd/kg/HM					
s1	0.49	0.73	1.04	0.92	-	-
s2	0.41	0.63	0.17	0.14	-	-
s3	0.46	0.66	0.73	0.61	-	-
s4	0.90	1.13	1.40	1.32	-	-
s5	0.96	1.20	1.40	1.31	-	-
s6	0.70	0.87	2.02	2.02	-	-

Table B- 3 K_{eff} and K_o values for various states as a function of burnup for MOX fuel assembly (V12).

State	TVS-M		HELIOS		WIMS-ABBN		MCU-RFFI/A	
	keff	k0	keff	k0	keff	k0	keff	k0
	Burnup 0. MWd/kg/HM							
s1	1.0486	1.2426	1.0483	1.2451	1.0367	1.2221	-	-
s2	0.8570	1.0142	0.8568	1.0161	0.8537	1.0067	-	-
s2*	0.8710	1.0309	0.8696	1.0313	-	-	0.8628	1.0230
s3	1.0795	1.2800	1.0788	1.2816	1.0665	1.2576	-	-
s4	1.0683	1.2661	1.0663	1.2665	1.0551	1.2440	1.0600	1.2560
s5	1.0826	1.2837	1.0812	1.2849	1.0718	1.2643	-	-
s6	1.1956	1.3376	1.1995	1.3445	1.1927	1.3293	1.1904	1.3310
	Burnup 10. MWd/kg/HM							
s1	0.9402	1.1144	0.9402	1.1167	0.9305	1.0975	-	-
s2	0.7654	0.9059	0.7669	0.9095	0.7638	0.9011	-	-
s3	0.9702	1.1507	0.9689	1.1511	0.9589	1.1313	-	-
s4	0.9714	1.1515	0.9707	1.1530	0.9610	1.1337	-	-
s5	0.9848	1.1679	0.9849	1.1705	0.9764	1.1524	-	-
s6	1.0852	1.2143	1.0892	1.2210	1.0838	1.2085	-	-
	Burnup 20. MWd/kg/HM							
s1	0.8715	1.0333	0.8744	1.0387	0.8663	1.0226	-	-
s2	0.7055	0.8353	0.7094	0.8414	0.7066	0.8341	-	-
s3	0.9021	1.0704	0.9039	1.0740	0.8952	1.0570	-	-
s4	0.9003	1.0677	0.9040	1.0740	0.8958	1.0577	-	-
s5	0.9126	1.0828	0.9174	1.0904	0.9099	1.0748	-	-
s6	1.0005	1.1199	1.0083	1.1304	1.0045	1.1209	-	-
	Burnup 30. MWd/kg/HM							
s1	0.8128	0.9642	0.8189	0.9731	0.8128	0.9602	-	-
s2	0.6542	0.7748	0.6603	0.7832	0.6583	0.7777	-	-
s3	0.8443	1.0023	0.8495	1.0097	0.8424	0.9957	-	-
s4	0.8394	0.9960	0.8472	1.0069	0.8409	0.9939	-	-
s5	0.8509	1.0101	0.8599	1.0225	0.8538	1.0095	-	-
s6	0.9266	1.0374	0.9376	1.0513	0.9360	1.0453	-	-
	Burnup 40. MWd/kg/HM							
s1	0.7624	0.9049	0.7709	0.9163	0.7665	0.9066	-	-
s2	0.6102	0.7229	0.6175	0.7327	0.6164	0.7288	-	-
s3	0.7947	0.9439	0.8025	0.9542	0.7969	0.9430	-	-
s4	0.7869	0.9341	0.7976	0.9483	0.7931	0.9384	-	-
s5	0.7978	0.9475	0.8097	0.9632	0.8049	0.9528	-	-
s6	0.8623	0.9658	0.8751	0.9815	0.8761	0.9791	-	-
	Burnup 50. MWd/kg/HM							
s1	0.7203	0.8553	0.7300	0.8682	0.7274	0.8611	-	-
s2	0.5735	0.6797	0.5812	0.6900	0.5811	0.6876	-	-
s3	0.7532	0.8951	0.7625	0.9073	0.7583	0.8984	-	-
s4	0.7428	0.8823	0.7552	0.8984	0.7523	0.8911	-	-
s5	0.7532	0.8951	0.7668	0.9126	0.7632	0.9044	-	-
s6	0.8084	0.9057	0.8217	0.9218	0.8251	0.9229	-	-
	Burnup 60. MWd/kg/HM							
s1	0.6861	0.8150	0.6962	0.8285	0.6953	0.8240	-	-
s2	0.5439	0.6448	0.5515	0.6550	0.5522	0.6540	-	-
s3	0.7194	0.8553	0.7295	0.8686	0.7268	0.8620	-	-
s4	0.7070	0.8400	0.7200	0.8571	0.7188	0.8523	-	-
s5	0.7170	0.8523	0.7311	0.8707	0.7289	0.8647	-	-
s6	0.7644	0.8566	0.7775	0.8726	0.7835	0.8770	-	-

Table B- 4 Comparison of K_{eff} and K_o for various states as a function of burnup for MOX fuel assembly (V12).

State	HELIOS		WIMS-ABBN		MCU-RFFI/A	
	keff	k0	keff	k0	keff	k0
	Burnup 0. MWd/kg/HM					
s1	-0.03	0.20	-1.13	-1.65	-	-
s2	-0.03	0.19	-0.39	-0.74	-	-
s2*	-0.17	0.04	-	-	-0.94	-0.76
s3	-0.06	0.13	-1.21	-1.75	-	-
s4	-0.19	0.03	-1.24	-1.74	-0.78	-0.80
s5	-0.13	0.10	-1.00	-1.51	-	-
s6	0.32	0.52	-0.24	-0.62	-0.44	-0.49
	Burnup 10. MWd/kg/HM					
s1	0.00	0.21	-1.03	-1.52	-	-
s2	0.20	0.40	-0.20	-0.53	-	-
s3	-0.14	0.04	-1.17	-1.68	-	-
s4	-0.07	0.13	-1.07	-1.54	-	-
s5	0.02	0.22	-0.84	-1.32	-	-
s6	0.37	0.56	-0.13	-0.48	-	-
	Burnup 20. MWd/kg/HM					
s1	0.34	0.52	-0.59	-1.04	-	-
s2	0.55	0.73	0.16	-0.14	-	-
s3	0.20	0.34	-0.77	-1.25	-	-
s4	0.41	0.59	-0.50	-0.93	-	-
s5	0.52	0.70	-0.30	-0.74	-	-
s6	0.78	0.94	0.40	0.09	-	-
	Burnup 30. MWd/kg/HM					
s1	0.75	0.92	-0.01	-0.41	-	-
s2	0.93	1.08	0.62	0.37	-	-
s3	0.61	0.74	-0.23	-0.66	-	-
s4	0.93	1.10	0.18	-0.21	-	-
s5	1.06	1.23	0.34	-0.06	-	-
s6	1.19	1.34	1.02	0.76	-	-
	Burnup 40. MWd/kg/HM					
s1	1.11	1.26	0.54	0.18	-	-
s2	1.20	1.35	1.02	0.82	-	-
s3	0.98	1.09	0.28	-0.10	-	-
s4	1.36	1.52	0.79	0.46	-	-
s5	1.50	1.66	0.90	0.56	-	-
s6	1.49	1.63	1.60	1.38	-	-
	Burnup 50. MWd/kg/HM					
s1	1.34	1.50	0.98	0.68	-	-
s2	1.34	1.51	1.32	1.16	-	-
s3	1.23	1.37	0.68	0.37	-	-
s4	1.66	1.83	1.27	1.00	-	-
s5	1.80	1.96	1.33	1.04	-	-
s6	1.65	1.78	2.08	1.90	-	-
	Burnup 60. MWd/kg/HM					
s1	1.48	1.66	1.35	1.11	-	-
s2	1.40	1.59	1.53	1.43	-	-
s3	1.41	1.56	1.03	0.78	-	-
s4	1.84	2.03	1.67	1.46	-	-
s5	1.97	2.16	1.67	1.45	-	-
s6	1.71	1.86	2.50	2.37	-	-

Table B- 5 Comparison of various reactivity effects values for several burnup points (LEU pin cell, variant V11)

Effect	Initial state	Final state	Effect value, $(K_i-K_j)/(K_i*K_j)$, %			Deviation from TVS-M,%	
			TVS-M	HELIOS	WIMS -ABBN	HELIOS	WIMS-ABBN
	Burnup 0. MWd/kgHM						
Doppler effect, T_f : 579K→ 1027K	S5	S4	-0.82	-0.85	-0.98	3.29	18.64
Boron effect, C_B : 0.0 → 0.6 g/kg	S3	S1	-3.91	-3.88	-3.91	-0.76	0.21
Poisoning effect	S4	S1	-3.04	-2.87	-2.97	-5.46	-2.17
Total temperature effect, Tm : 300K → 579K	S6	S5	-1.11	-1.15	-1.45	4.07	30.94
Control rods worth, B_4C	S1	S2	-21.73	-22.05	-21.85	1.47	0.55
	Burnup 10. MWd/kgHM						
Doppler effect, T_f : 579K→ 1027K	S5	S4	-0.94	-0.98	-1.10	4.02	17.16
Boron effect, C_B : 0.0 → 0.6 g/kg	S3	S1	-4.08	-3.97	-3.97	-2.54	-2.63
Poisoning effect	S4	S1	-3.16	-3.16	-3.24	0.01	2.69
Total temperature effect, Tm : 300K → 579K	S6	S5	-1.76	-1.82	-2.21	3.53	25.29
Control rods worth, B_4C	S1	S2	-23.37	-23.31	-22.87	-0.23	-2.11
	Burnup 20. MWd/kgHM						
Doppler effect, T_f : 579K→ 1027K	S5	S4	-1.12	-1.18	-1.27	4.86	13.71
Boron effect, C_B : 0.0 → 0.6 g/kg	S3	S1	-4.42	-4.29	-4.26	-2.90	-3.61
Poisoning effect	S4	S1	-3.29	-3.41	-3.50	3.51	6.18
Total temperature effect, Tm : 300K → 579K	S6	S5	-2.10	-2.14	-2.61	1.83	24.32
Control rods worth, B_4C	S1	S2	-25.12	-25.02	-24.71	-0.41	-1.63
	Burnup 30. MWd/kgHM						
Doppler effect, T_f : 579K→ 1027K	S5	S4	-1.28	-1.35	-1.41	5.33	10.01
Boron effect, C_B : 0.0 → 0.6 g/kg	S3	S1	-4.87	-4.73	-4.65	-2.80	-4.56
Poisoning effect	S4	S1	-3.42	-3.63	-3.71	6.13	8.38
Total temperature effect, Tm : 300K → 579K	S6	S5	-2.07	-2.05	-2.62	-1.07	26.70
Control rods worth, B_4C	S1	S2	-27.16	-27.01	-26.84	-0.53	-1.17
	Burnup 40. MWd/kgHM						
Doppler effect, T_f : 579K→ 1027K	S5	S4	-1.42	-1.49	-1.50	5.01	6.08
Boron effect, C_B : 0.0 → 0.6 g/kg	S3	S1	-5.40	-5.24	-5.10	-2.90	-5.40
Poisoning effect	S4	S1	-3.53	-3.81	-3.87	8.03	9.84
Total temperature effect, Tm : 300K → 579K	S6	S5	-1.71	-1.59	-2.31	-6.87	35.31
Control rods worth, B_4C	S1	S2	-29.40	-29.26	-29.21	-0.50	-0.66
	Burnup 50. MWd/kgHM						
Doppler effect, T_f : 579K→ 1027K	S5	S4	-1.54	-1.62	-1.57	5.07	1.98
Boron effect, C_B : 0.0 → 0.6 g/kg	S3	S1	-5.96	-5.82	-5.60	-2.32	-5.98
Poisoning effect	S4	S1	-3.62	-3.97	-4.01	9.89	10.81
Total temperature effect, Tm : 300K → 579K	S6	S5	-1.03	-0.79	-1.71	-23.41	66.39
Control rods worth, B_4C	S1	S2	-31.74	-31.60	-31.95	-0.45	0.64
	Burnup 60. MWd/kgHM						
Doppler effect, T_f : 579K→ 1027K	S5	S4	-1.66	-1.72	-1.63	3.51	-2.11
Boron effect, C_B : 0.0 → 0.6 g/kg	S3	S1	-6.51	-6.38	-6.10	-1.98	-6.31
Poisoning effect	S4	S1	-3.68	-4.11	-4.10	11.70	11.39
Total temperature effect, Tm : 300K → 579K	S6	S5	-0.12	0.26	-0.91	-317.70	668.94
Control rods worth, B_4C	S1	S2	-34.00	-33.90	-34.88	-0.28	2.62

Table B- 6 Comparison of various reactivity effects values for several burnup points (MOX pin cell, variant V12)

Effect	Initial state	Final state	Effect value, $(K_i-K_j)/(K_i*K_j)$, %			Deviation from TVS-M, %	
			TVS-M	HELIOS	WIMS-ABBN	HELIOS	WIMS-ABBN
	Burnup 0. MWd/kgHM						
Doppler effect, T_f : 579K→ 1027K	S5	S4	-1.08	-1.13	-1.29	4.35	19.04
Boron effect, C_B : 0.0 → 0.6 g/kg	S3	S1	-2.35	-2.29	-2.31	-2.64	-1.77
Poisoning effect	S4	S1	-1.49	-1.36	-1.44	-8.92	-3.41
Total temperature effect, Tm : 300K → 579K	S6	S5	-3.14	-3.45	-3.87	9.90	23.16
Control rods worth, B_4C	S1	S2	-18.02	-18.01	-17.51	-0.08	-2.83
	Burnup 10. MWd/kgHM						
Doppler effect, T_f : 579K→ 1027K	S5	S4	-1.22	-1.30	-1.44	6.20	17.53
Boron effect, C_B : 0.0 → 0.6 g/kg	S3	S1	-2.83	-2.68	-2.72	-5.37	-3.66
Poisoning effect	S4	S1	-2.89	-2.82	-2.91	-2.45	0.78
Total temperature effect, Tm : 300K → 579K	S6	S5	-3.27	-3.53	-4.02	8.09	23.09
Control rods worth, B_4C	S1	S2	-20.66	-20.40	-19.86	-1.25	-3.86
	Burnup 20. MWd/kgHM						
Doppler effect, T_f : 579K→ 1027K	S5	S4	-1.31	-1.40	-1.50	6.94	14.70
Boron effect, C_B : 0.0 → 0.6 g/kg	S3	S1	-3.35	-3.16	-3.19	-5.55	-4.76
Poisoning effect	S4	S1	-3.11	-3.16	-3.25	1.62	4.39
Total temperature effect, Tm : 300K → 579K	S6	S5	-3.06	-3.25	-3.82	6.16	25.12
Control rods worth, B_4C	S1	S2	-22.94	-22.58	-22.09	-1.61	-3.73
	Burnup 30. MWd/kgHM						
Doppler effect, T_f : 579K→ 1027K	S5	S4	-1.41	-1.52	-1.56	7.73	10.78
Boron effect, C_B : 0.0 → 0.6 g/kg	S3	S1	-3.94	-3.73	-3.71	-5.37	-5.78
Poisoning effect	S4	S1	-3.30	-3.45	-3.53	4.50	6.83
Total temperature effect, Tm : 300K → 579K	S6	S5	-2.61	-2.68	-3.39	2.76	29.86
Control rods worth, B_4C	S1	S2	-25.36	-24.92	-24.45	-1.74	-3.57
	Burnup 40. MWd/kgHM						
Doppler effect, T_f : 579K→ 1027K	S5	S4	-1.51	-1.63	-1.61	7.91	6.37
Boron effect, C_B : 0.0 → 0.6 g/kg	S3	S1	-4.56	-4.33	-4.26	-5.02	-6.65
Poisoning effect	S4	S1	-3.45	-3.68	-3.74	6.64	8.44
Total temperature effect, Tm : 300K → 579K	S6	S5	-2.00	-1.94	-2.82	-3.15	41.24
Control rods worth, B_4C	S1	S2	-27.82	-27.35	-26.90	-1.71	-3.33
	Burnup 50. MWd/kgHM						
Doppler effect, T_f : 579K→ 1027K	S5	S4	-1.62	-1.73	-1.65	6.94	1.86
Boron effect, C_B : 0.0 → 0.6 g/kg	S3	S1	-5.19	-4.96	-4.82	-4.37	-7.23
Poisoning effect	S4	S1	-3.57	-3.87	-3.91	8.46	9.53
Total temperature effect, Tm : 300K → 579K	S6	S5	-1.31	-1.09	-2.21	-16.21	69.51
Control rods worth, B_4C	S1	S2	-30.21	-29.75	-29.30	-1.53	-3.00
	Burnup 60. MWd/kgHM						
Doppler effect, T_f : 579K→ 1027K	S5	S4	-1.72	-1.82	-1.68	6.08	-2.21
Boron effect, C_B : 0.0 → 0.6 g/kg	S3	S1	-5.78	-5.57	-5.34	-3.55	-7.51
Poisoning effect	S4	S1	-3.66	-4.03	-4.03	10.13	10.10
Total temperature effect, Tm : 300K → 579K	S6	S5	-0.59	-0.25	-1.62	-57.64	174.56
Control rods worth, B_4C	S1	S2	-32.40	-31.97	-31.56	-1.32	-2.60

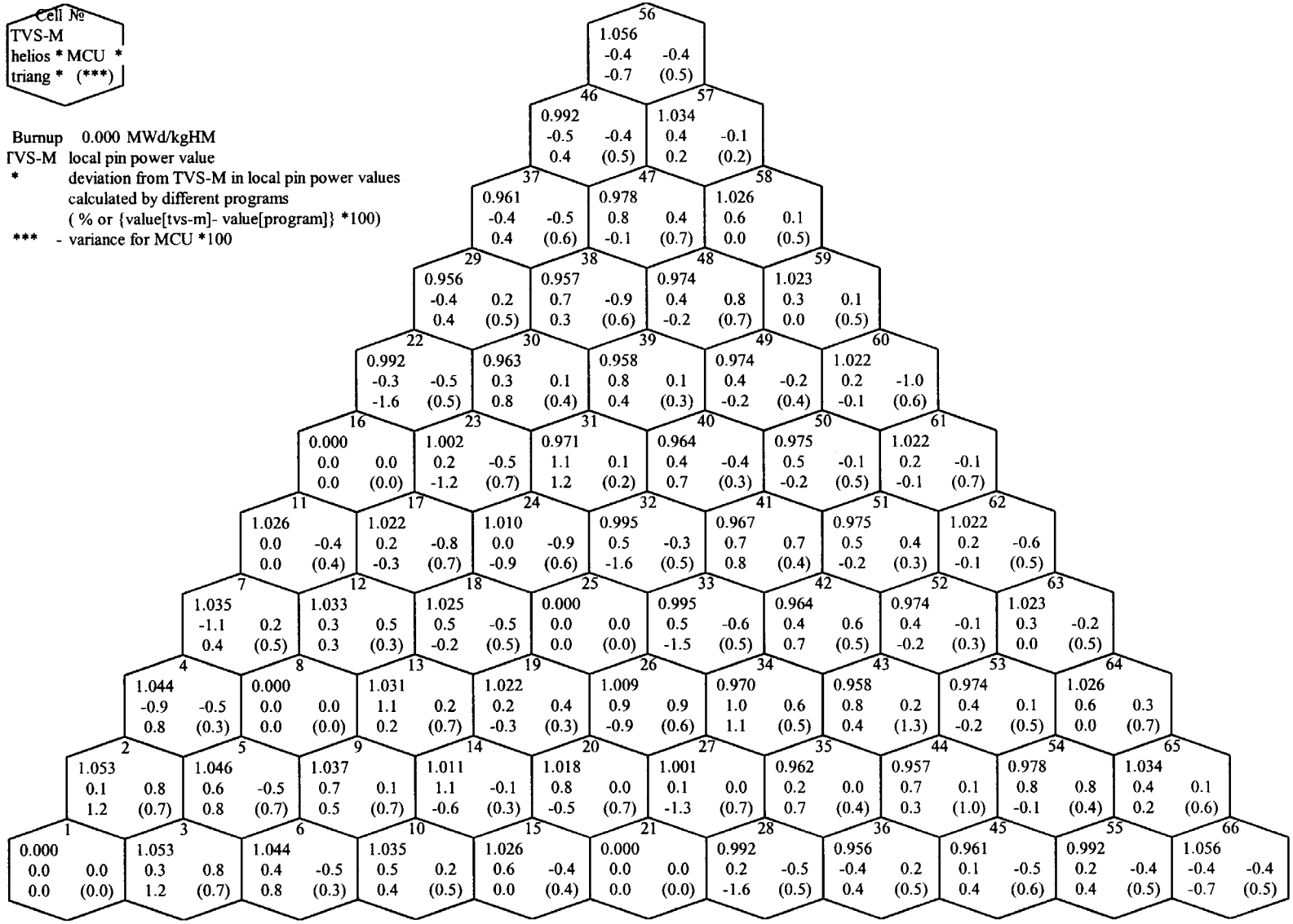

Figure B- 2 Deviation from TVS-M in local pin power values for state S1. Burnup 0 MWd/kgHM. Variant V11 (%)

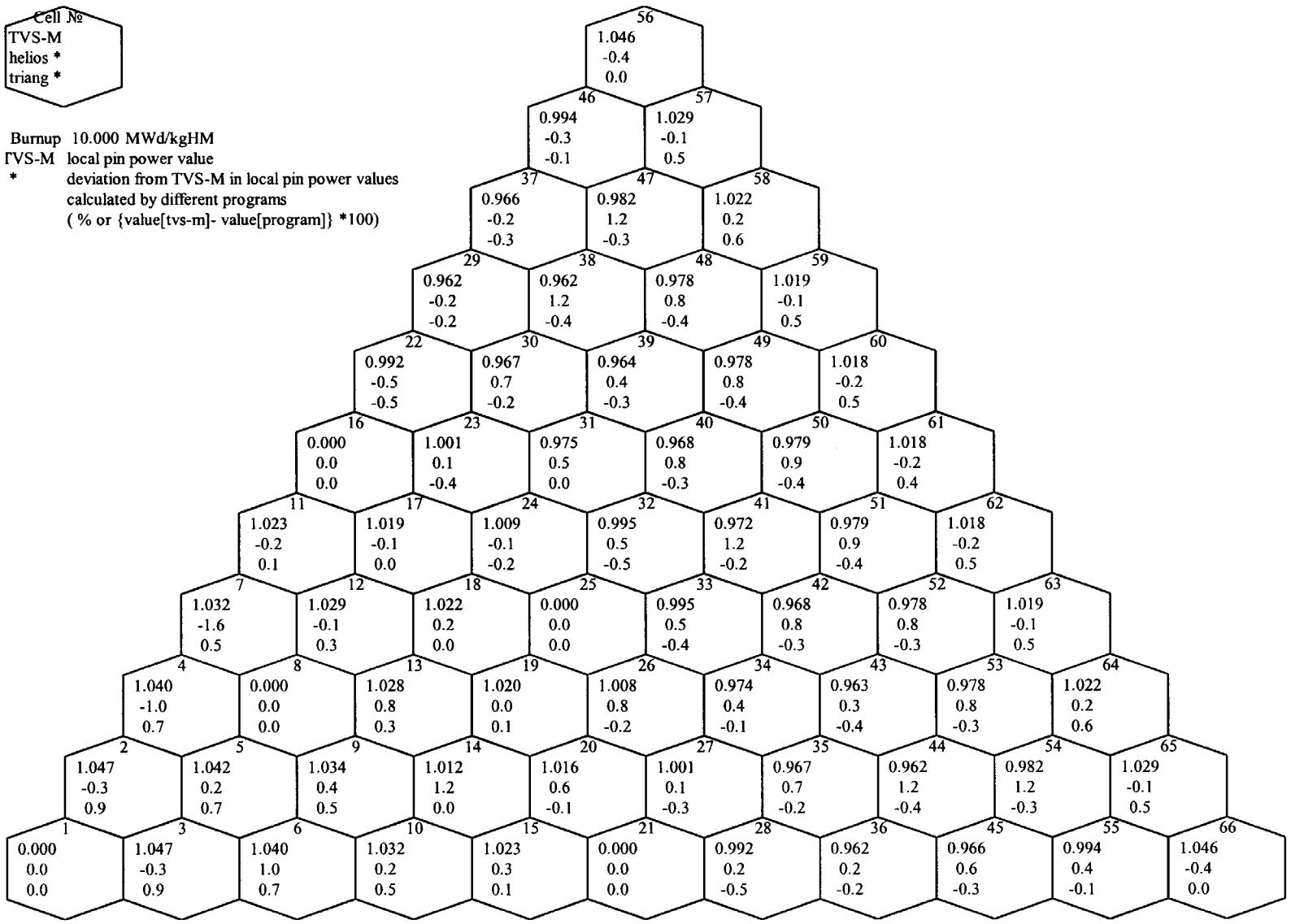

Figure B- 3 Deviation from TVS-M in local pin power values for state S1. Burnup 10 MWd/kgHM. Variant V11 (%)

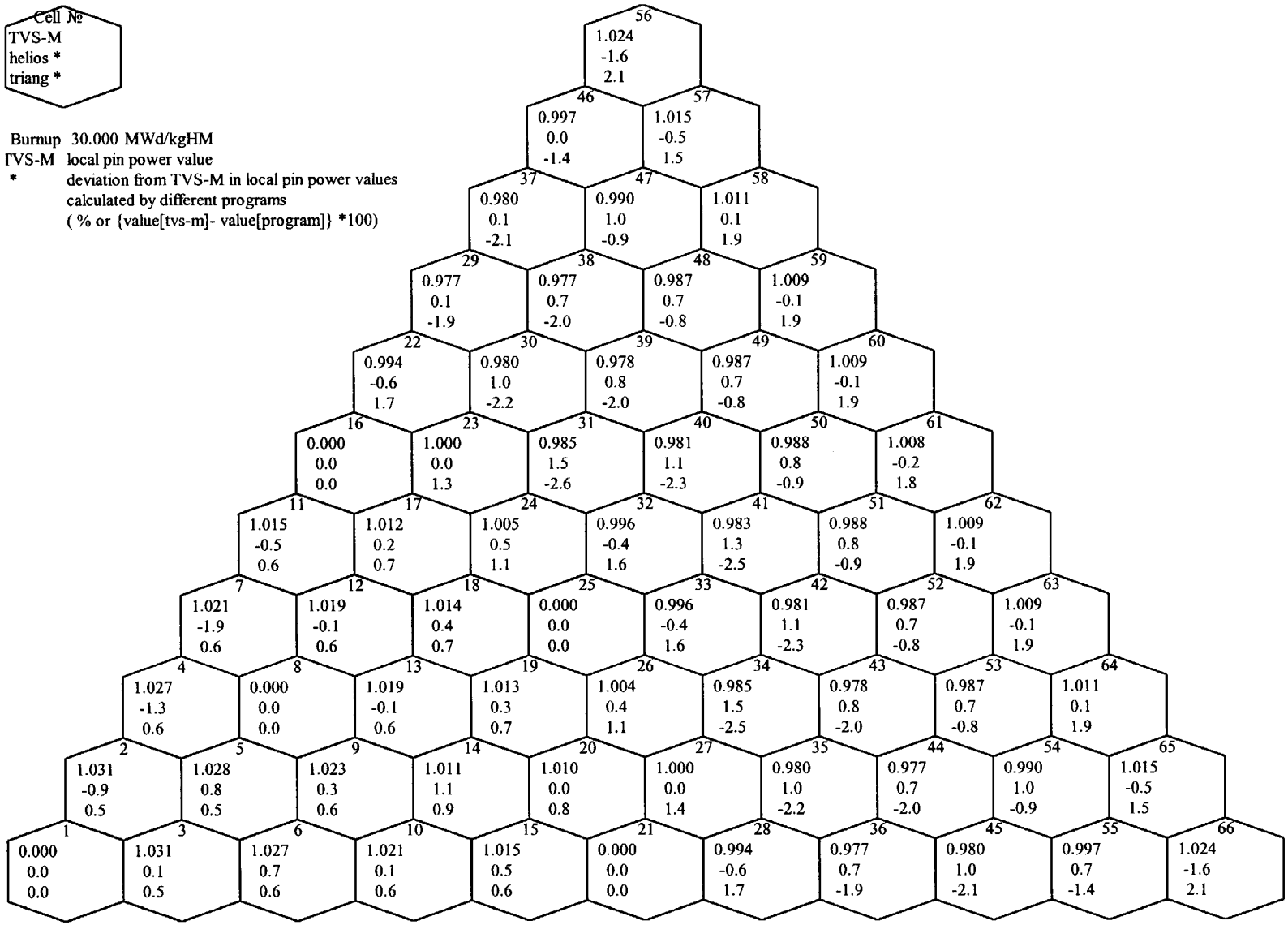

Figure B- 4 Deviation from TVS-M in local pin power values for state S1. Burnup 30 MWd/kgHM. Variant V11 (%)

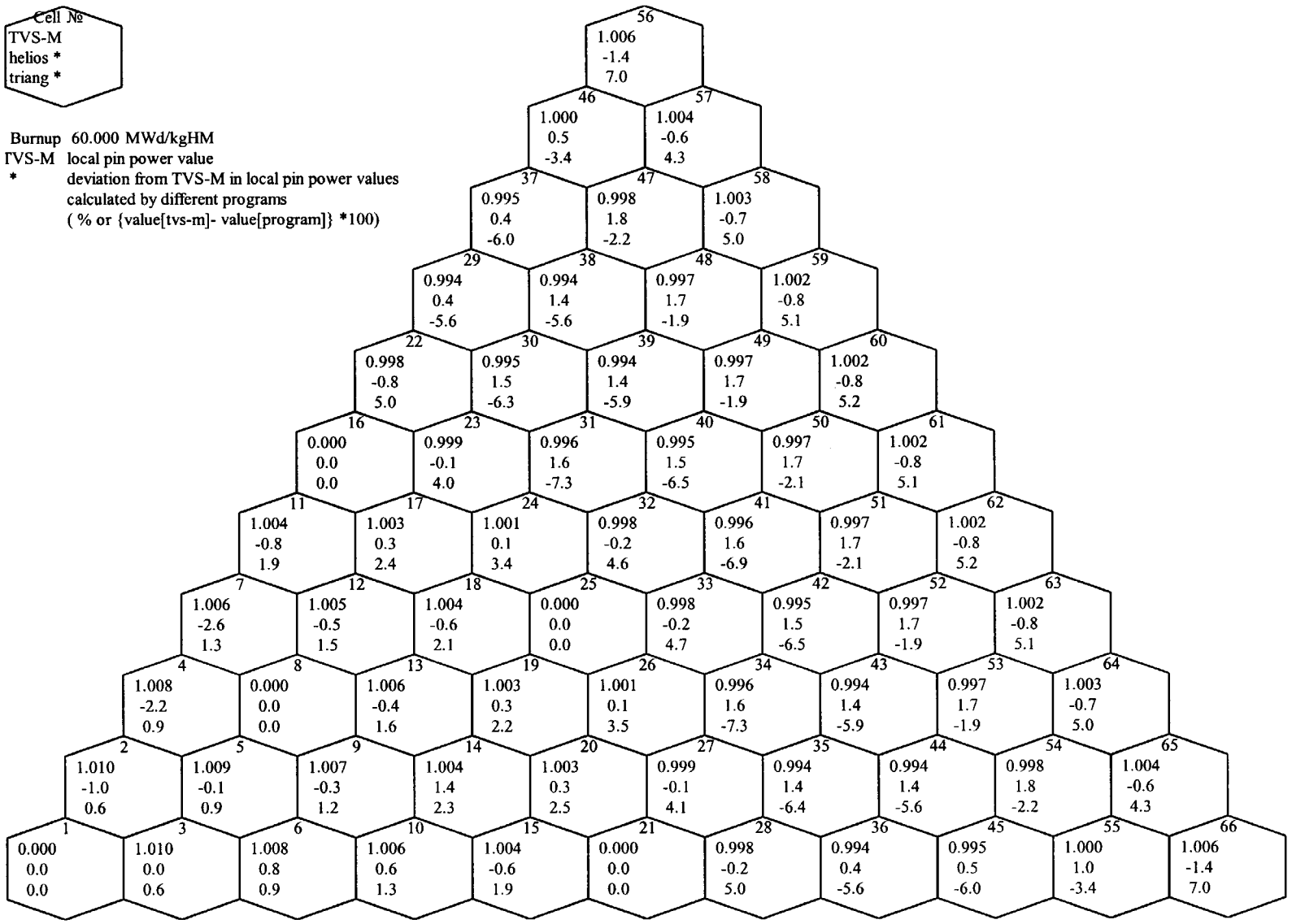

Figure B- 5 Deviation from TVS-M in local pin power values for state S1. Burnup 60 MWd/kgHM. Variant V11 (%)

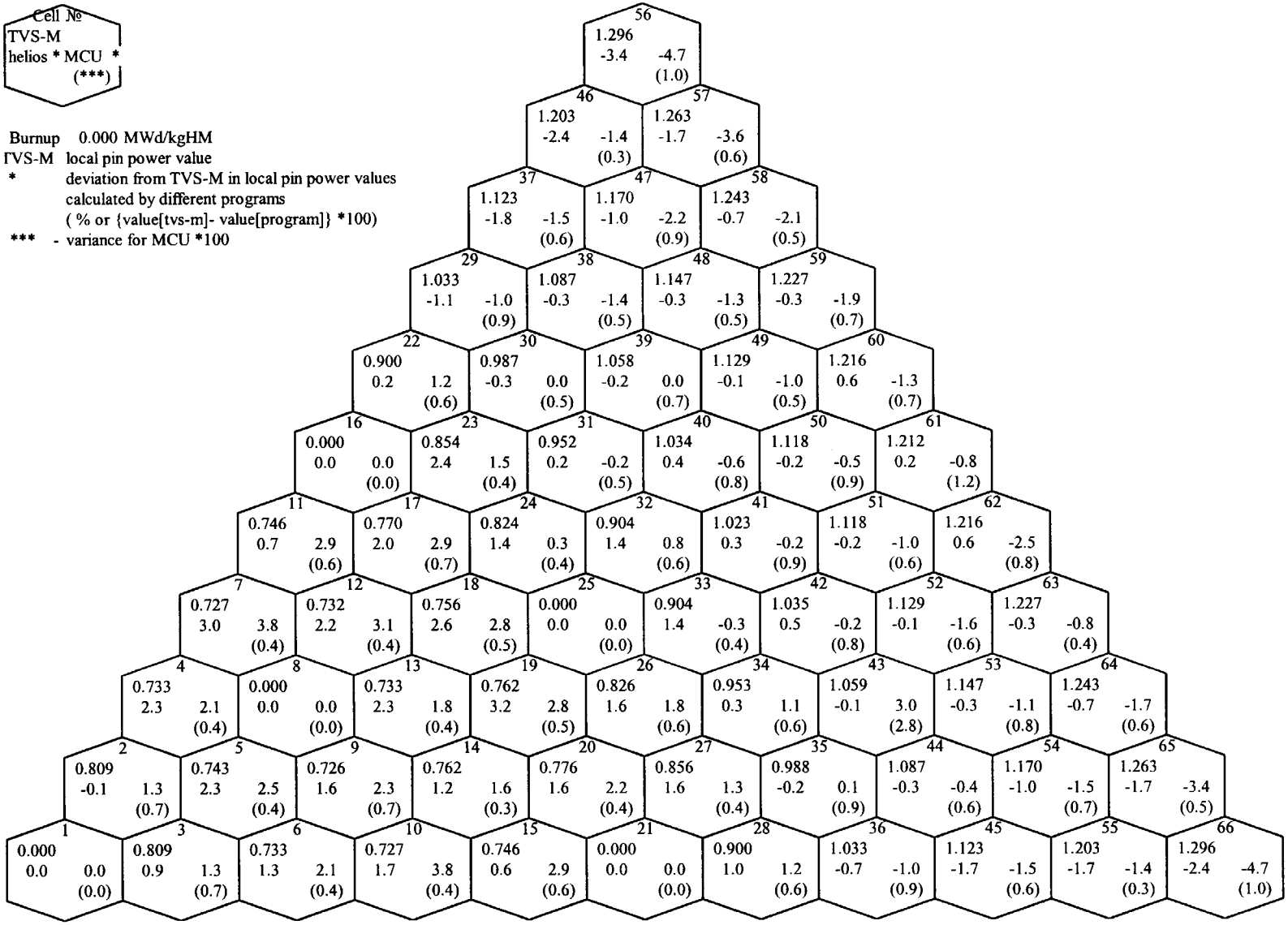

Figure B- 6 Deviation from TVS-M in local pin power values for state S2. Burnup 0 MWd/kgHM. Variant V11 (%)

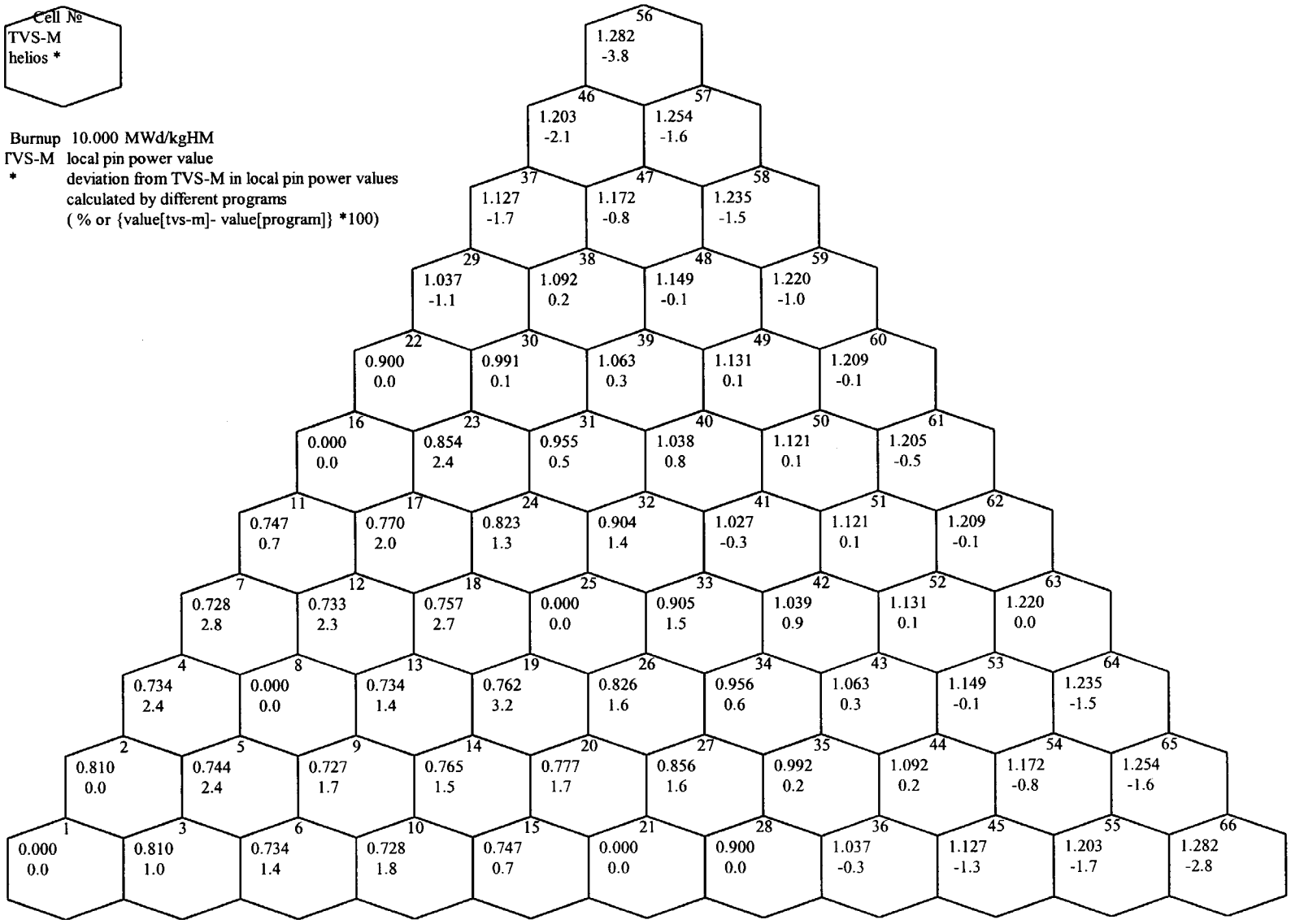

Figure B- 7 Deviation from TVS-M in local pin power values for state S2. Burnup 10 MWd/kgHM. Variant V11 (%)

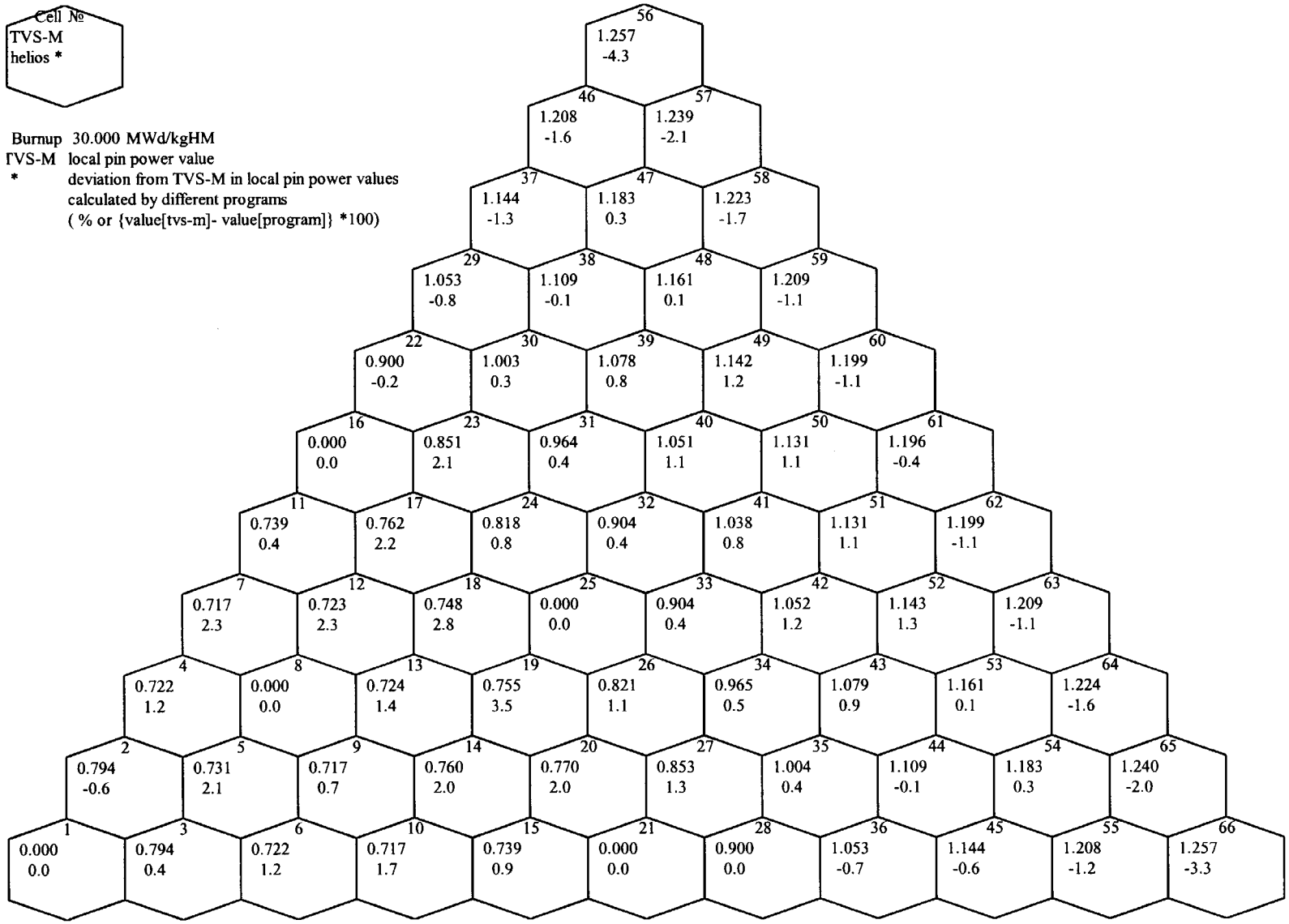

Figure B- 8 Deviation from TVS-M in local pin power values for state S2. Burnup 30 MWd/kgHM. Variant V11 (%)

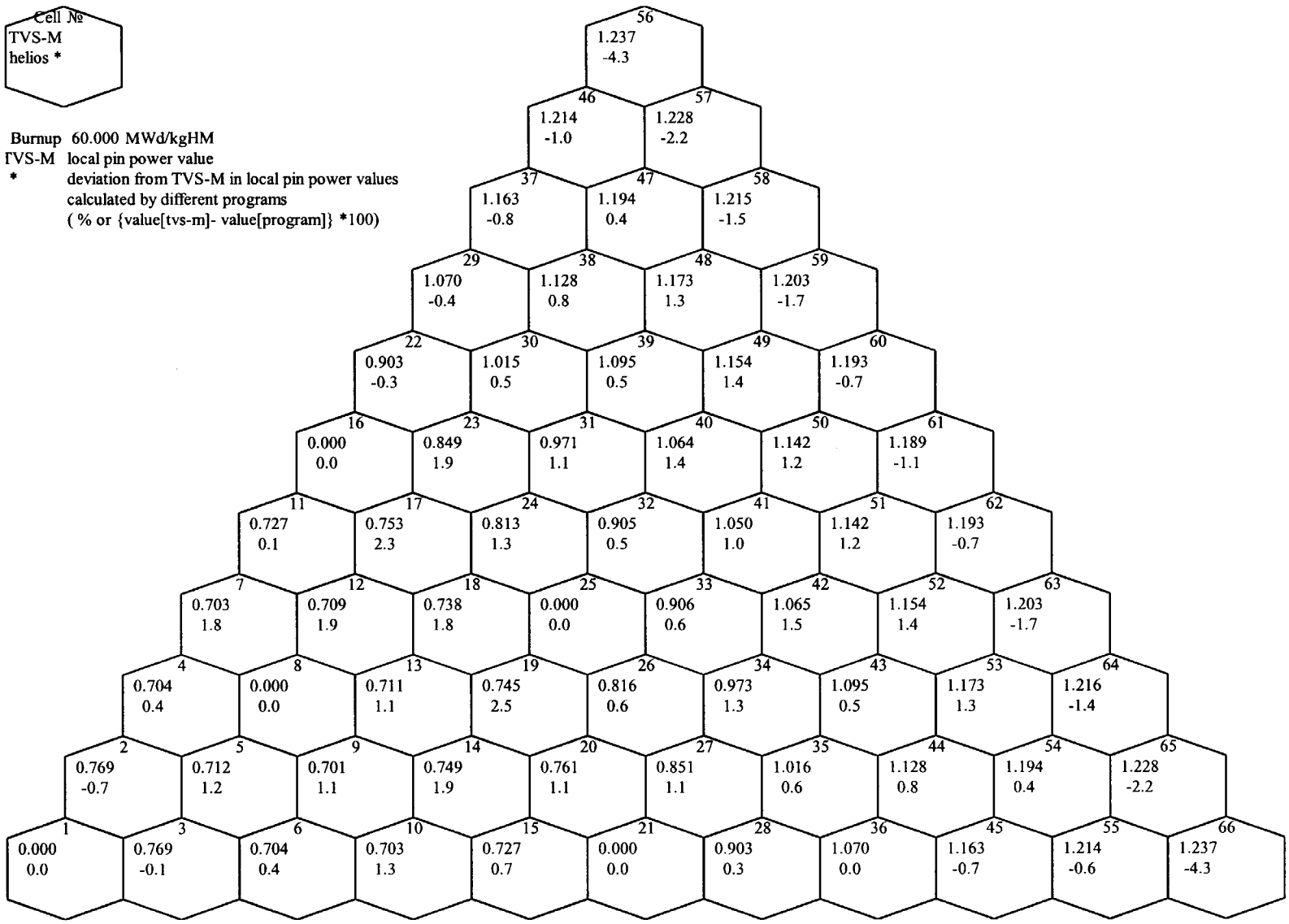

Figure B- 9 Deviation from TVS-M in local pin power values for state S2. Burnup 60 MWd/kgHM. Variant V11 (%)

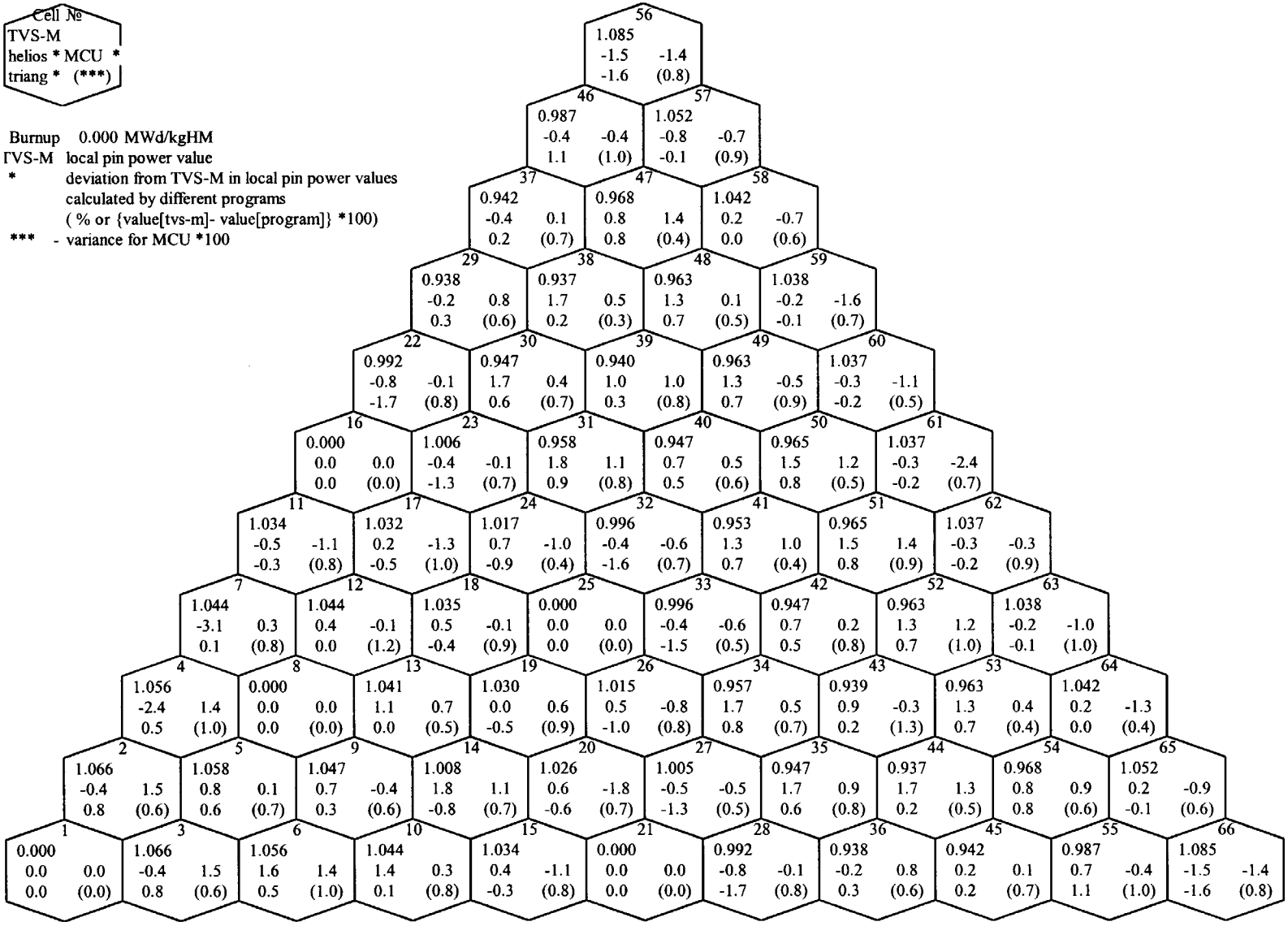

Figure B- 10 Deviation from TVS-M in local pin power values for state S1. Burnup 0 MWd/kgHM. Variant V12 (%)

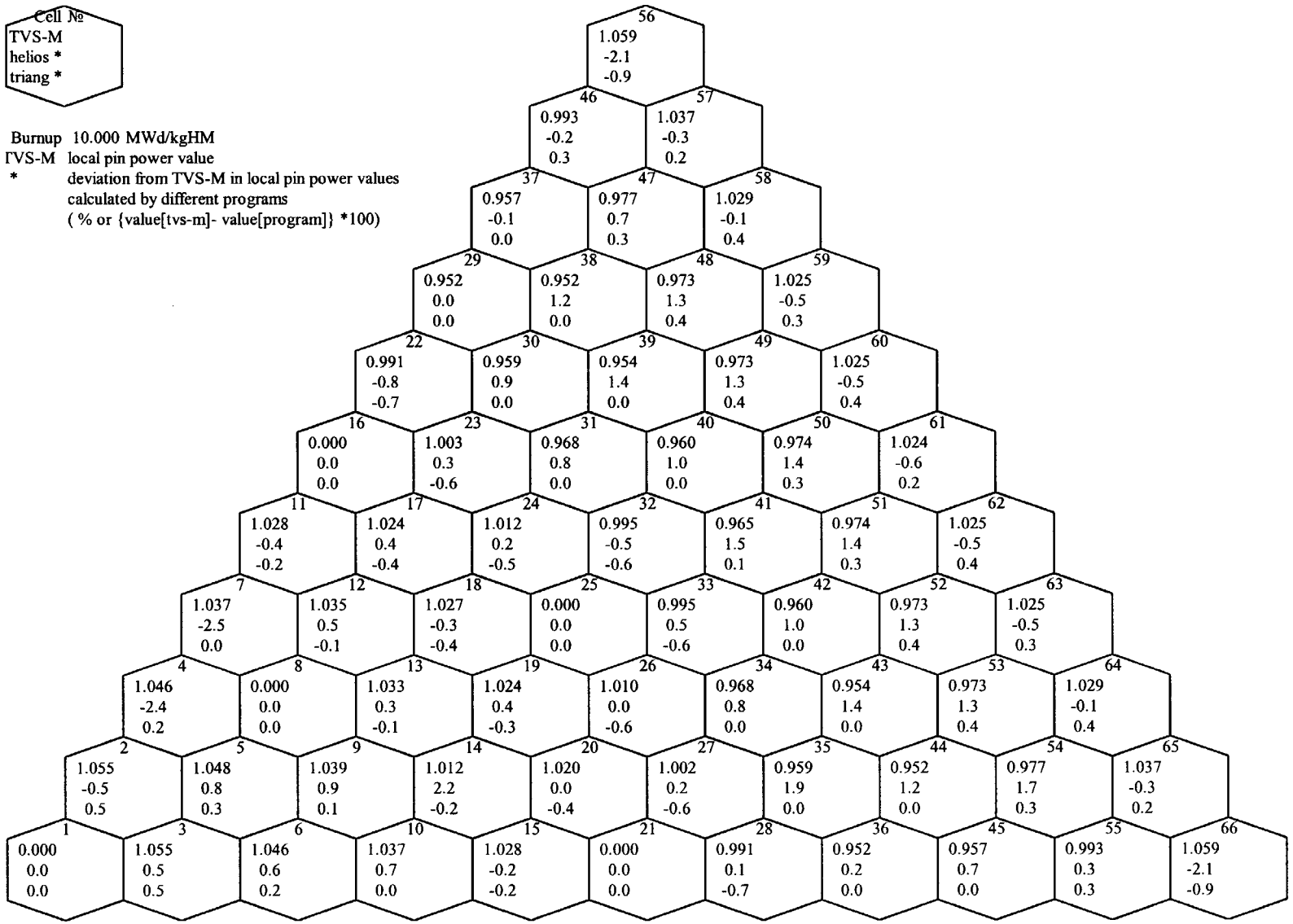

Figure B- 11 Deviation from TVS-M in local pin power values for state S1. Burnup 10 MWd/kgHM. Variant V12 (%)

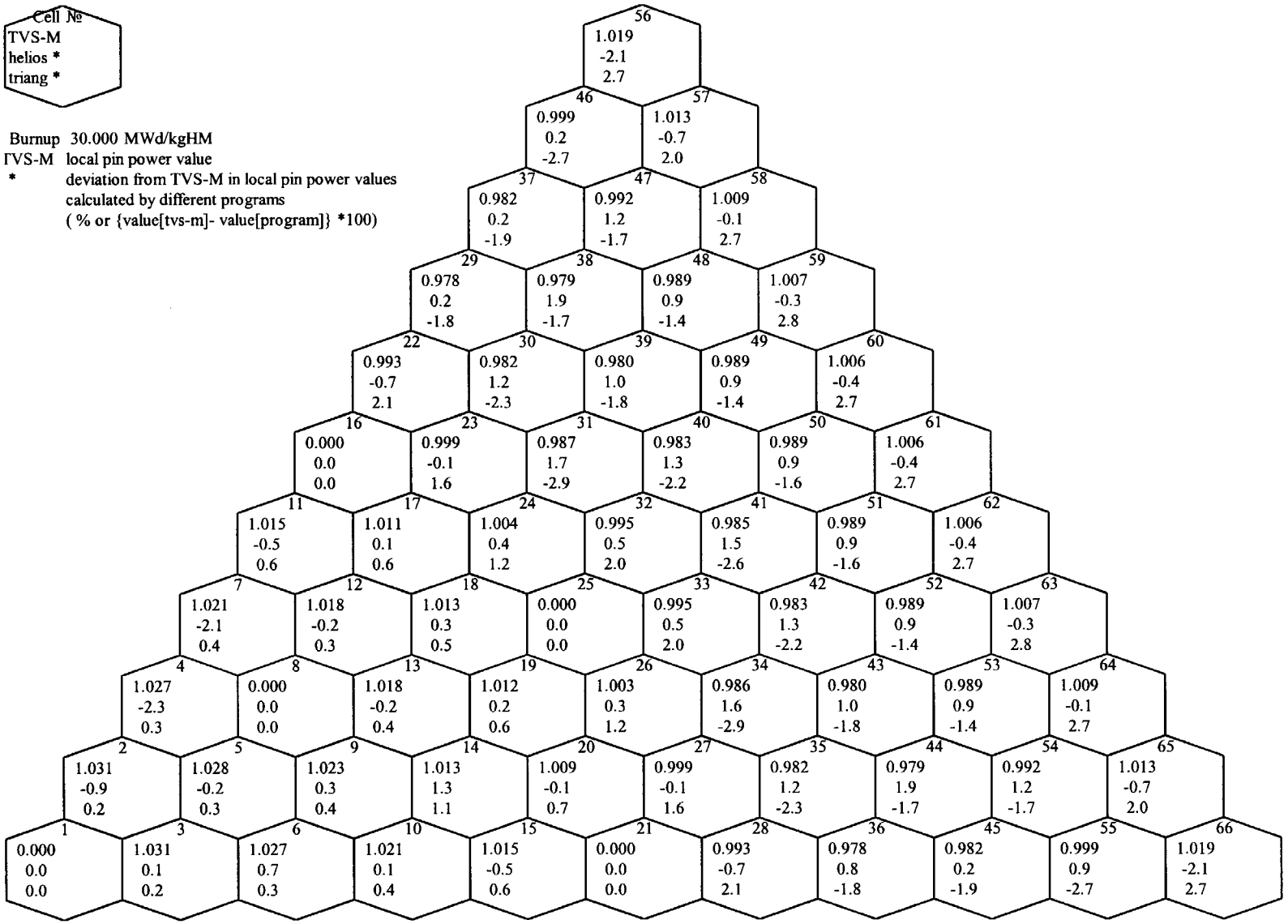

Figure B- 12 Deviation from TVS-M in local pin power values for state S1. Burnup 30 MWd/kgHM. Variant V12 (%)

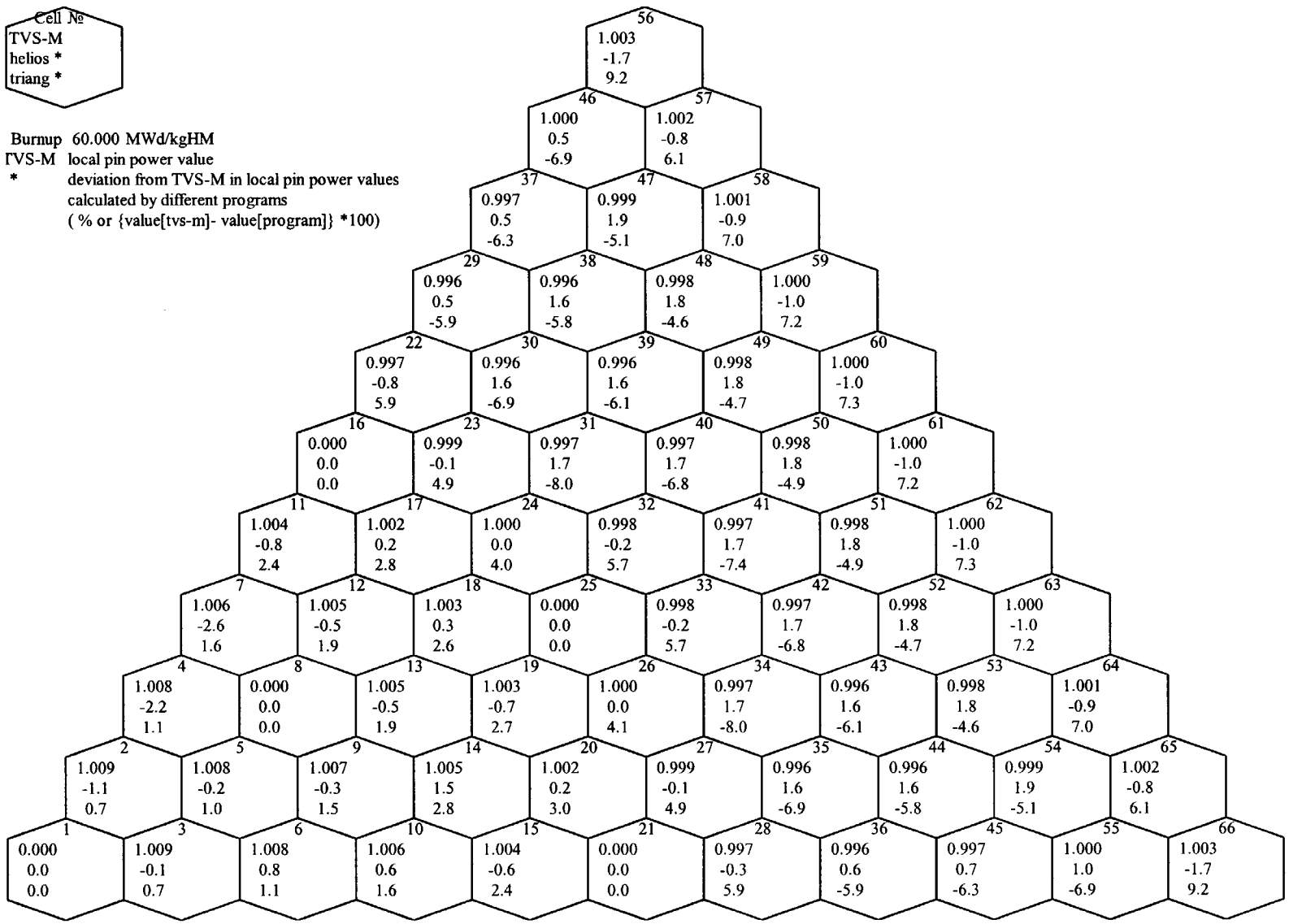

Figure B- 13 Deviation from TVS-M in local pin power values for state S1. Burnup 60 MWd/kgHM. Variant V12 (%)

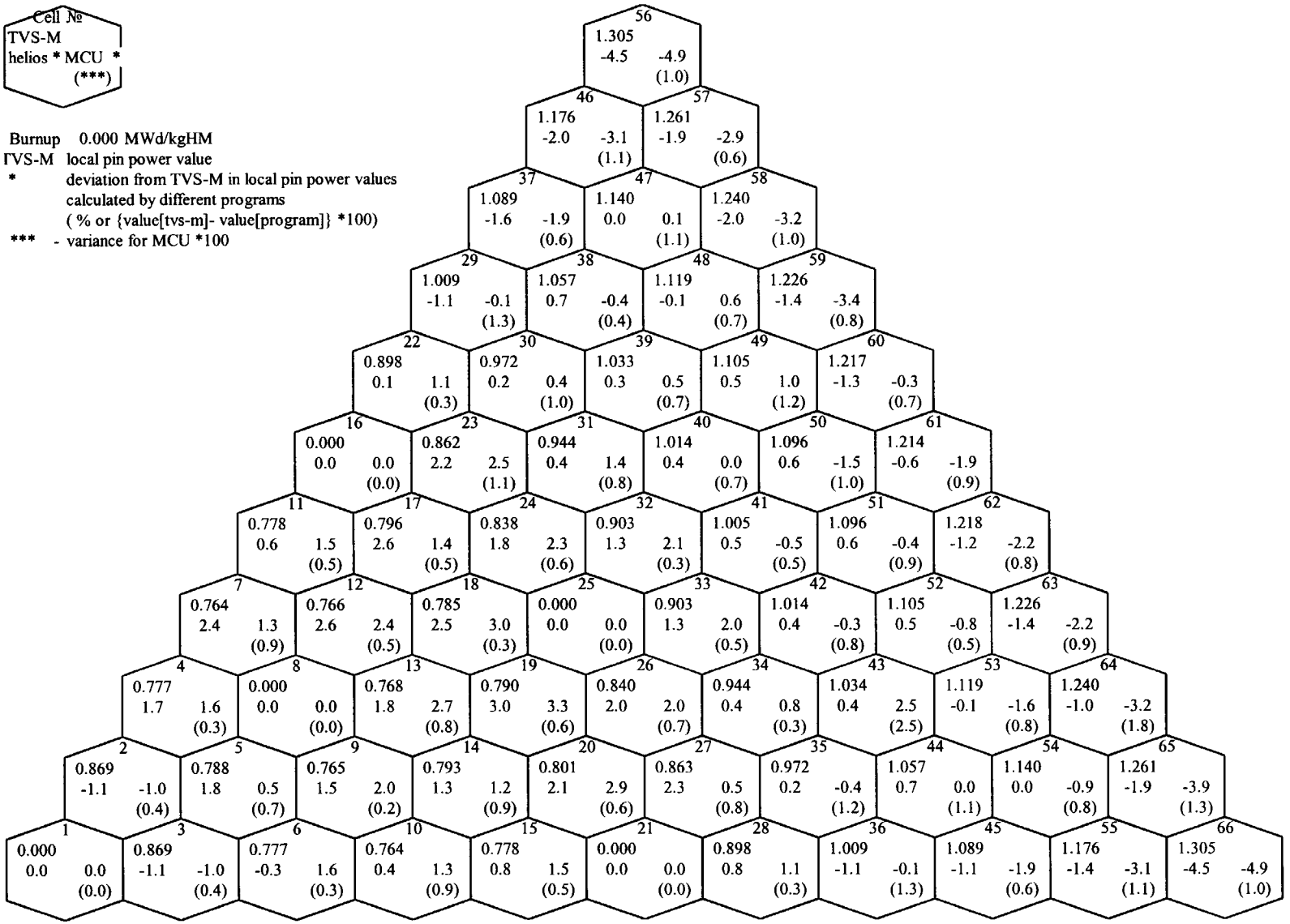

Figure B- 14 Deviation from TVS-M in local pin power values for state S2. Burnup 0 MWd/kgHM. Variant V12 (%)

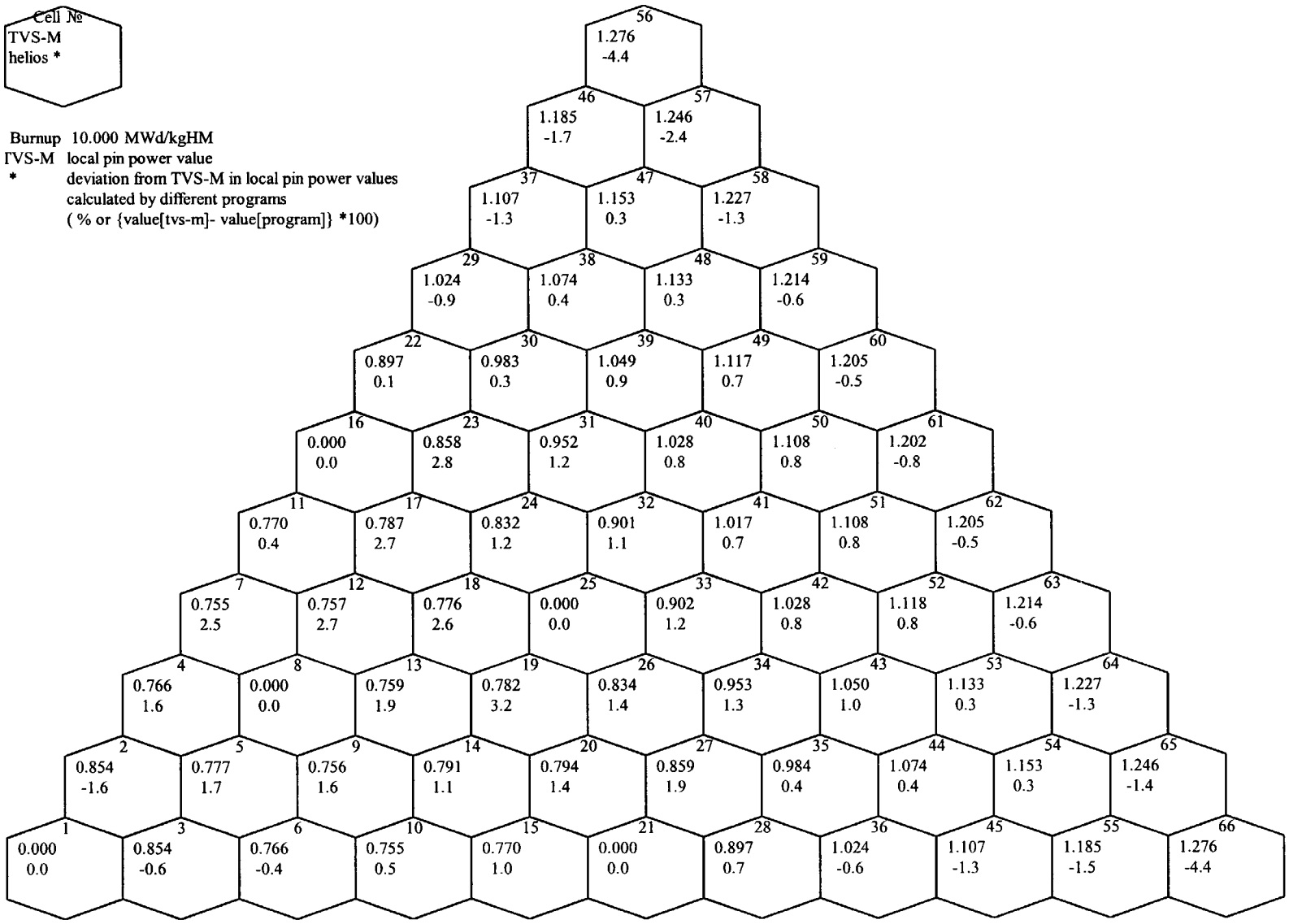

Figure B- 15 Deviation from TVS-M in local pin power values for state S2. Burnup 10 MWd/kgHM. Variant V12 (%)

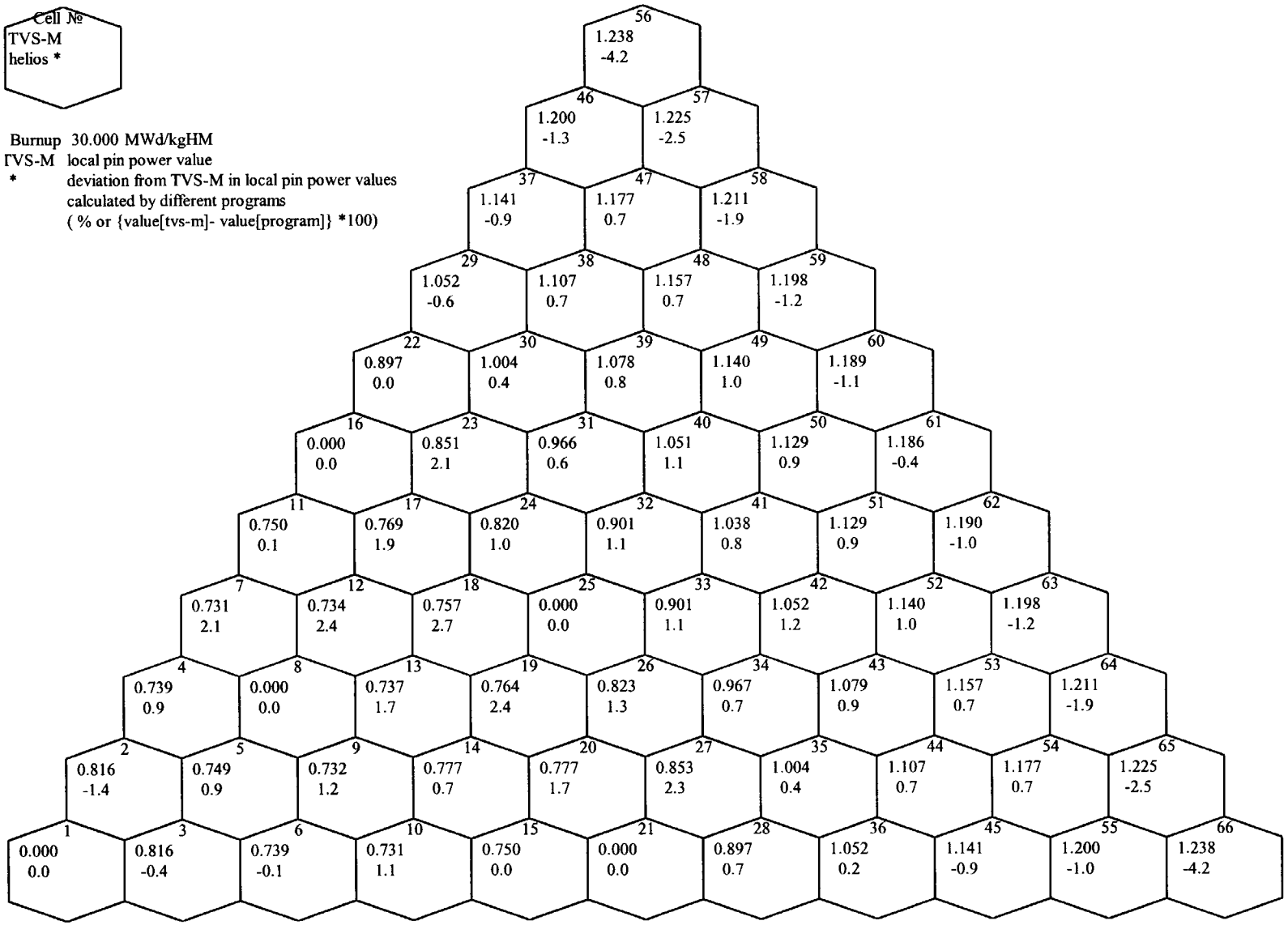

Figure B- 16 Deviation from TVS-M in local pin power values for state S2. Burnup 30 MWd/kgHM. Variant V12 (%)

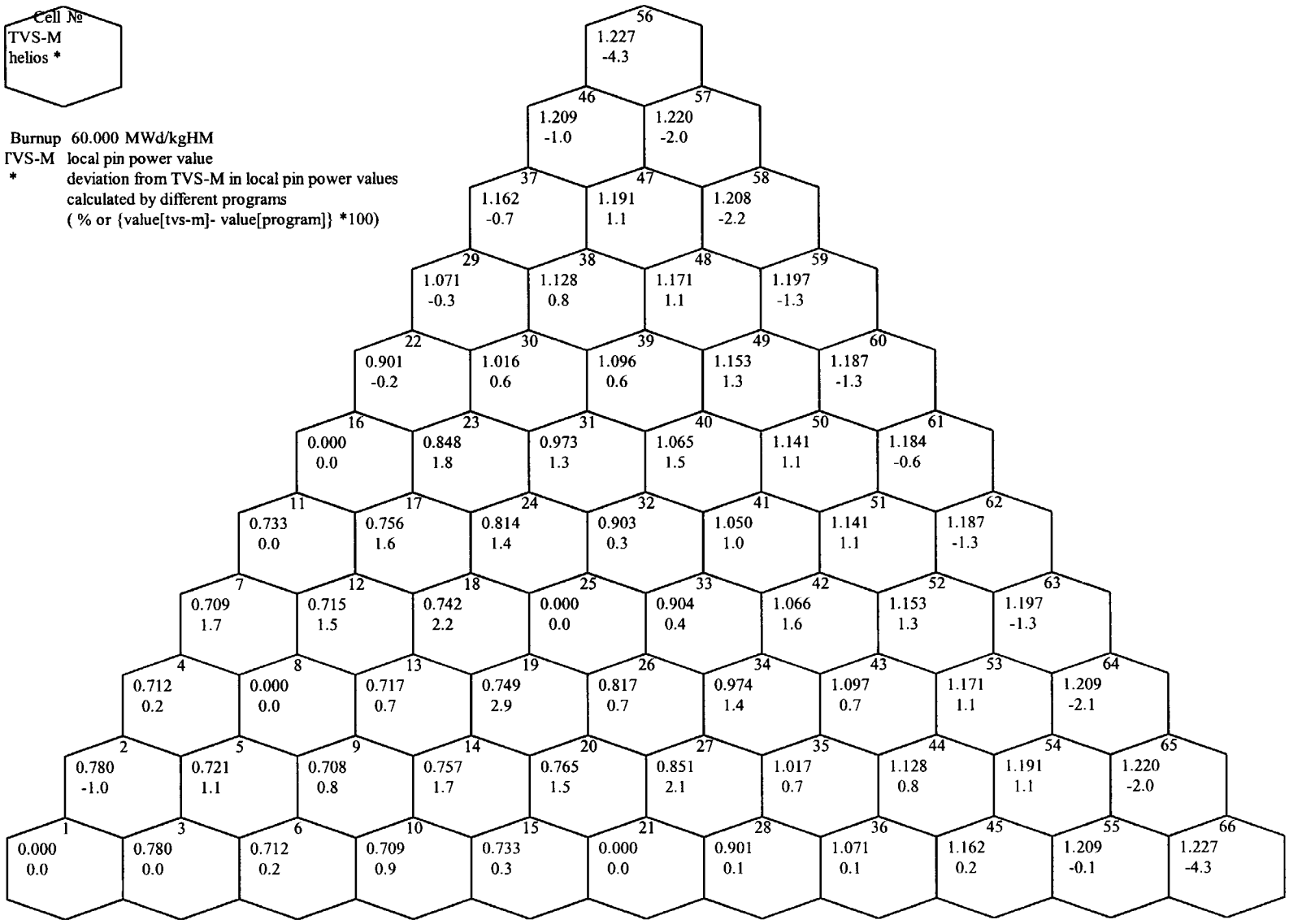

Figure B- 17 Deviation from TVS-M in local pin power values for state S2. Burnup 60 MWd/kgHM. Variant V12 (%)

APPENDIX C. MULTI ASSEMBLIES CALCULATION RESULTS

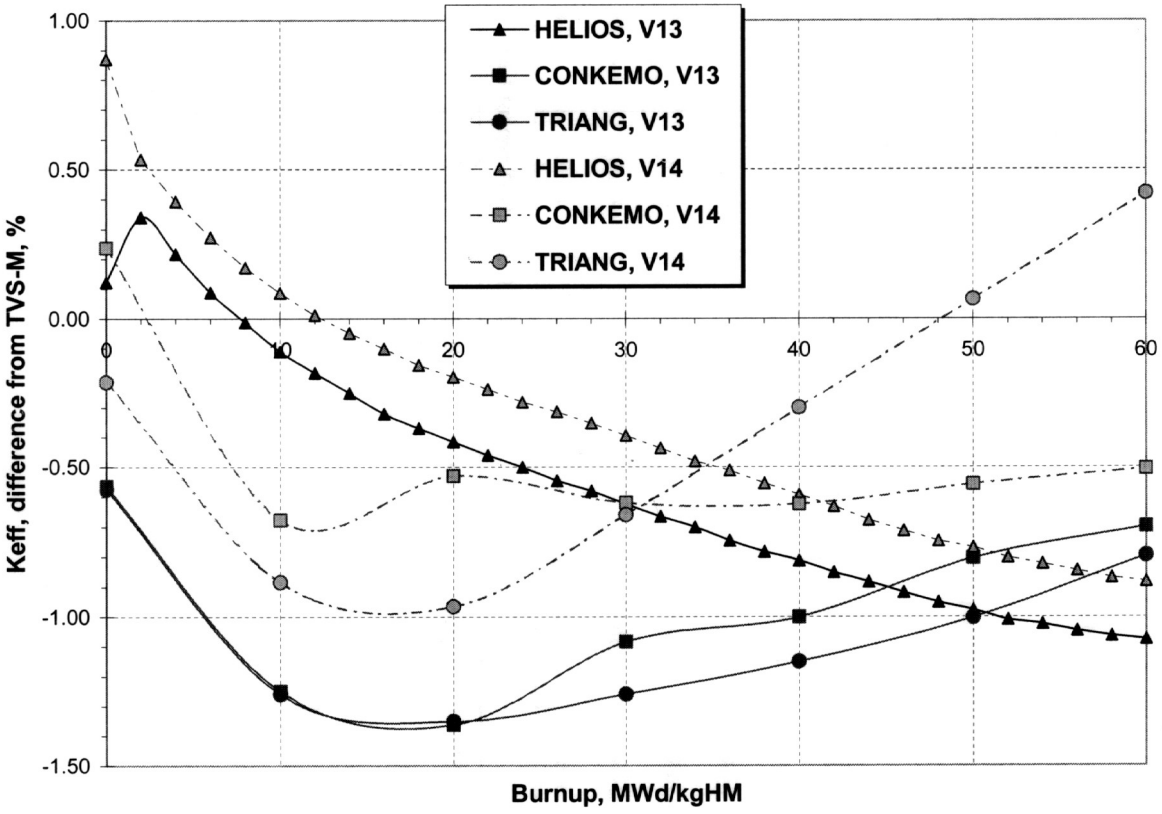

Fig. C- 1 Comparison of K_{eff} burnup dependence for multi-assembly variants (V13-V14)

Table C- 1 Comparison of K_{eff} calculations at zero burnup point (variants V19-V20)

State	K_{eff}						Deviation from TVS-M (U8 - LIPAR-3)				
	MCU-RFFI/A		TVS-M (U8 - LIPAR-5)	TVS-M (U8 - LIPAR-3)	WIMS-ABBN/ TRIANG	HELIOS	MCU-RFFI/A		TVS-M (U8 - LIPAR-5)	WIMS-ABBN/ TRIANG	HELIOS
	Pointwise	Multigroup					Pointwise	Multigroup			
	V19, fresh LEU+fresh MOX						V19, fresh LEU+fresh MOX				
S7	1.3639	1.3666	1.3655	1.3686	1.3520	1.3743	-0.34	-0.14	-0.22	-1.21	0.42
S8	-	-	1.3384	1.3412	1.3264	1.3457	-	-	-0.21	-1.10	0.33
S9	-	-	1.0621	1.0667	1.0948	1.0684	-	-	-0.43	2.63	0.16
S10	-	-	1.2534	1.2562	1.2456	1.2619	-	-	-0.23	-0.85	0.45
S11	-	-	1.3565	1.3595	1.3468	1.3646	-	-	-0.22	-0.93	0.38
S12	-	-	1.4442	1.4468	1.4361	1.4521	-	-	-0.18	-0.74	0.36
	V20, fresh MOX+spent LEU						V20, fresh MOX+spent LEU				
S7	1.1614	1.1680	1.1665	1.1691	1.1581	1.1759	-0.66	-0.10	-0.22	-0.94	0.58
S8	-	-	1.1397	1.1421	1.1318	1.1471	-	-	-0.21	-0.90	0.44
S9	-	-	0.8598	0.8635	0.8959	0.8706	-	-	-0.43	3.75	0.82
S10	-	-	1.0786	1.0812	1.0776	1.0888	-	-	-0.24	-0.34	0.70
S11	-	-	1.1638	1.1664	1.1583	1.1726	-	-	-0.23	-0.70	0.53
S12	-	-	1.2581	1.2606	1.2529	1.2677	-	-	-0.19	-0.61	0.57

Table C- 2 Comparison of various reactivity effects values for multi-assembly variants (V19-V20).

Effect	Initial state	Final state	Effect value, $(K_i-K_j)/(K_i*K_j)$, %				Deviation from TVS-M (Lipar3)		
			TVS-M (Lipar5)	TVS-M (Lipar3)	HELIOS	WIMS-ABBN	TVS-M (Lipar5)	HELIOS	WIMS-ABBN
	V19, fresh LEU+fresh MOX								
Doppler effect, T_f : 1027K→ 2000K	S7	S8	-1.48	-1.49	-1.55	-1.43	-0.47	3.80	-4.18
Boron effect, C_B : 0.0 → 1.2 g/kg	S7	S10	-6.55	-6.53	-6.48	-6.32	0.25	-0.79	-3.29
Voiding effect, γ_m : 0.716 → 0.2 g/cm3	S7	S9	-20.92	-20.67	-20.83	-17.38	1.19	0.77	-15.95
	V20, fresh MOX+spent LEU								
Doppler effect, T_f : 1027K→ 2000K	S7	S8	-2.02	-2.03	-2.14	-2.01	-0.51	5.38	-0.97
Boron effect, C_B : 0.0 → 1.2 g/kg	S7	S10	-6.99	-6.95	-6.80	-6.45	0.49	-2.15	-7.22
Voiding effect, γ_m : 0.716 → 0.2 g/cm3	S7	S9	-30.58	-30.27	-29.82	-25.27	1.02	-1.48	-16.51

Table C- 3 β_{eff} comparison in case of multi-assembly variants (V19-V20).

State	β_{eff}				Deviation from TVS-M		
	MCU-RFFI/A	TVS-M	WIMS-ABBN/ TRIANG	HELIOS	MCU-RFFI/A	WIMS-ABBN/ TRIANG	HELIOS
	V19, fresh LEU+fresh MOX						
S7	6.140E-03	6.071E-03	6.326E-03	6.172E-03	1.14	4.20	1.67
S8	-	6.076E-03	6.325E-03	6.179E-03	-	4.10	1.69
S9	-	6.333E-03	6.610E-03	6.596E-03	-	4.37	4.16
S10	-	6.066E-03	6.286E-03	6.161E-03	-	3.63	1.56
S11	-	6.926E-03	7.144E-03	7.083E-03	-	3.15	2.27
S12	-	7.093E-03	7.270E-03	7.191E-03	-	2.50	1.38
	V20, fresh MOX+spent LEU						
S7	4.530E-03	4.603E-03	4.560E-03	4.650E-03	-1.59	-0.93	1.02
S8	-	4.611E-03	4.334E-03	4.645E-03	-	-6.01	0.74
S9	-	5.236E-03	5.321E-03	5.453E-03	-	1.62	4.15
S10	-	4.620E-03	4.564E-03	4.667E-03	-	-1.21	1.03
S11	-	4.943E-03	4.934E-03	5.027E-03	-	-0.18	1.71
S12	-	5.167E-03	5.060E-03	5.198E-03	-	-2.07	0.59

Table C- 4 β_{eff}/β comparison in case of multi-assembly variants (V19-V20).

State	β/β_{eff}			
	MCU-RFFI/A	TVS-M	WIMS-ABBN/ TRIANG	HELIOS
	V19, fresh LEU+fresh MOX			
S7	9.780E-01	9.780E-01	9.840E-01	9.739E-01
S8	-	9.770E-01	9.820E-01	9.724E-01
S9	-	9.260E-01	9.240E-01	9.161E-01
S10	-	9.710E-01	9.770E-01	9.678E-01
S11	-	1.105E+00	1.089E+00	1.102E+00
S12	-	1.146E+00	1.130E+00	1.145E+00
	V20, fresh MOX+spent LEU			
S7	9.620E-01	9.670E-01	9.530E-01	9.621E-01
S8	-	9.660E-01	9.530E-01	9.601E-01
S9	-	8.930E-01	8.870E-01	8.787E-01
S10	-	9.600E-01	9.490E-01	9.557E-01
S11	-	1.030E+00	1.007E+00	1.029E+00
S12	-	1.076E+00	1.043E+00	1.079E+00

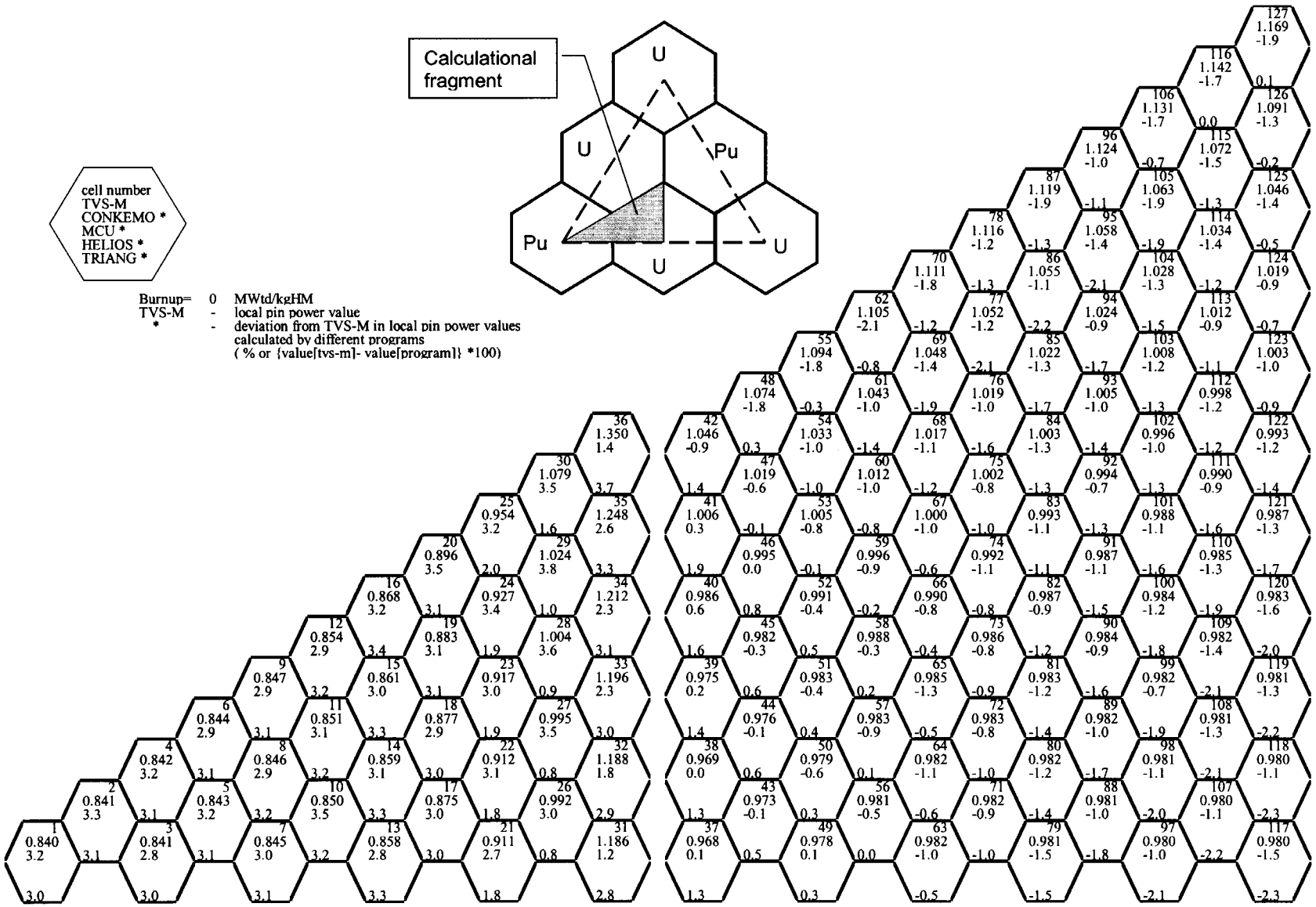

Fig. C- 2 Deviation from TVS-M in local pin power values calculated by various codes for state S1. Burnup 0 MWd/kgHM. Variant V13 (%)

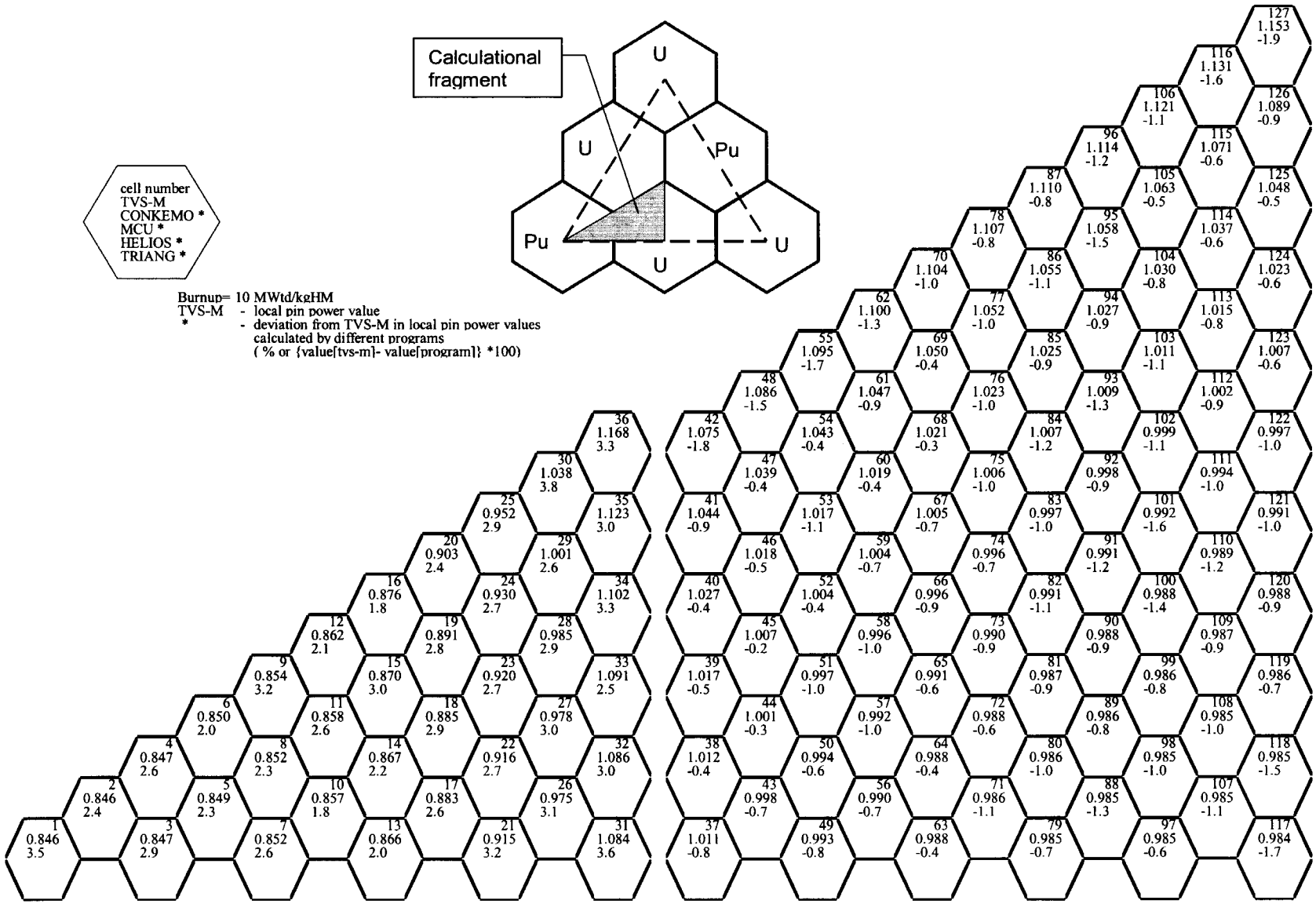

Fig. C- 3 Deviation from TVS-M in local pin power values calculated by various codes for state S1. Burnup 10 MWd/kgHM. Variant V13 (%)

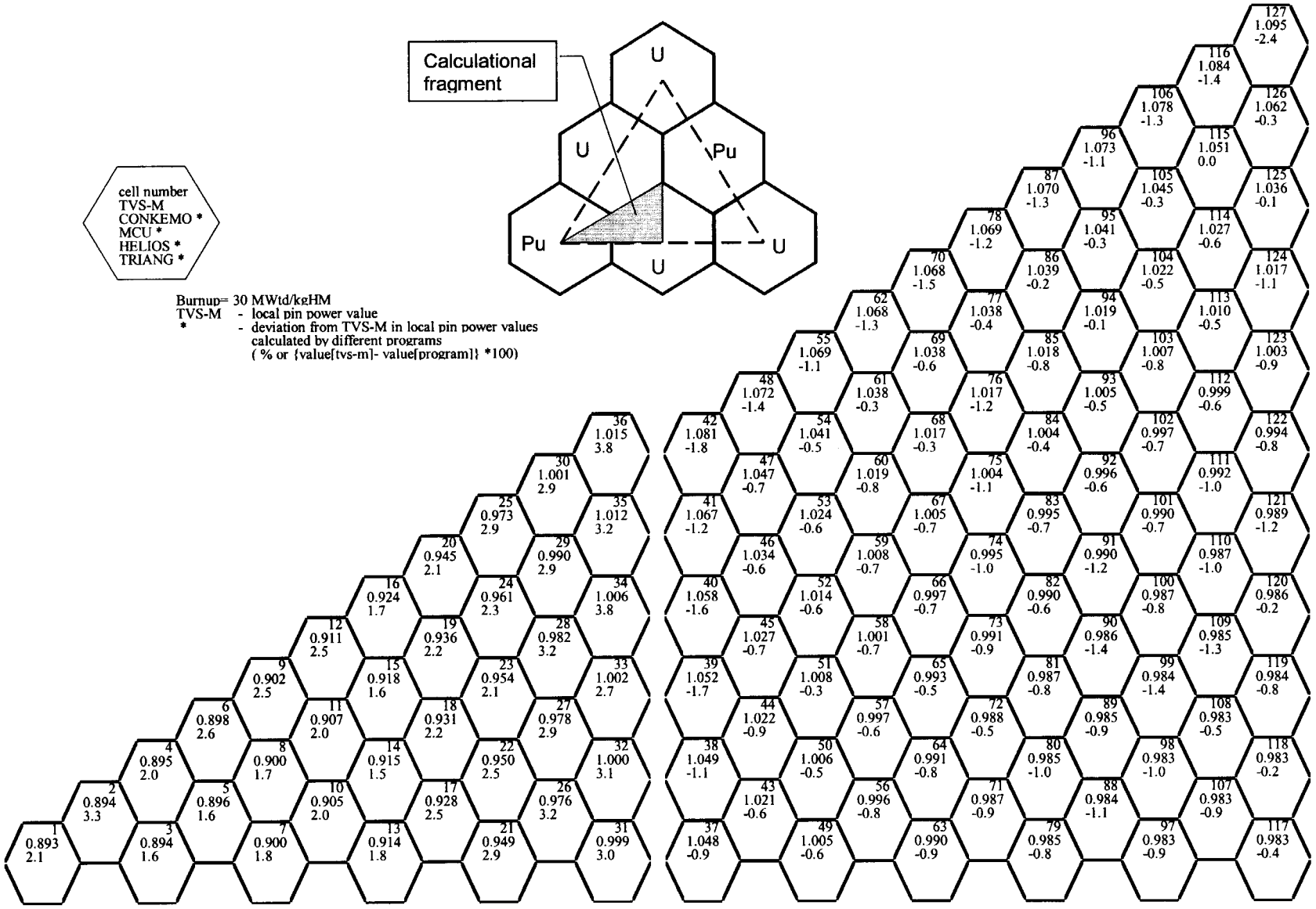

Fig. C- 4 Deviation from TVS-M in local pin power values calculated by various codes for state S1. Burnup 30 MWd/kgHM. Variant V13 (%)

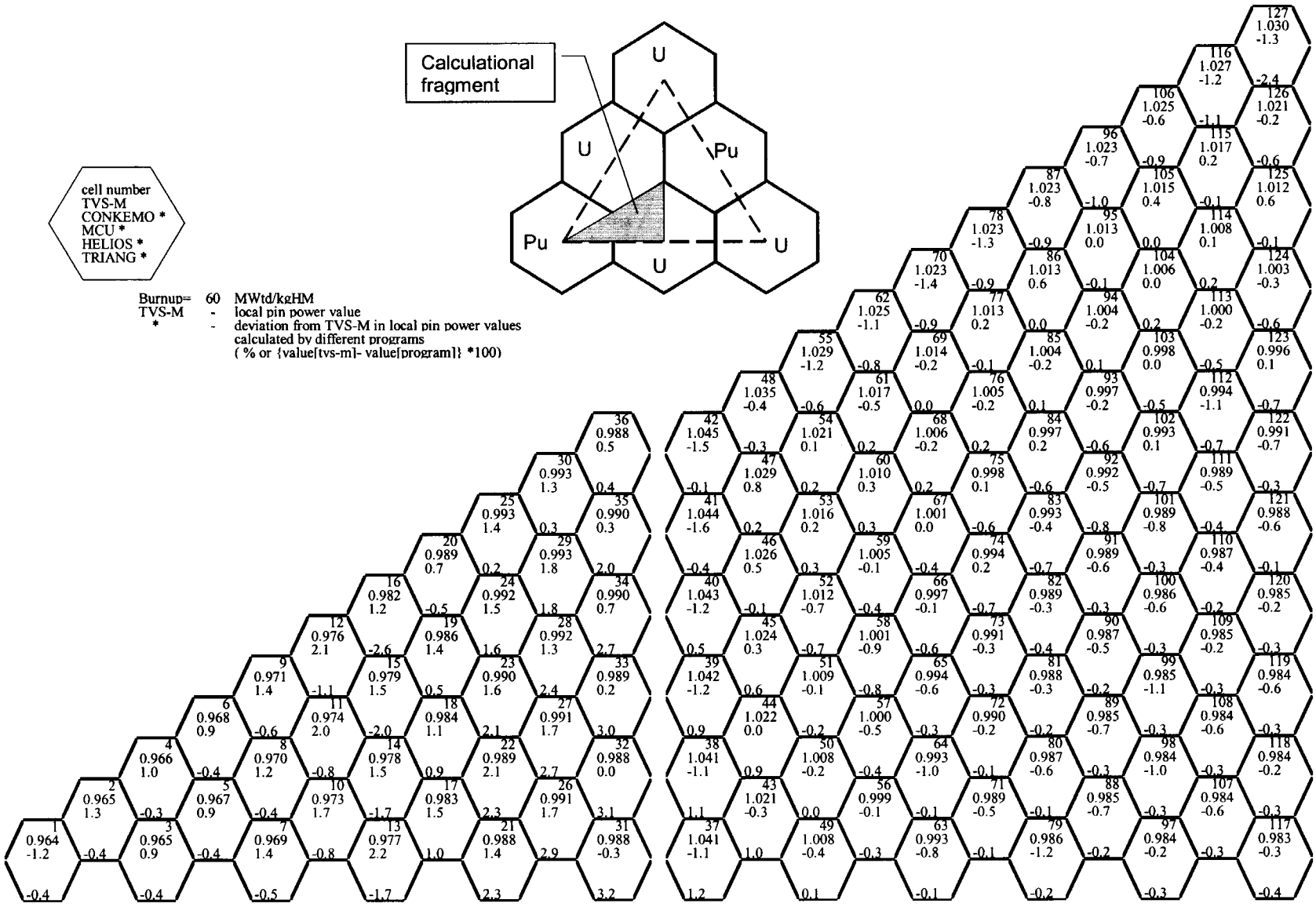

Fig. C- 5 Deviation from TVS-M in local pin power values calculated by various codes for state S1. Burnup 60 MWd/kgHM. Variant V13 (%)

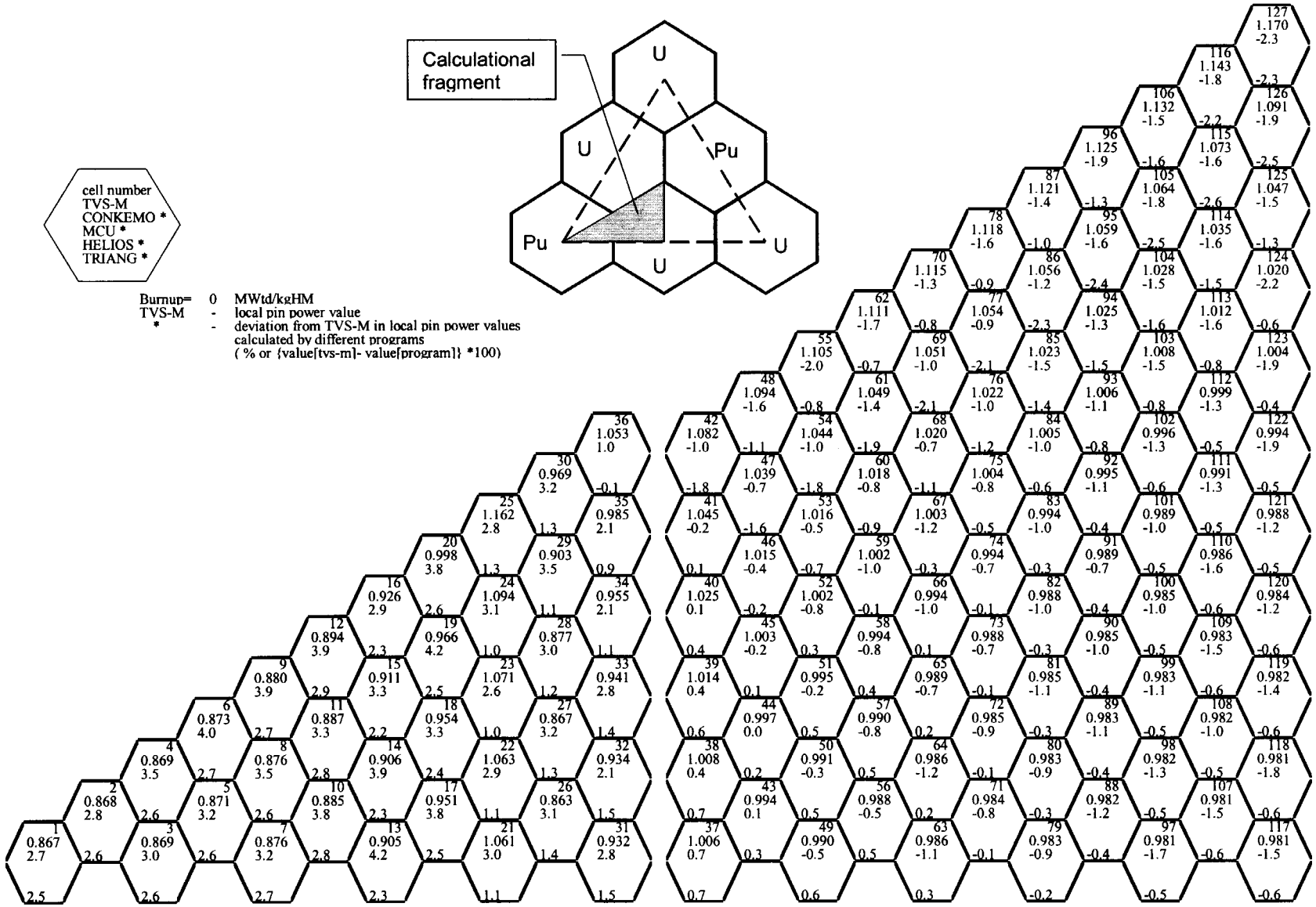

Fig. C- 6 Deviation from TVS-M in local pin power values calculated by various codes for state S1. Burnup 0 MWd/kgHM. Variant V14 (%)

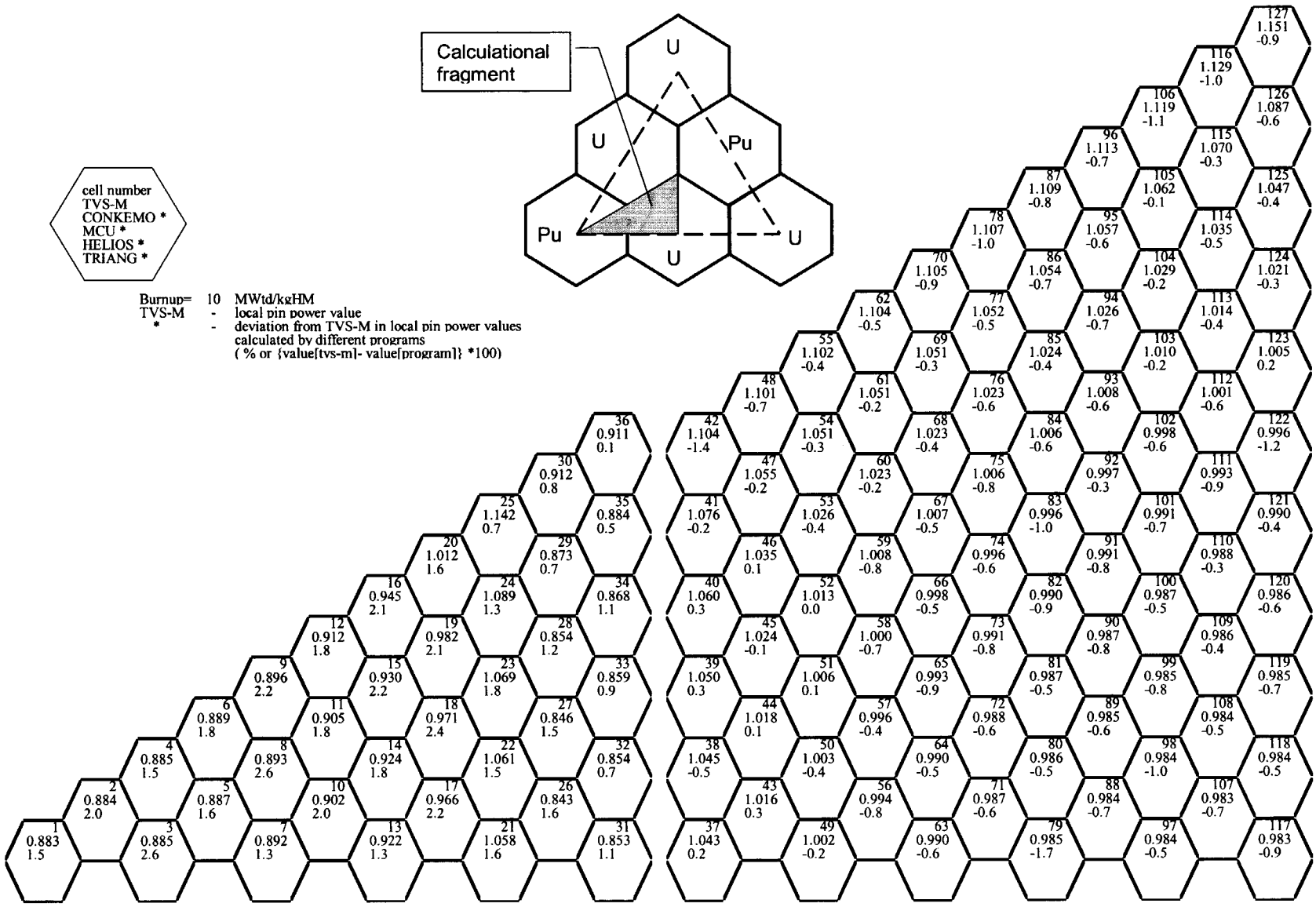

Fig. C- 7 Deviation from TVS-M in local pin power values calculated by various codes for state S1. Burnup 10 MWd/kgHM. Variant V14 (%)

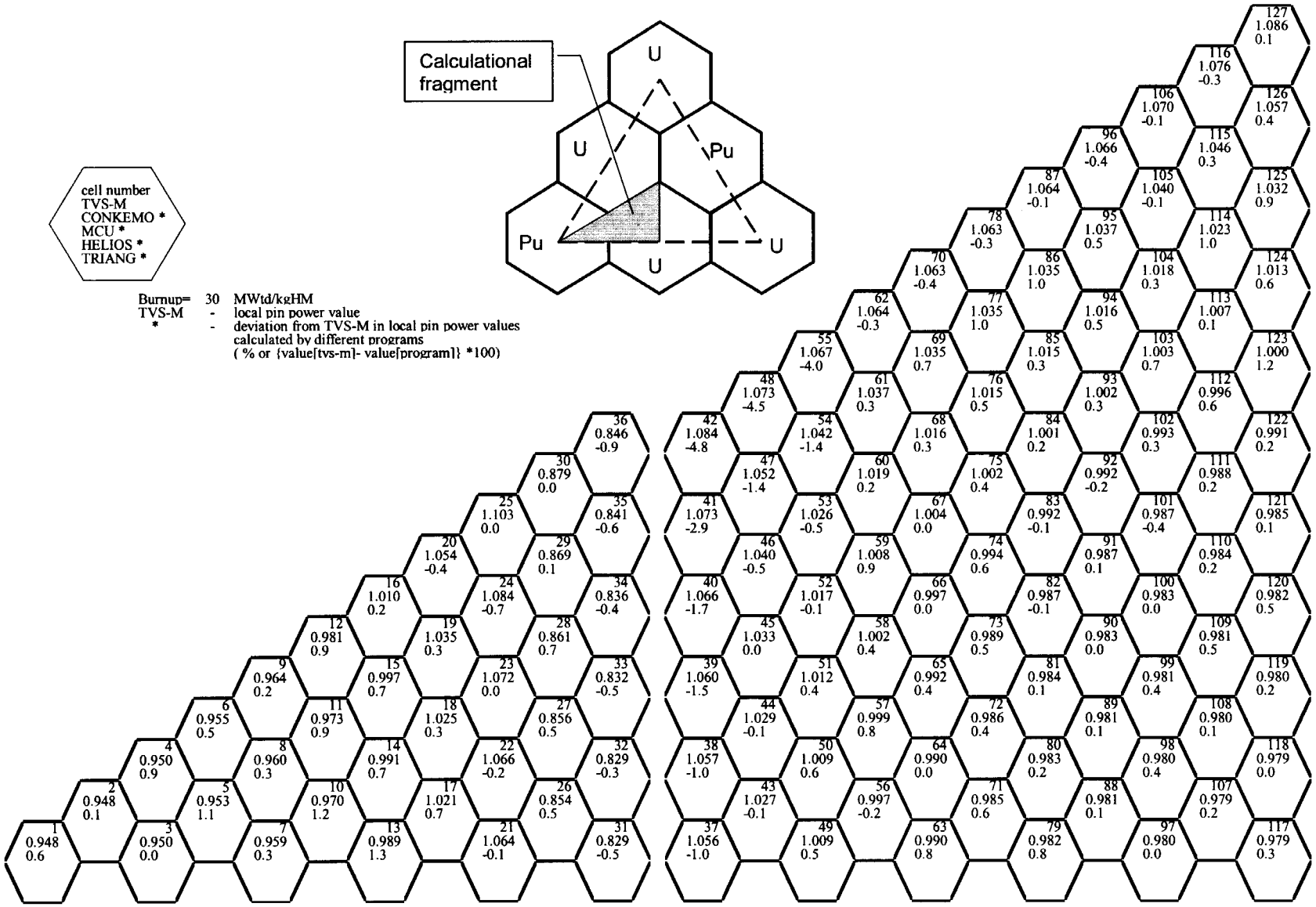

Fig. C- 8 Deviation from TVS-M in local pin power values calculated by various codes for state S1. Burnup 30 MWd/kgHM. Variant V14 (%)

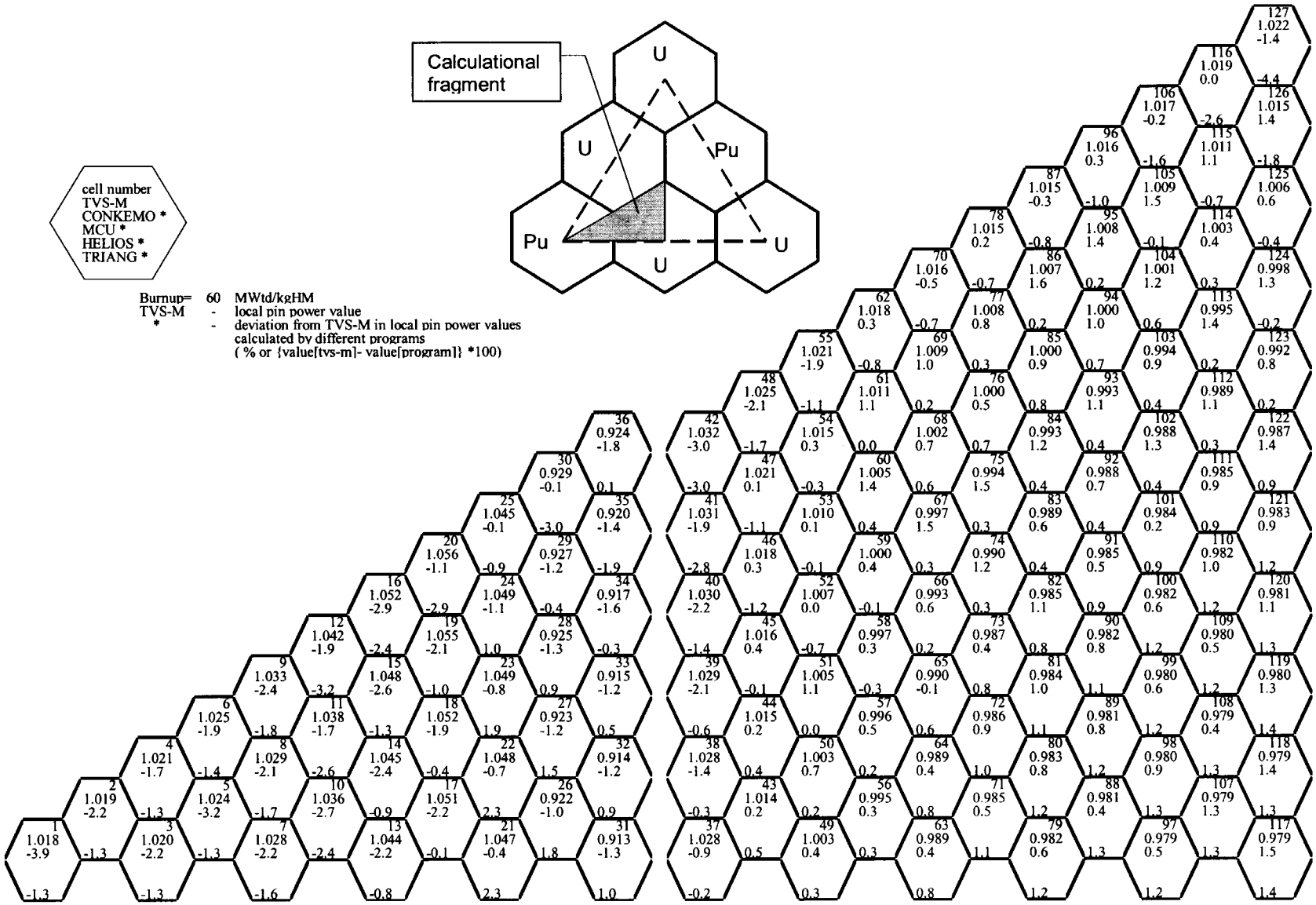

Fig. C- 9 Deviation from TVS-M in local pin power values calculated by various codes for state S1. Burnup 60 MWd/kgHM. Variant V14 (%)

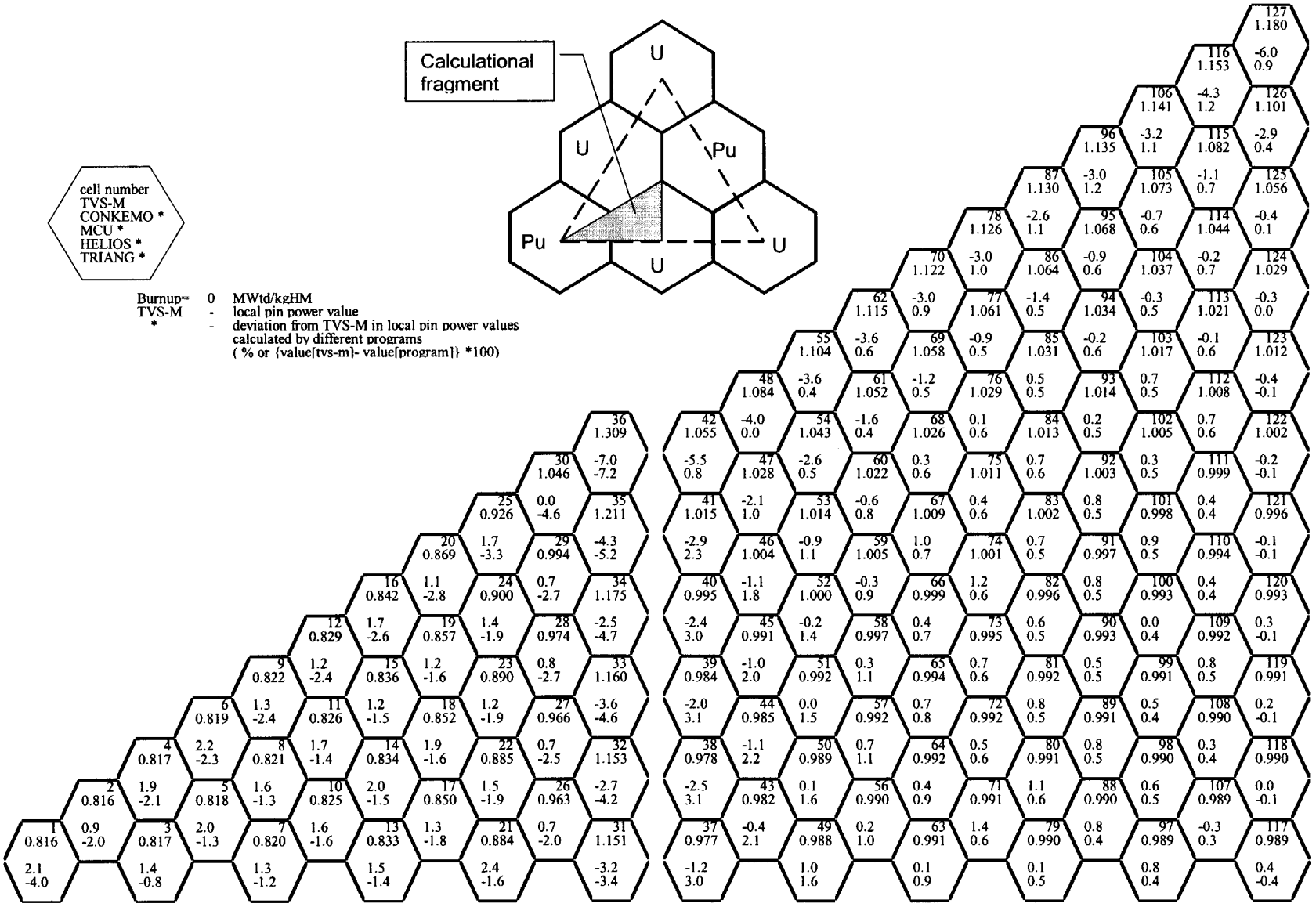

Fig. C- 10 Deviation from TVS-M in local fission rates calculated by various codes for state S1. Burnup 0 MWd/kgHM. Variant V13 (%)

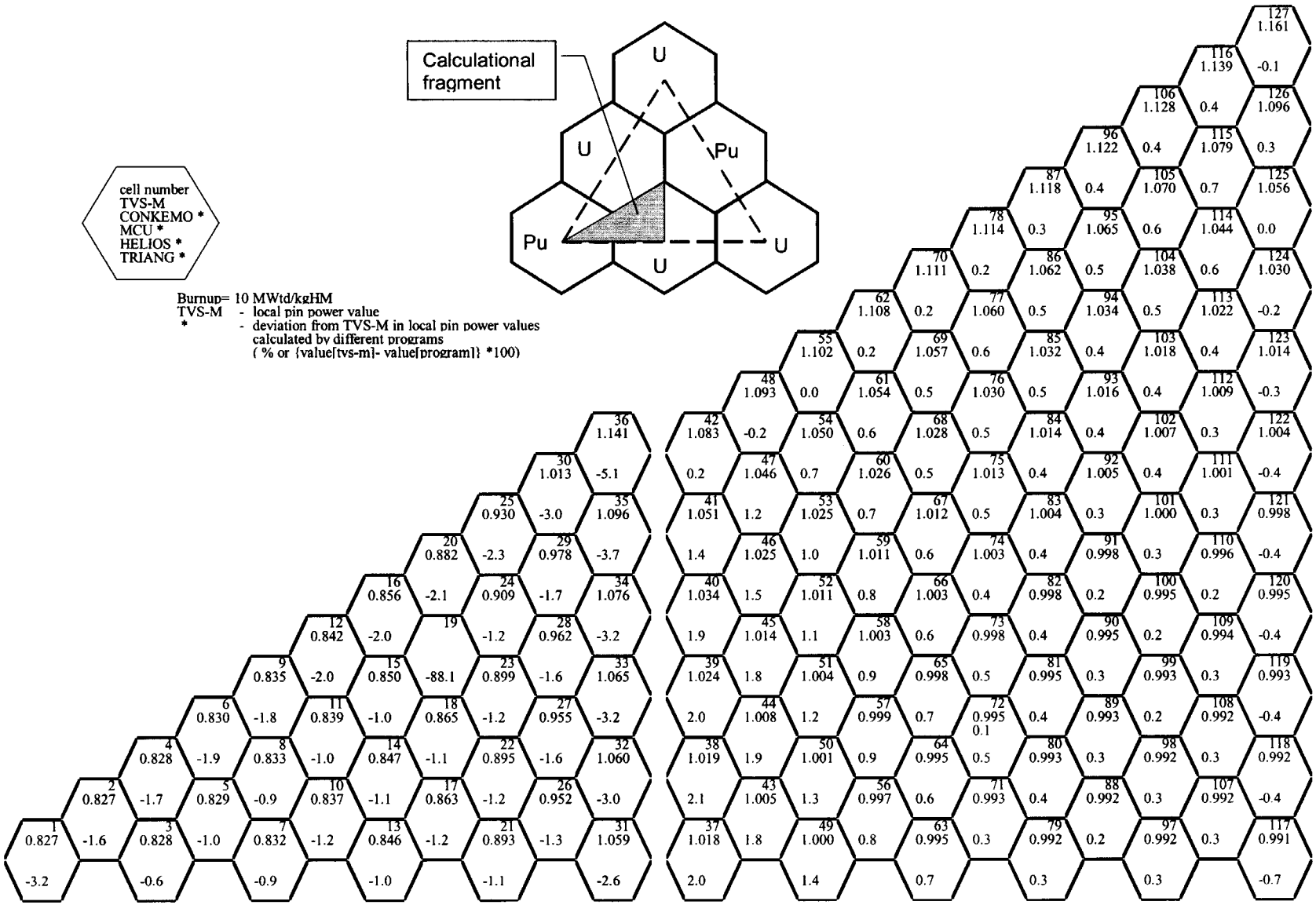

Fig. C- 11 Deviation from TVS-M in local fission rates calculated by various codes for state S1. Burnup 10 MWd/kgHM. Variant V13 (%)

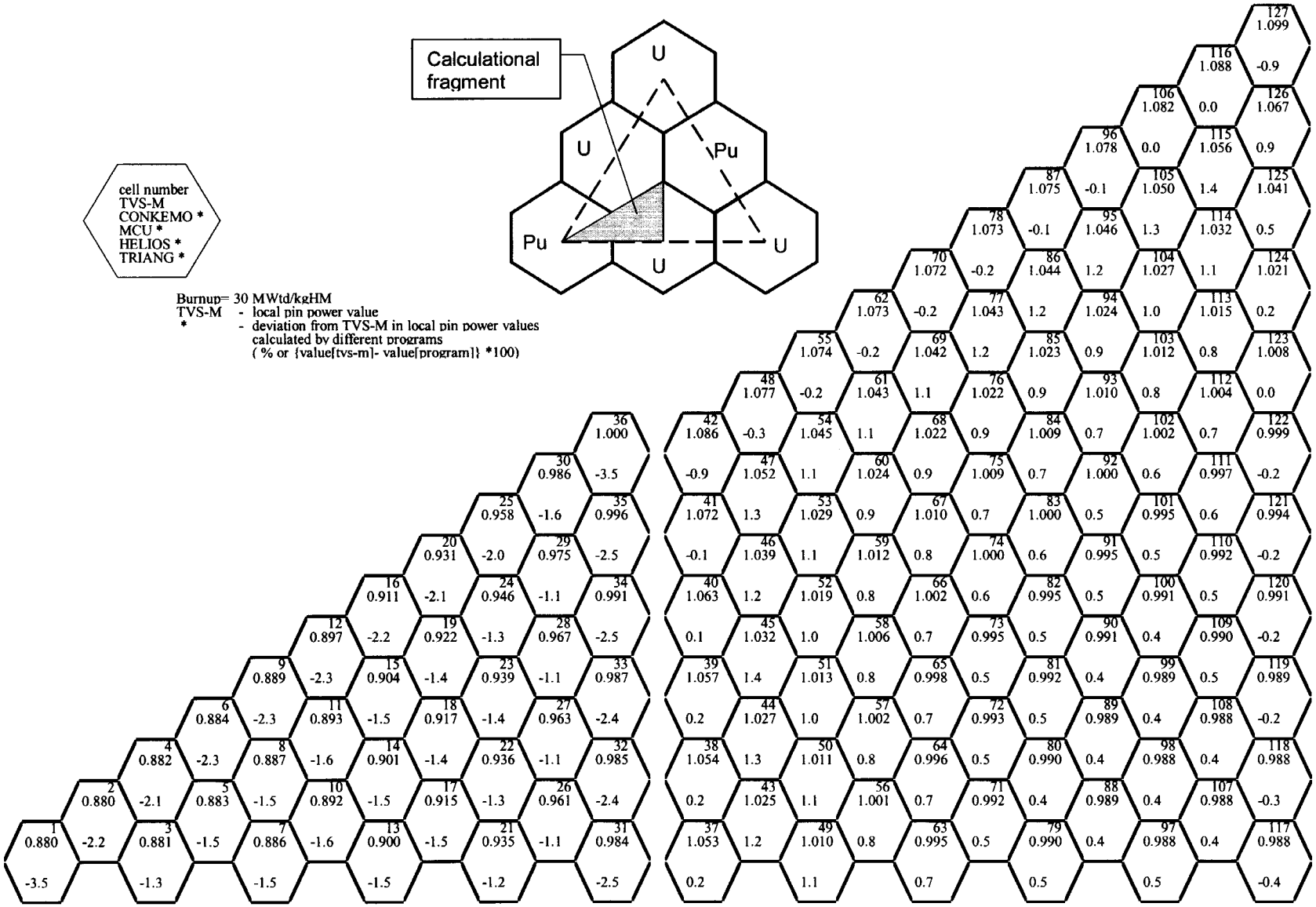

Fig. C- 12 Deviation from TVS-M in local fission rates calculated by various codes for state S1. Burnup 30 MWd/kgHM. Variant V13 (%)

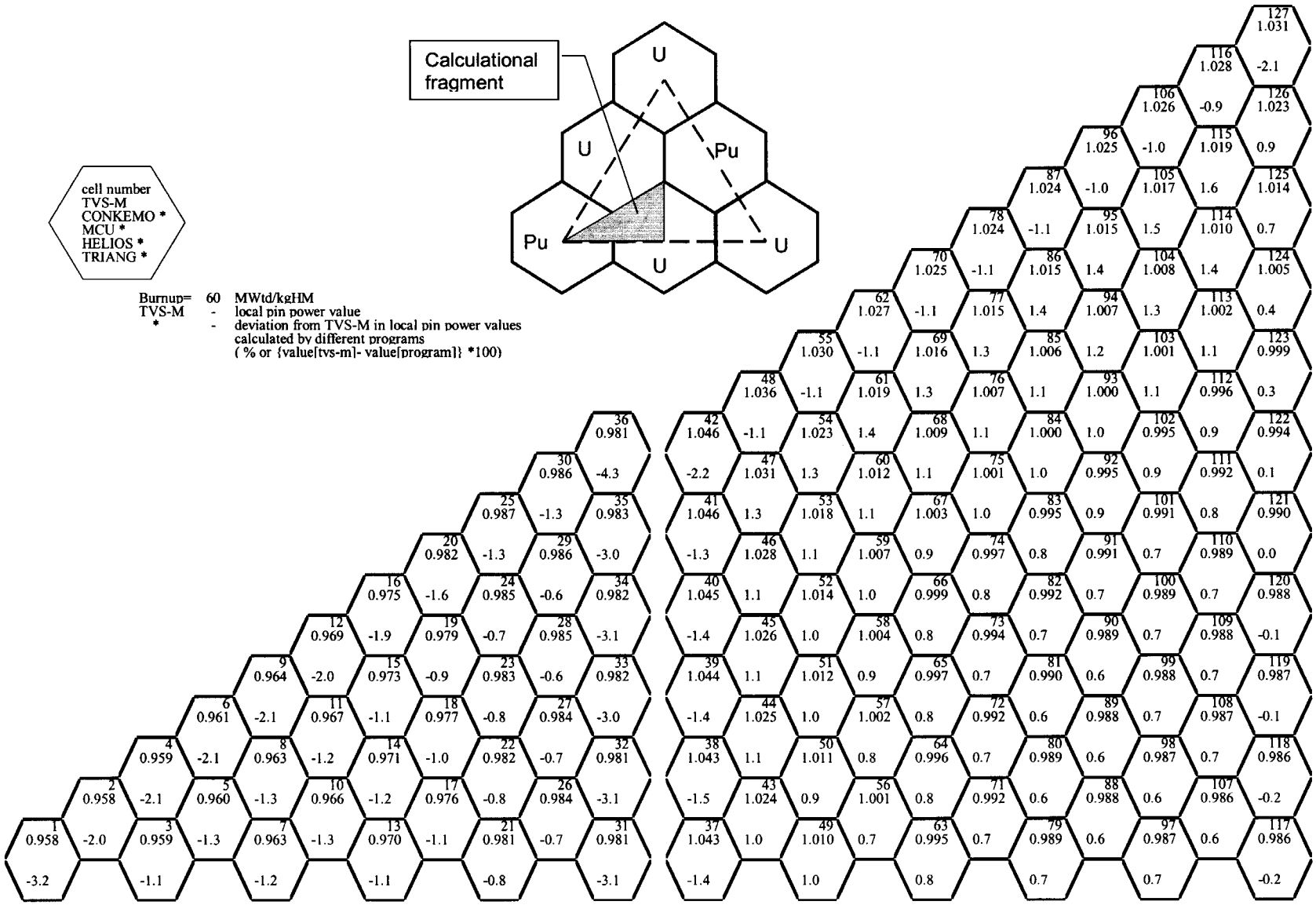

Fig. C- 13 Deviation from TVS-M in local fission rates calculated by various codes for state S1. Burnup 60 MWd/kgHM. Variant V13 (%)

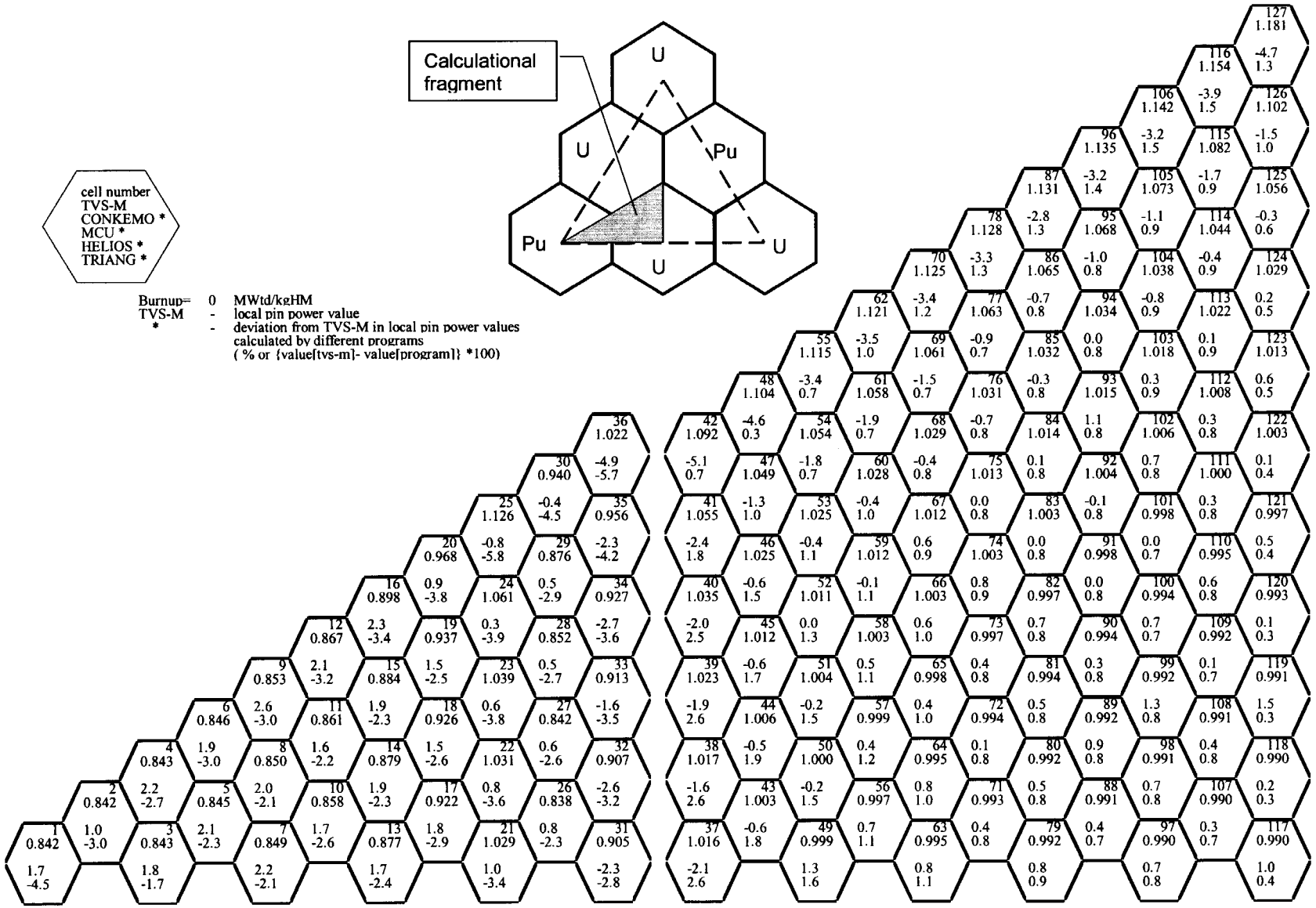

Fig. C- 14 Deviation from TVS-M in local fission rates calculated by various codes for state S1. Burnup 0 MWd/kgHM. Variant V14 (%)

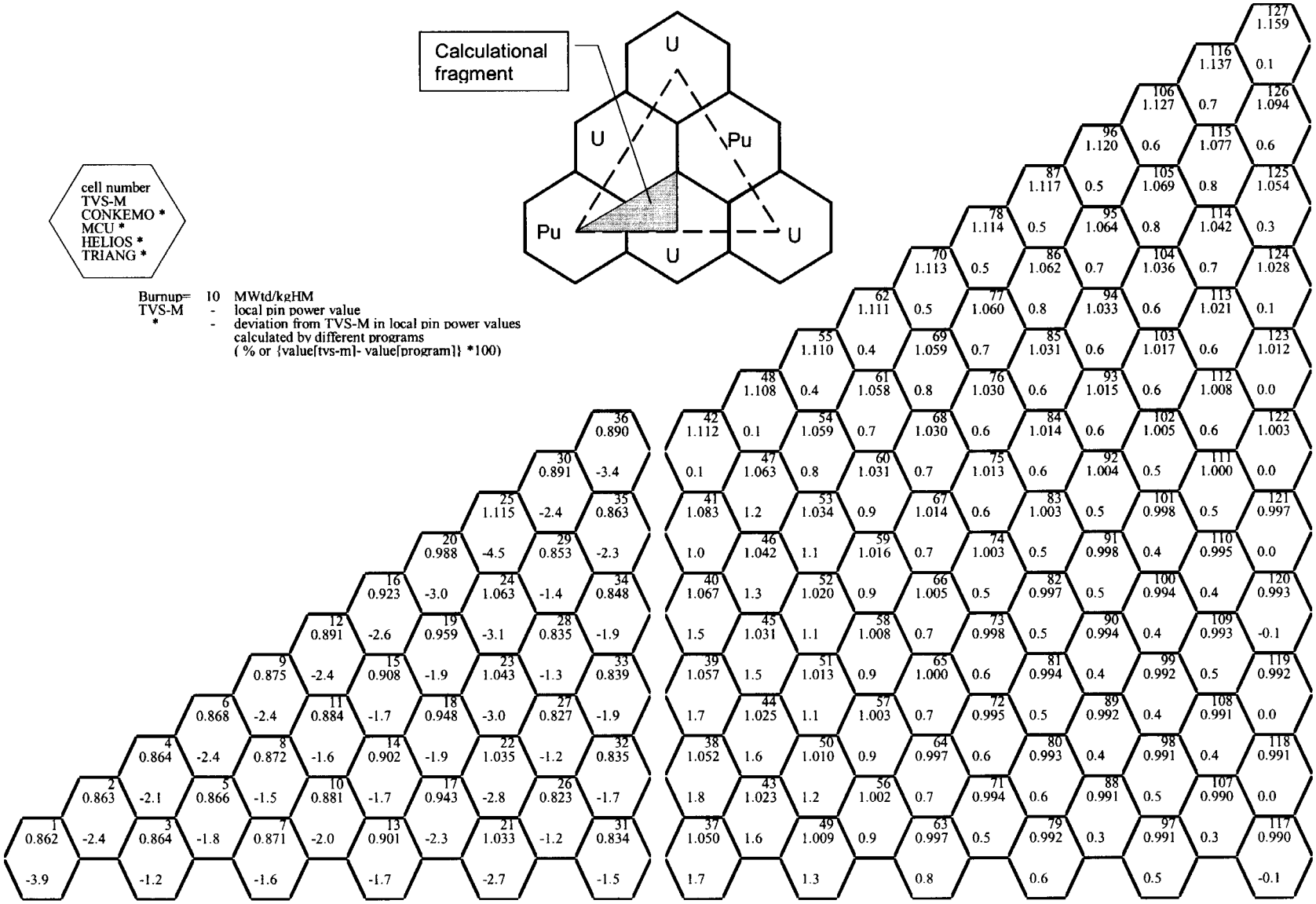

Fig. C- 15 Deviation from TVS-M in local fission rates calculated by various codes for state S1. Burnup 10 MWd/kgHM. Variant V14 (%)

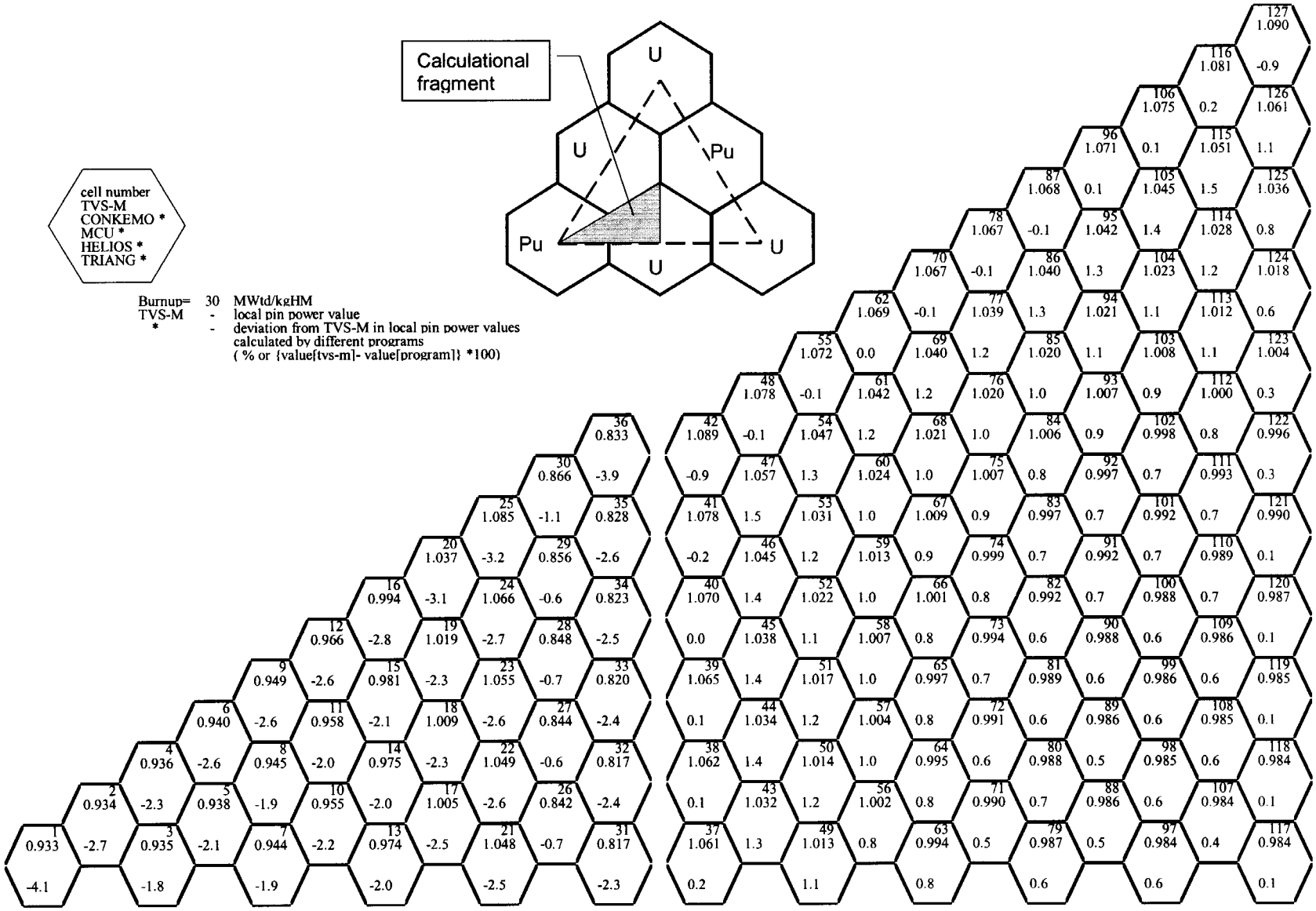

Fig. C- 16 Deviation from TVS-M in local fission rates calculated by various codes for state S1. Burnup 30 MWd/kgHM. Variant V14 (%)

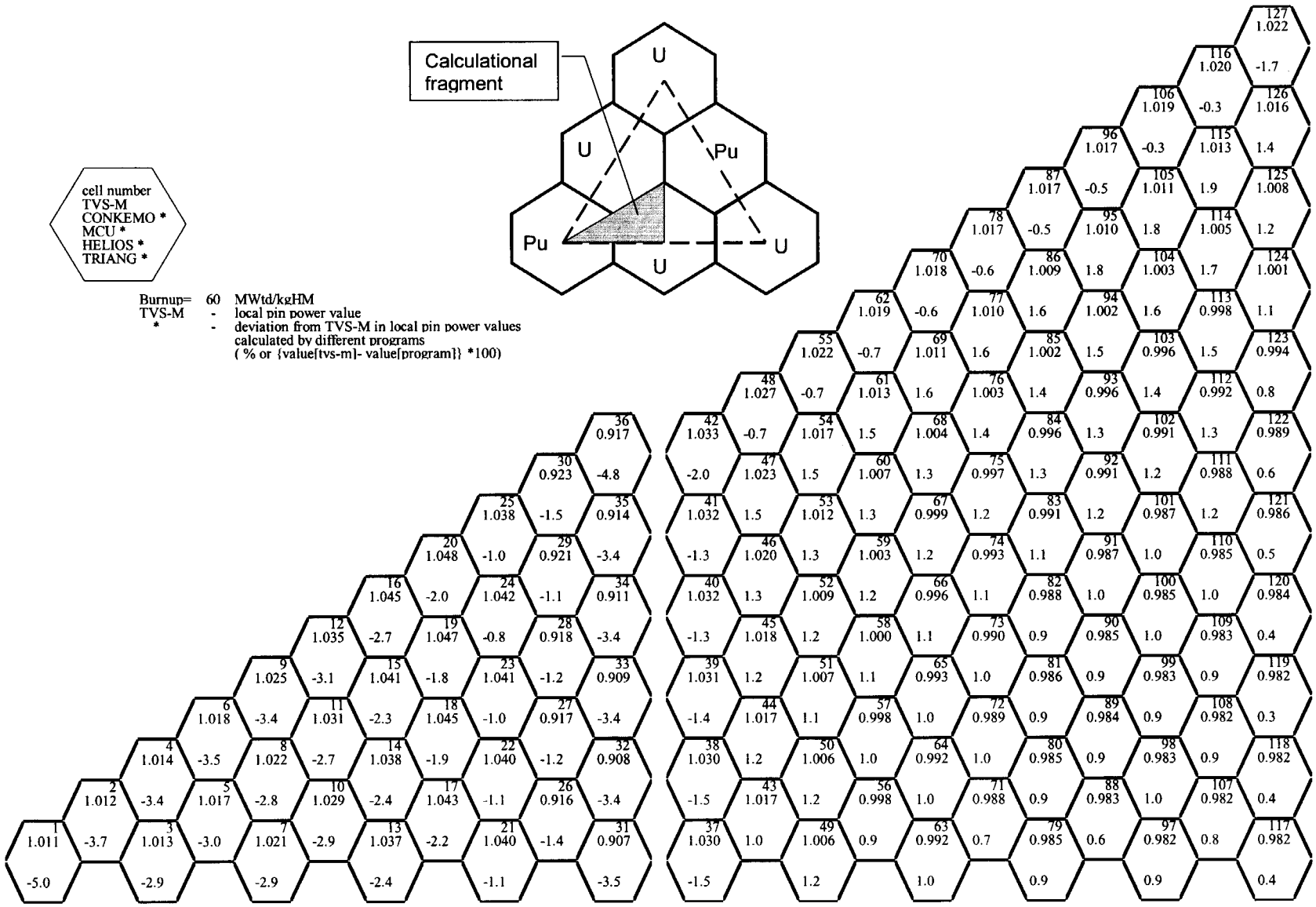

Fig. C- 17 Deviation from TVS-M in local fission rates calculated by various codes for state S1. Burnup 60 MWd/kgHM. Variant V14 (%)

Review comments on the *Validation Report for FY 1997* by R. J. Ellis and J. C. Gehin

General Comments

1. Page 3, Abstract: Change to "…with various codes: RRC KI design code TVS-M and precision code MCU-REA; IPPE codes WIMS-ABBN, TRIANG-PWR, and CONKEMO; and the 2-D n,γ-transport lattice physics code HELIOS, developed by Studsvik Scandpower"
2. Also with the above item: should MCU-RFFI/A be mentioned here too (it is mentioned on page 12)?
3. Page 5, Table of Contents: re 1.3: What is a "code complex," as the other entries simply say "codes"? Is it a "code system" or "code package"?
4. Page 5, Table of Contents: In the REFERENCES entry, the "28" should be at the right margin, with leading "…" in front of it. I think a "tab" before the "28" will force it far enough toward the right side so that the "…" appear properly.
5. Pages 6–9, in the Lists: Do not underline the table numbers and titles, and the figure numbers and titles. Some are not underlined, and these look much better.
6. Page 11: Change to "with colleagues in the U.S.A."
7. Page 11: Change to "Institute of Physics."
8. Page 13 and many other places in the document: "cross-sections" become "cross sections;" it is only to be written as "cross-sections" if it is an adjective.
9. Page 13: Perhaps indicate that the epithermal energy region usually has a defined upper limit, such as "(1 keV > E_n > 0.625 eV)."
10. Page 13: Change "the rest ones the group" to "the other ones, the group" or "the rest, the group."
11. Page 13: Change to "water molecules."
12. Page 13: Change from "the standard one by the only file" to "the standard one only by the file."
13. Page 13, under "Uniform Lattice:" The neutron energy group interval range is shown incorrectly, in the wrong order; it should be "(10.5 MeV > E_n > 0.625 eV)."
14. Page 13: Does "inertia center system" become "i.c.s."?
15. Page 14: Change "^{232} Th" to "^{232}Th" (that is, no space between isotope number and the element symbol).
16. Page 14: Change "Runge-Kutt method" to "Runge-Kutta method;" also, what order of Runge-Kutta method is intended?
17. Page 14 (as mentioned earlier): Change "group cross-sections" to "group cross sections" of media(?).
18. Page 17: Change "the more detailed" to "a more detailed."
19. Page 17: I believe HELIOS Version 1.4 (or HELIOS-1.4) was used for these cases; it should be identified as such as the libraries are dependent on the code version.
20. Page 18: The state definitions would be much better displayed in a table.
21. Page 19: Change "comparing of two" to "comparison of two."
22. Page 19, Section 2.1.3: Again, change "cross-sections" to "cross sections."
23. Page 19: Please revise or reword the following: "TVS-M overestimates somewhat (up to 6%) a fission products efficiency." What does the sentence mean? Is the FP production rate involved?
24. Page 20, Section 2.1.4: What is meant by the "neutron value function" used to calculate β_{eff} and l?
25. Page 20, Section 2.1.5: Regarding the statement "…TVS-M code shows a slight tendency to underestimate k_{eff} at high-burnups in comparison with other codes, especially WIMS-ABBN…":

Code	At zero burnup	At 60 MWd/kgHM	i-f reactivity diff
SAS2H	1.0800	0.7411	–42.342%
HELIOS	1.0648	0.7161	–45.731%
TVS-M	1.0609	0.7143	–45.738%
WIMS-ABBN	1.0572	0.7179	–44.706%

The tabulated informative above comes from ORNL/TM-2000/4, *Analyses of Weapons-Grade MOX VVER-1000 Neutronics Benchmarks: Pin-Cell Calculations with SCALE/SAS2H*, by R. J. Ellis. The main observations are that there are similarities between k_{eff} vs burnup behavior for all four codes, and HELIOS and TVS-M are very similar. The $\Delta k_{eff}/\Delta$burnup value is only slightly smaller in magnitude for the WIMS-ABBN code results.

26. Page 23, end of Section 2.2.1: Change or fix the "÷" symbol in "Table B-1 ÷ Table B-3."
27. Page 26: The authors of the report state that "HELIOS systematically overvalues fission rate in the MOX pins located in the central region…" This behavior was documented in Ref. 4 of this report and at the time was not understood. Since that time, this systematic error has been traced to the choice of surface divisions on the HELIOS cells. The cell surfaces on the edges and near the assembly center represent partial pins (the HELIOS model was based on 1/6-assembly geometry) and therefore have faces that are subdivided into finer regions than the whole fuel-pin cells. This results in an asymmetry in the collision probability/currently coupling solution, leading to an overprediction of the pin power in the central pin. In other studies of VVER-1000 assemblies this behavior was not observed because an instrument tube occupied the central location, not a fuel pin as for these benchmark studies. An alternate model has been created in which none of the fuel pins are subdivided, thereby eliminating this symmetry problem.
28. Page 26, top of Section 2.3.4: Change "of pin power one" to "of a pin power distribution."
29. Page 26: Change or fix the "÷" symbol in "Table C-2 ÷ Table C-9."
30. Page 26: Change or fix the "÷" symbol in "Table C-10 ÷ Table C-17."
31. Page 26: Change "agree satisfactory" to "agree satisfactorily."
32. Page 26: Change "…for the most of pins deviations do not exceed 2%" to "…most of the pin deviations do not exceed 2%."
33. Page 27: Please define or explain what you mean by "spectral codes."
34. Page 27: Change "And another parts" to "Other parts."
35. Page 27: Change "calculation" to "calculations."
36. Pages 28–29, References: Some of the entries do not have a space between initials and last names, and some entries are written as last name first. A consistent format needs to be used.
37. Page 28, Ref. 2: Change "Portlend" to "Portland."
38. Page 28, Ref. 5: Change "et all." to "et al."
39. Page 28, Ref. 9: Change the far future date "11973" to "1973."
40. Page 28, Ref. 10: Some of the text is in Cyrillic.
41. Page 28, Ref. 15: Change "Bildup" to "Buildup," and change "Assosiation" to "Associated."
42. Page 29, Ref. 17: Change "neutronics calculation" to "neutronics calculations."
43. Page 33, etc., the bar-graph figures such as Fig. A-1: The color and texture/design of the "bars" for HELIOS and MCU-RFFI/A are difficult to distinguish, especially for the graphs that only have one or the other "bars."
44. Page 36, etc., Tables A-4, A-5, A-10, A-11, and some others: The deviations presented should be stated as "% differences."
45. Pages 44–46, Figs. A-5, A-6, A-7: The y-axes and curves are mislabeled. These are not curves of k_o nor k_{eff}; these are curves of the percent differences between the k_o and k_{eff} results of a specific code with respect to the results from TVS-M.

46. Page 49, Fig. A-10: Why is the presented curve for “TVS-M (U8-LI5)” so erratic? Furthermore, are not these curves supposed to be the differences from TVS-M? If there is a comparison between TVS-M results using two different nuclear data libraries, then this should be clearly described.
47. Page 50, Fig. A-11: Why is the plotted curve solid, not dashed? And why is it erratic and not smooth?
48. Page 51, etc., Fig. A-12 and others: As mentioned above, if the results from “TVS-M (U8-LI5)” are not the same as the “reference” TVS-M, this should be made much more evident.
49. Page 54, Fig. A-15: The curves are solid, but the legend says the curves should be dashed lines.
50. Page 57, Fig. A-18: The curves are solid, but the legend says the curves should be dashed lines.
51. Page 59, Table A-9, for example: k_i and k_j are identified. Is k_j supposed to be the k for the final burnup state? What does the “j” signify?
52. Pages 66–68, Tables B-2, B-4: What is presented in the tables? These values are not k_o nor k_{eff}; they appear to be the percent reactivity differences. If so, how are they defined or determined?
53. Page 89, Table C-2: It is confusing comparing percent Δk reactivity effect values, and the percent differences between these values in the same table. Perhaps more description or explanation in the table headers or column titles will help?
54. In multiple places: In some cases, lowercase “k” is used for multiplicative constants, and in other cases, uppercase “K” is used.

INTERNAL DISTRIBUTION

1–4. B. B. Bevard
5. R. J. Belles
6. B. L. Broadhead
7. M. D. DeHart
8. F. C. Difilippo
9. M. E. Dunn
10. R. J. Ellis
11. J. C. Gehin
12. S. Goluoglu
13. S. R. Greene
14. D. Hollenbach
15. C. M. Hopper
16. D. T. Ingersoll
17. M. A. Kuliasha
18. S. B. Ludwig
19. G. E. Michaels
20. B. D. Murphy
21. C. V. Parks
22–23. R. T. Primm III
24. C. C. Southmayd
25. D. L. Spellman
26. D. L. Williams, Jr.
27. G. L.Yoder, Jr.
28. Central Research Library
29. ORNL Laboratory Records-RC

EXTERNAL DISTRIBUTION

30. M. L. Adams, Department of Nuclear Engineering, Texas A&M University, Zachry 129, 3133 TAMU, College Station, TX 77843
31. D. Alberstein, Los Alamos National Laboratory, P.O. Box 1663, MS-K551, Los Alamos, NM 87545
32. J. B. Briggs, Idaho National Environmental and Engineering Laboratory, P.O. Box 1625-3855, Idaho Falls, ID 83415-3855
33. J. Baker, Office of Fissile Materials Disposition, U.S. Department of Energy, NN-63, 1000 Independence Avenue SW, Washington, DC 20585
34. K. Chidester, Los Alamos National Laboratory, P.O. Box 1663, MS-E502, Los Alamos, NM 87545
35. W. Danker, U.S. Department of Energy, NN-62, 1000 Independence Avenue SW, Washington, DC 20585
36. T. Gould, Lawrence Livermore National Laboratory, P.O. Box 808, MS-L186, Livermore, CA 94551
37. L. Jardine, Lawrence Livermore National Laboratory, P.O. Box 808, MS-L166, Livermore, CA 94551
38. Dr. Alexander Kalashnikov, Institute of Physics and Power Engineering, 1 Bondarenko Square, Obninsk, Kaluga Region, Russia 249020
39–43. Dr. Alexander Pavlovichev, Russian Research Center “Kurchatov Institute,” Institute of Nuclear Reactors, VVER Division, VVER Physics Department, 123182, Kurchatov Square, 1, Moscow, Russia
44. K. L. Peddicord, Associate Vice Chancellor, Texas A&M University, 120 Zachry, College Station, TX 77843-3133

45. J. Thompson, Office of Fissile Materials Disposition, U.S. Department of Energy, NN-61, 1000 Independence Avenue SW, Washington, DC 20585
46. F. Trumble, Westinghouse Savannah River Company, Building 730R, Room 3402, WSRC, Aiken, SC 29808
47. R. H. Clark, Duke/Cogema/Stone & Webster, 400 South Tryon Street, WC-32G, P.O. Box 1004, Charlotte, NC 28202
48. S. Nesbit, Duke/Cogema/Stone & Webster, 400 South Tryon Street, WC-32G, P.O. Box 1004, Charlotte, NC 28202
49. M. S. Chatterton, Office of Nuclear Reactor Regulation, MS O10B3, U.S. Nuclear Regulatory Commission, Washington, DC 20555-0001
50. R. W. Lee, Office of Nuclear Reactor Regulation, MS O10B3, U.S. Nuclear Regulatory Commission, Washington, DC 20555-0001
51. U. Shoop, Office of Nuclear Reactor Regulation, MS O10B3, U.S. Nuclear Regulatory Commission, Washington, DC 20555-0001
52. Aldo Ferri, Scandpower, Inc., 101 Lakeforest Blvd., Suite 340, Gaithersburg, MD 20877.
53. Nagao Ogawa; Director and General Manager; Plant Engineering Department; Nuclear Power Engineering Corporation; Shuwa-Kamiyacho Building, 2F; 3-13, 4-Chome Toranomon; Minato-Ku, Tokyo 105-0001, Japan
54. Dr. Kiyonori Aratani; Surplus Weapons Plutonium Disposition Group; International Cooperation and Nuclear Material Control Division; Japan Nuclear Cycle Development Institute; 4-49 Muramatsu, Tokai-mura, Naka-gun, Ibaraki-ken, Japan
55. Boris E. Volkov; Head of Division; EDO Gidropress; 21 Ordzhonikidze Street; Podolsk, Moscow District, Russia 142103
56. Dr. Alexandre Ermolaev; Balakovo Nuclear Power Plant, Saratov Region, Balakovo-26, Russia, 413866